Pakistan Journal of Scientific and Industrial Research

Vol. 52, No. 4 **Contents** **July - August 2009**

Physical Sciences

Biological Sciences

Technology

Physical Sciences

Pak. J. Sci. Ind. Res. 2009 **52** (4) 173-179

Solvent Extraction of Zn(II) from Aqueous Sulphate Media by Di(2-Ethylhexyl) Phosphoric Acid in Kerosene

D. A. Begum, M. Alauddin, M. F. Islam and M. S. Rahman*

Department of Applied Chemistry and Chemical Technology, University of Rajshahi, Rajshahi - 6205, Bangladesh

(received October 27, 2008; revised June 18, 2009; accepted June 30, 2009)

Abstract. The extraction equilibrium studies of Zn(II) from sulphate medium by di(2-ethylhexyl) phosphoric acid (D2EHPA, H_2A_2) in kerosene revealed that the distribution ratio (D) decreased with the increase of initial [Zn(II)] in the aqueous phase and increased with the increase of equilibrium pH and extractant concentration. The equilibration is reached within 2 min. The species extracted into the organic phase is thought to be ZnA_2.HA. The pH and extractant dependencies were about 2 and 1.67, respectively. The distribution ratio decreased with the increase in sulphate ion concentration in the aqueous phase. The extraction equilibrium reaction is suggested as $Zn^{2+}_{aq} + 1.5\ (H_2A_2)_{org} \leftrightarrow [ZnA_2.HA]_{org} + 2H^+_{aq}$. The extraction equilibrium constant (k_{ex}) for the above reaction was calculated to be $10^{-2.26}$. The extraction process was endothermic in nature having positive D*H* value of 16.27 kJ/mol. The loading of D2EHPA by Zn(II) is about 4.50 g of Zn(II) by 0.10 M D2EHPA. Possible reaction mechanism has been suggested based on distribution data, extractant concentration and equilibrium pH of the aqueous phase.

Keywords: solvent extraction, Zn(II) ion, sulphate media, D2EHPA, di(2-ethylhexyl) phosphoric acid, kerosene

Introduction

Solvent extraction has been one of the most important extraction and separation processes in hydrometallurgy. Especially phosphorus-based extractant, D2EHPA, a commercial extractant, has proved to be of particular importance for its wide range of extraction (from divalent to heptavalent) ability as well as separations of metal ions such as iron, copper, silver, cadmium, cobalt, nickel, manganese, magnesium, calcium, sodium, potassium, arsenic and antimony from different acidic solutions (Park and Fray, 2009; Fouad and Bart, 2008; Keng Xie *et al*., 2008; Mansur *et al*., 2008, 2002; Samaniego *et al*., 2007; Sarangi *et al*., 2007; Kumar Vinay *et al*., 2006; Jianbing Ryszard *et al*., 2006; Takeshita *et al*., 2003; Singh and Dhadke, 2002; Morters and Bart, 2000).

All the studies made on the extraction of Zn(II) by D2EHPA were done mostly from chloride solutions and with purified D2EHPA (Amer and Luis, 1995; Devi *et al*., 1995; Alguacil *et al*., 1992). As the extraction characteristics of a metal ion by an extractant depends on the concentration levels of the metal ions and coexisting anions in the aqueous phase as well as on the diluents used, the objective of the present work was to make an investigation on the possibility of extraction of Zn(II) by commercial grade D2EHPA in kerosene diluent. Presently the kerosene medium is used as the industrial diluent for solvent extraction technology. Zinc extraction from waste leach solution has assumed importance in view of the world-wide shortage of zinc and consequently its high price. Recovery of zinc from waste zinc containing materials is now a major interest in hydrometallurgy. The present study was undertaken to explore the possibility of extraction of zinc from comparatively concentrated zinc solutions in presence of sulphate ions. Various waste zinc materials are best leached by dilute H_2SO_4.

*Author for correspondence; E-mail: saeed_hamim@yahoo.com

Materials and Methods

A standard solution of Zn(II) (1 g/litre) was prepared by dissolving and diluting calculated amount of their respective sulphate salts ($ZnSO_4.7H_2O$) with distilled water after adding 2.90 cc of 18.337 M H_2SO_4 and standardized by using atomic absorption spectrophotometric method [Atomic Absorption Spectrophotometer (AAS), ANA 180, Tokyo Photoelectric Co. Ltd., Japan] at wavelength 217 nm. The test solution was prepared by taking calculated amount of respective aqueous stock solution of metal ion in a volumetric flask and then adding calculated amount of sulphate ion as either H_2SO_4 or Na_2SO_4 and made up to the mark by distilled water. After mixing, the solution was taken in a beaker for pH adjustment using dilute H_2SO_4 or anhydrous Na_2CO_3.

The extractant D2EHPA having 98% purity was used without further purification. All other chemicals were of reagent grade and used without further purification. The diluent, kerosene, was purchased from the local market and distilled when the colourless fraction was obtained in the range of 200-260 °C.

A stock solution of D2EHPA (1 M) was prepared by weighing out exactly 658.02 g of D2EHPA in a 1 litre volumetric flask and diluting with distilled kerosene. Working solutions of different concentrations (0.01-0.50 M) were prepared by proper dilution of this stock solution with distilled kerosene.

A definite aliquot of an aqueous phase (20 ml) was taken in a 125 ml reagent bottle and to it, same aliquot of organic phase (20 ml) was added. The bottle was stoppered and shaken for 5 min in a thermostatic water bath at 30±1 °C (except for temperature dependence). After attainment of equilibrium, the phases were allowed to settle and disengaged by a separating funnel. The aqueous phase was subjected to equilibrium pH measurement and the metal ion content by AAS. Distilled water was used as blank solution. In all the cases, phase separation occurred readily. pH value of aqueous solutions was measured by Mettler Toledo 320 pH meter and checked time to time to set the desired pH.

The equilibrium organic phase metal ion concentrations were estimated by the method of difference. The organic phase Zn(II) concentration was determined by the formula: initial aqueous phase - aqueous phase concentration of Zn(II) after extraction. The distribution ratio (D) of a metal ion was calculated as the ratio of metal ion concentration in the organic phase to that in the aqueous phase at equilibrium. In the case of loading test, the organic phase was repeatedly contacted with fresh equal volume of aqueous solutions until saturation of the organic phase with the metal was attained and tested by measuring aqueous phase concentration.

Results and Discussion

Effect of distribution ratio of Zn(II) by D2EHPA on contact time. Figure 1 represents contact time (in minutes) and the distribution ratio for two different sets of pH 4 and 5. In both the cases, it was found that the extraction ratio of Zn(II) increased continuously with the increase of phase contact time upto 2 min and then remained unchanged with further increase of contact time. The slopes of the lines decreased to zero at around 2 min. Moreover, it was also observed that 96.70 ± 0.05% and 97.45 ± 0.05% [n = 8] of Zn(II) got extracted at pH 4 and 5, respectively, and on further shaking for a long time, extraction ratio did not increase. The extraction of Zn(II) by Cyanex 302 was studied by Alguacil *et al.* (1992) and obtained equilibrium time above 10 min. Therefore, the extraction of Zn(II) by D2EHPA is faster than that of Cyanex 302. It is concluded that the extraction of Zn(II) from sulphate solution by analytical grade D2EHPA in kerosene system takes 2 min. Thus in subsequent experiments, mixing was carried out for 5 min to ensure equilibrium.

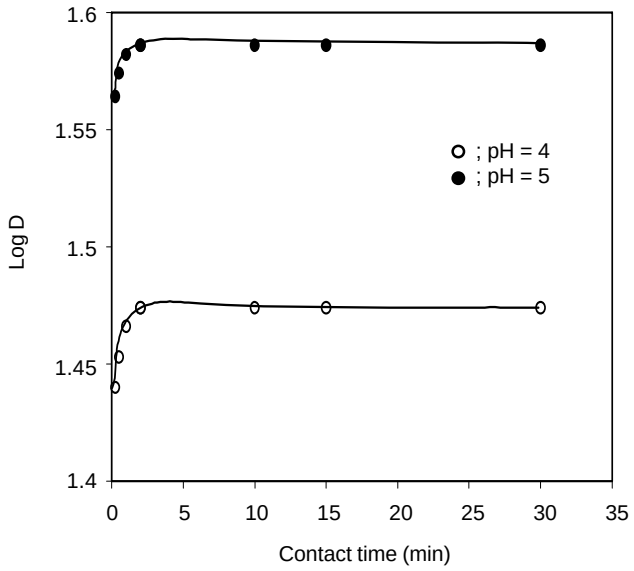

Fig. 1. Effect of distribution ratio of Zn(II) by D2EHPA on contact time.
[Zn(II)] = 0.200 g/litre; $[SO_4^{=}]_{(ini)}$ = 0.10 M; pH = 4.00 and 5.00; phase mixing time = moderate; [D2EHPA] = 0.05 M; O/A=1; temperature = (30±1) °C.

Effect of metal ion concentration on Zn(II) by D2EHPA. The results obtained from the experiments are plotted as log D *vs.* log {$[Zn(II)]_{(ini)}$mol/litre} which represent variation of distribution ratio on initial metal ion concentration. It is seen that the distribution ratio decreases with increase in initial Zn(II) ion concentration (Fig. 2). The slopes of the plots are steeper at higher concentration region than those at lower concentration. In general, log D should be independent of initial metal ion concentration, provided the equilibrium pH and the equilibrium extractant concentration remain constant, which can occur with very low metal concentration only.

The decrease in extraction ratio with the increase of Zn(II) ion concentration may be explained as follows:

a) ***Non-constant aqueous phase acidity, pH.*** With the increase in Zn(II) ion concentration in the aqueous phase, the equilibrium pH may drop down due to the liberation of H^+ by the extraction process. The decreased equilibrium pH with increase of Zn(II) ion concentration will decrease the extraction ratio according to the simplified extraction reaction as follows:

$$Zn^{2+} + H_2A_2 \Leftrightarrow ZnA_2 + 2H^+ \quad (1)$$

where, H_2A_2 is the dimer of D2EHPA

b) ***Non-constant equilibrium extractant concentration.*** With the increase in initial Zn(II) ion concentration, more extractant

will be consumed to form the extractable Zn(II) complex. As a result, the equilibrium pH and extractant concentration will decrease with the increase in the initial Zn(II) ion concentration in the aqueous phase and eventually, the extraction ratio will decrease and may be expressed according to the following equation:

$$\log D = \log K_{ex} + z \log [H_2A_2]_{(ini)} + z\,pH - S \qquad (2)$$

where:

D = distribution or extraction ratio; z = extractant dependence;

S = concentration of the extractant which is used in forming the metal complex; $[H_2A_2]_{(ini)}$ = initial extractant concentration in the organic phase; pH = equilibrium pH of the aqueous phase.

Besides these two reasons, the decrease in the extraction ratio with increasing initial Zn(II) ion concentration may be attributed to the non-ideality of the aqueous phase, hydrolysis and polymerization of Zn(II) species in the aqueous phase.

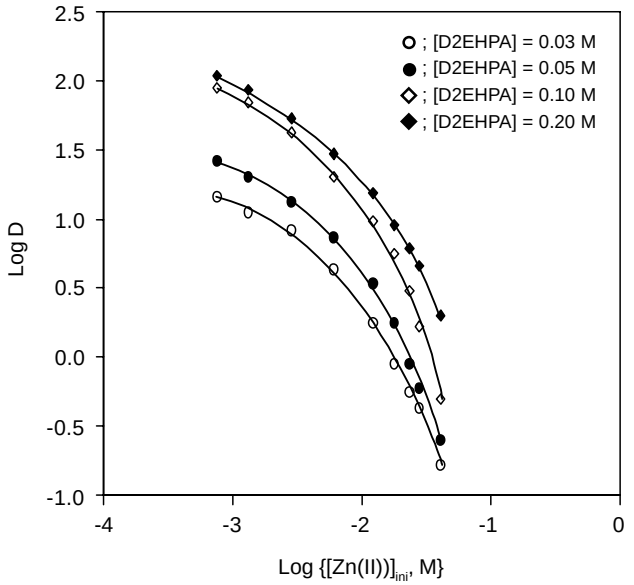

Fig. 2. Effect of distribution ratio (D) on Zn(II) ion concentration.
$[SO_4^{=}]_{(ini)}$ = 0.10 M; pH=3.00; phase mixing time = 5 min; [D2EHPA] = 0.03, 0.05, 0.10, 0.20 M; O/A=1; temperature= (30±1) °C.

Effect of equilibrium pH on the extraction of Zn (II) by D2EHPA. The results obtained from the experiments at different constant equilibrium pH and at constant [Zn(II)] concentration are plotted as log D (distribution ratio) *vs.* equilibrium pH (Fig. 3). It can be seen that the extraction of Zn(II) ions increases with increase of aqueous phase equilibrium pH. The slopes of the lines were calculated and the values are 1.99, 2.09, 2.06, 2.03, 2.12 and 1.96 for 0.01, 0.02, 0.05, 0.10, 0.20 and 0.50 M D2EHPA systems, respectively. The average slope obtained from this investigation is equal to 2 (two). Similar results were obtained from the extraction of Zn(II) by D2EHPA by other workers (Bart *et al*., 1992; Svendsen *et al*., 1990). The intercepts of the lines are -5.58, -5.21, -4.44, -3.80, -3.70 and -2.40 for 0.01, 0.02. 0.05, 0.10, 0.20 and 0.50 M D2EHPA systems, respectively. The slope of the line of Zn(II) is ~ 2, which indicates that two moles of H^+ are liberated per mole of Zn(II) during extraction. From intercept of the line, the value of extraction equilibrium constant (k_{ex}) was calculated after knowing the extractant dependence. The calculated value was found to be $10^{-2.26}$.

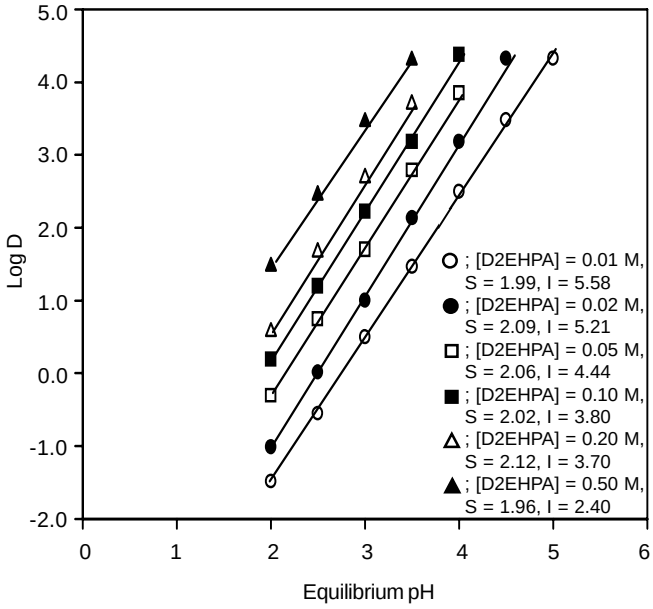

Fig. 3. Effect of distribution ratio (D) on equilibrium pH. $[Zn(II)]_{(ini)}$ = 0.215 g/litre; $[SO_4^{=}]_{(ini)}$ = 0.10 M; [D2EHPA] = 0.01, 0.02, 0.05, 0.10, 0.20, 0.50 M; D2EHPA, phase mixing time = 5 min; O/A=1; temperature = (30±1) °C.

Effect of extractant concentration on the extraction of Zn(II) by D2EHPA. The results obtained from the experiments carried out at different equilibrium pH and for the effect of extractant concentration were plotted as log D *vs.* log $[H_2A_2]$ at fixed Zn(II) ion concentration (Fig. 4). The figure represents the effect of variation of distribution ratio (D) on the extractant concentrations. It was observed that the extraction ratio increased with increasing extractant concentration in the organic phase, and a straight-line relationship was obtained.

The slopes (S) and intercepts (I) of the lines were: S=1.78, I=2.14; S=1.70, I=3.80; S=1.60, I=5.66 and S=1.60, I=7.82 for equilibrium pH values of 2, 3, 4, and 5, respectively. Average slope of the lines was 1.67. Similar observations were found by other workers (Bart *et al.*, 1992; Svendsen *et al.*, 1990). Here the linear relationship of the extraction ratio with the D2EHPA concentration indicates that the more is extractant concentration, the more is the extraction of Zn(II). This is the normal behavior of extraction process. The slope of the line indicates that normal ion exchange mechanism for Zn(II) is followed. Since for a particular initial pH system, the equilibrium pH varies with the variation of extractant concentration, to get actual extractant dependence, it is necessary to get log D *vs.* log $[H_2A_2]$ plots at constant equilibrium pH values. Such type of correction has been made with the help of acidity dependence data. First of all the difference between the initial and equilibrium pH values are determined (termed as ΔpH). As the acidity dependence is always 2, the correction term for

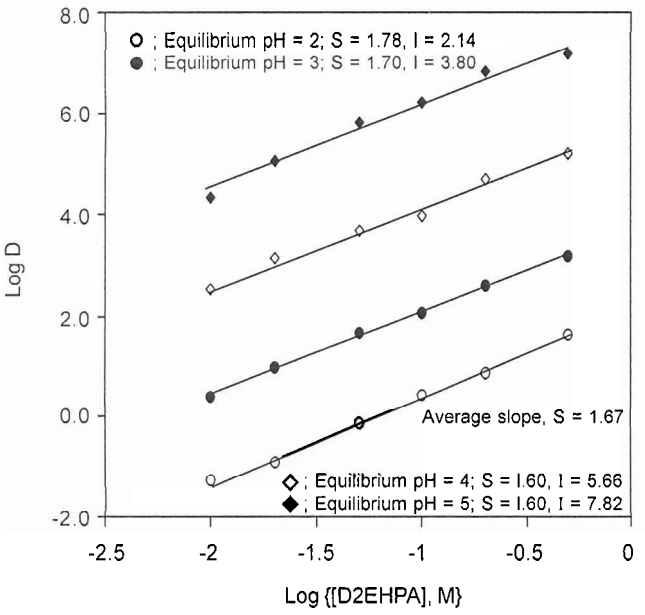

Fig. 4. Effect of distribution ratio (D) on extractant concentration.
$[Zn(II)]_{(ini)}$ = 0.215 g/litre; $[SO_4^{=}]_{(ini)}$ = 0.10 M; phase mixing time = 5 min; O/A=1; temperature = (30±1) °C.

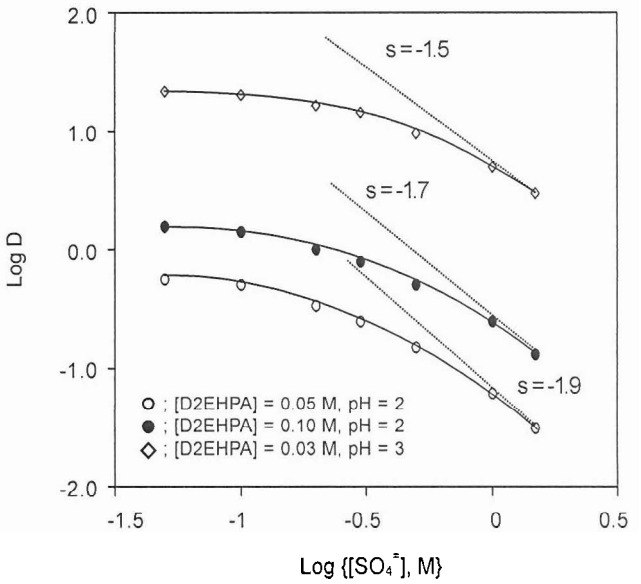

Fig. 5. Effect of distribution ratio (D) on sulphate ion concentration.
$[Zn(II)]_{(ini)}$ = 0.215 g/litre; [D2EHPA] = 0.03; 0.05, 0.10 M; phase mixing time = 5 min; O/A=1; temperature = (30±1) °C.

Table 1. Evaluation of the extraction equilibrium constant log k_{ex} for Zn(II) ion (based on Figs. 3 and 4)

Figure No	Equilibrium pH	[D2EHPA], M	Intercept, *I*	Log k_{ex}	Average log k_{ex}	Standard deviation
3		0.01	-5.58	-2.240		
		0.02	-5.21	-2.373		
		0.05	-4.44	-2.267		
		0.10	-3.80	-2.130		
		0.20	-3.70	-2.533		
		0.50	-2.40	-1.897		
					-2.258	0.204
4	2.0		2.14	-1.94		
	3.0		3.80	-2.32		
	4.0		5.66	-2.50		
	5.0		7.82	-2.38		

log D is calculated as ΔpH x 2. Then the corrected log D value is calculated as log D (experimental) + ΔpH x 2, which corresponds to the data at equilibrium, equal to initial pH.

Extractant dependence of about 1.67 indicates the association of 1.67 moles of extractant with 1 mole of ion Zn(II). From the intercept of the line in Fig. 3 and Fig. 4, the value of log k_{ex} has been calculated to be -2.258 with the standard deviation of log k_{ex} being 0.204 (Table 1).

Effect of sulphate ion concentration on the extraction of Zn(II) by D2EHPA. Figure 5 represents the results obtained from the experiments involving the variations of sulphate ion concentration at three constant initial pH (2, 2 and 3) and at three extractant concentrations (0.03, 0.05 and 0.10 M), respectively. Herein, log D has been plotted *vs.* log [$SO_4^{=}$], M. The variation of extraction ratio with the variation of sulphate ion concentration depends on the extractant concentration as well as on the pH of the aqueous solution. When the pH of the aqueous solution is kept constant, the extraction ratio decreases with the increase in sulphate ion concentration in the aqueous phase. In all the cases, the tangential negative slopes of these curves increased gradually with the increase in sulphate ion concentration. At lower sulphate region, the slope approaches to zero, whereas in the higher region, it approaches to -2.00 depending upon the pH-D2EHPA values.

Effect of temperature on the extraction of Zn(II) by D2EHPA. Figure 6 (plot of log D *vs.* inverse of absolute temperature) shows the effect of variation of distribution ratio on temperature i.e. the effect of temperature on extraction. The extraction ratio increases with increase in temperature. The slopes of this line are -0.844×10^3 and -0.857×10^3 for 0.05 and 0.10 M D2EHPA, respectively, in kerosene system. The extraction reaction enthalpy values (ΔH) has been calculated using Vant-Hoff equation. The calculated values are found to be 16.15 and 16.40 kJ/mol respectively for 0.05 and 0.10 M D2EHPA. The average value of apparent enthalpy change is 16.27 kJ/mol. The positive enthalpy change suggests that the extraction process of Zn(II) by D2EHPA is endothermic in nature. The extraction ratio-temperature relationship indicates that the equilibrium reaction of Zn(II) is moderately influenced by temperature. Thus, extraction of Zn(II) by D2EHPA in kerosene system moderately increases by using extraction at a higher temperature.

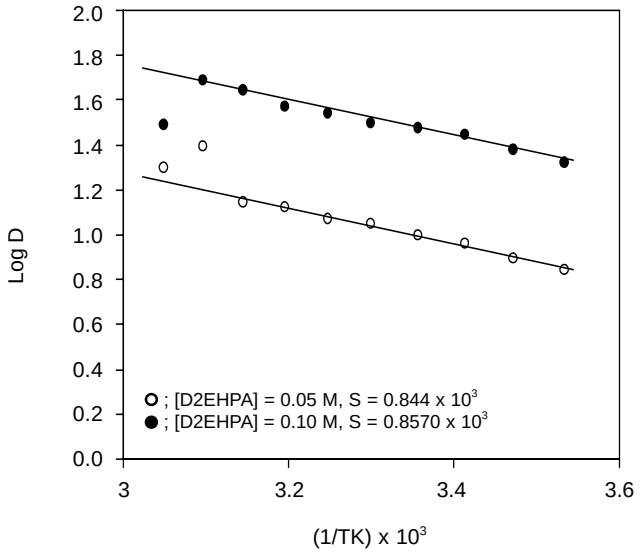

Fig. 6. Effect of distribution ratio (D) on temperature. $[Zn(II)]_{(ini)}$ = 0.205 g/litre; $[SO_4^{=}]_{(ini)}$ = 0.10 M; pH = 3.00, phase mixing time = 5 min., O/A=1.

Effect of loading on the extraction of Zn(II) by D2EHPA. Loading is an important factor for the study of mechanism of extraction and also for the industrial evaluation of the extractant. High values of loading capacity are desirable for any particular extractant metal system for industrial applications.

The organic phases (20 ml) were repeatedly contacted for 5 min at 30±1 °C with fresh equal volume of aqueous solution containing fixed concentration of metal ions [Zn(II)] 1.08 g/litre at pH 2 and 3. After equilibration, the phases were disengaged and the aqueous phases were analyzed for Zn(II) contents. The amount of metal ions [Zn(II)] transferred into the organic phase for each contact was then determined by difference and the cumulative concentration of Zn(II) in the organic phase, after each stage of contact, was estimated. The result obtained from the experiments, plotted as cumulative [Zn(II)], g/litre *vs.* contact number is given in Fig. 7. It can be seen the organic phase is saturated with Zn(II) after the 7th and the 11th contact, respectively, for pH 2 and 3. The loading of 0.10 M D2EHPA by Zn(II) was as much as 0.92 g and 4.455 g of Zn(II) at pH 2 and 3, respectively, which indicates that the loading capacity of D2EHPA is 1.40 g and 6.77 g of Zn(II)/100 g extractant for pH 2 and 3, respectively. The loading data suggests the ratio Zn : D2EHPA is 1, at pH 3, but at pH 2, the ratio is very low. At pH 2, most of D2EHPA remains uncombined having low distribution ratio.

Extraction mechanism. The extractant-dependence of ~1.6 suggests that 1.5 moles of extractant is required for each ion of Zn(II) ion for the extracted species. The hydrogen ion and extractant dependence suggests the following equation for the extraction reaction:

$$Zn^{2+}_{aq} + 1.5\,(H_2A_2)_{org} \Leftrightarrow [ZnA_2.HA]_{org} + 2H^{+}_{aq} \qquad (1)$$

Here the extracted species contains coordinated monomer di-2-ethylhexyl phosphoric acid molecules. The extraction of coordinated extracted species (adducts) is a general observation in the solvent extraction process. The extraction reaction is supported by Mellah and Benachour (2006) and Breno *et al.* (2004).

Sulphate dependence, almost zero below 0.1 M [$SO_4^{=}$], suggests that Zn(II) ion is the predominant species in the extraction process. However, at higher [$SO_4^{=}$] ion, the species $Zn(HSO_4)_2$ may form to some extent, indicating the reaction involving non-ionized zinc species:

$$Zn(HSO_4)_2\,aq + 1.5\,(H_2A_2)_{org} \Leftrightarrow [ZnA_2.HA]_{org} + 2H_2SO_{4\,aq} \quad (2)$$

This supports the slopes approaching -2.00 with increasing [$SO_4^{=}$] ion concentration in the aqueous phase.

The loading test suggested that the neutral unreacted HA in the extracted species [ZnA_2.HA] gradually increased to give Zn **:** D2EHPA(H_2A_2) ratio of 1:1 corresponding to the species ZnA_2 for high (pH 3) loading. At the low pH the organic phase is not saturated with zinc even after the 11th contact.

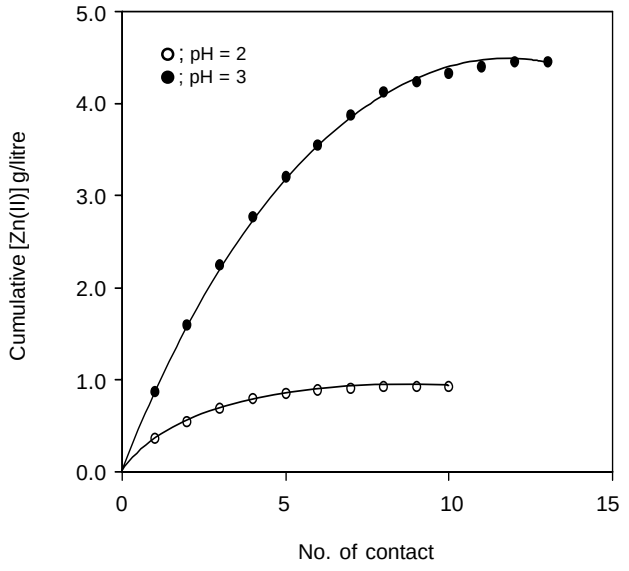

Fig. 7. Loading of Zn(II) in D2EHPA. $[Zn(II)]_{(ini)}$ = 1.08 g/litre; $[SO_4^{=}]_{(ini)}$ = 0.10 M; phase mixing time = 5 min; [D2EHPA] = 0.10 M; O/A=1; temperature = (30±1) °C.

Conclusion

Zn(II) solution can be obtained as leach solution in different industries especially in the pickling industry with acids. Dilute solution can be a good source for Zn(II) if it can be separated. Solvent extraction can be a good technique for simultaneous separation and concentration of weak Zn(II) solution. Di-2-ethylhexyl phosphoric acid is a moderately effective extractant for Zn(II) from low acidic and low sulphate media. The extractant and hydrogen ion dependence suggests a simple extraction reaction for the process. Temperature has moderate influence on the extraction process. The extracted species is suggested to be $[ZnA_2.HA]_{org}$ in the kerosene phase. However, complete saturation of the organic phase occurs at high loading, corresponding to ZnA_2 as extracted species. Low extraction equilibrium constant (k_{ex}) suggests that stripping from the organic phase is much favoured.

References

Alguacil, F.J., Cobo, A., Caravaca, C. 1992. Study of the extraction of Zn(II) in the aqueous chloride media by Cyanex 302. *Hydrometallurgy* **31:** 163-174.

Amer, S., Luis, A.1995. The extraction of zinc and other minor metals from concentrated ammonium chloride solutions with D2EHPA and CYANEX 272. *Revista de Metalurgia* **31:** 351-360.

Bart, H.J., Marr, R., Scheks, J., Konkar, M. 1992. Modelling of solvent extraction equilibria of Zn(II) from sulphate solutions with bis(2-ethylhexyl) phosphoric acid. *Hydrometallurgy* **31:** 13-28.

Breno, S., Morais, Marcelo, B., Mansur. 2004. Characterisation of the reactive test system $ZnSO_4$/D2EHPA in *n*-heptane, *Hydrometallurgy* **74:** 11-18.

Devi, N.B., Nathsarma, K.C., Chakravorthy, V. 1995. Solvent extraction of zinc(II) using sodium salts of D2EHPA, PC-88A and CYANEX 272 in kerosene. In: *Mineral Processing*: *Recent Advances and Future Trends*. S. P. Mehrotra and R. Shekhar (eds.), pp. 537-547, Allied Publishers, New Delhi, India.

Fouad, E.A., Bart, H.J. 2008. Emulsion liquid membrane extraction of zinc by a hollow-fiber contactor. *Journal of Membrane Science* **307:** 156-168.

Jianbing, J., Kathryn, H.M., Jilska, M.P., Geoff, W.S. 2006. The role of kinetics in the extraction of zinc with D2EHPA in a packed column. *Hydrometallurgy* **84:** 139-148.

Keng Xie, Jian-Kang Wen, Yi-Xin Hua, Ren-Man Ruan. 2008. Selective separation of Cu(II), Zn(II), and Cd(II) by solvent extraction. *Rare Metals* **27:** 228-232.

Kumar, V., Bagchi, D., Pandey, B.D. 2006. Extraction of zinc-cobalt from sulphate solution of cobalt cake by D2EHPA in the processing of Indian Ocean nodules. *Steel Research* **77:** 299-304.

Mansur, M.B., Slater, M.J., Biscaia, E.C. 2002. Kinetic analysis of the reactive liquid-liquid test system $ZnSO_4$/D2EHPA/*n*-heptane. *Hydrometallurgy* **63:** 107-116.

Mansur, M.B., Rocha, S.D.F., Magalhaes, F.S., Benedetto, J.D.S.

2008. Selective extraction of zinc(II) over iron(II) from spent hydrochloric acid pickling effluents by liquid-liquid extraction. *Journal of Hazardous Materials* **150:** 669-678.

Mellah, A., Benachour, D. 2006. The solvent extraction of zinc and cadmium from phosphoric acid solution by di-2-ethyl hexyl phosphoric acid in kerosene diluent; *Chemical Engineering and Processing* **45:** 684-690.

Morters, M., Bart, H.J. 2000. Extraction equilibria of zinc with bis(2-ethylhexyl)phosphoric acid. *Journal of Chemical and Engineering Data* **45:** 82-85.

Park, Y.J., Fray, D.J. 2009. Separation of zinc and nickel ions in a strong acid through liquid-liquid extraction. *Journal of Hazardous Materials* **163:** 259-265.

Samaniego, H., Roman, M.F.S., Ortiz, I. 2007. Kinetics of zinc recovery from spent pickling effluents. *Industrial and Engineering Chemistry Research* **46:** 907-912.

Sarangi, K., Parhi, P.K., Padhan, E., Palai, A.K., Nathsarma, K.C., Park, K.H. 2007. Separation of iron(III), copper(II) and zinc(II) from a mixed sulphate/chloride solution using TBP, LIX 84I and Cyanex 923, *Separation and Purification Technology* **55:** 44-49.

Singh, R.K., Dhadke, P.M. 2002. Extraction and separation studies of zinc(II) and copper(II) with D2EHPA and *pc*-88*a* from perchlorate media. *Journal of the Serbian Chemical Society* **67:** 41-51.

Svendsen, H.F., Schei, G., Osman, M. 1990. Kinetics of extraction of zinc by di(2-ethylhexyl) phosphoric acid in cumene. *Hydrometallurgy* **25:** 197-212.

Takeshita, K., Watanabe, K., Nakano, Y., Watanabe, M. 2003. Solvent extraction separation of Cd(II) and Zn(II) with the organophosphorus extractant D2EHPA and the aqueous nitrogen-donor ligand TPEN. *Hydrometallurgy* **70:** 63-71.

Pak. J. Sci. Ind. Res. 2009 **52** (4) 180-185

Synthesis, Characterization and Antimicrobial Evaluation of Some Arylidenehydrazonofuropyrimidines and Thienopyrimidines

Md. Mosharef Hossain Bhuiyan*, Khandker M. M. Rahman and Md. Imjamul Islam

Department of Chemistry, University of Chittagong, Chittagong-4331, Bangladesh

(received March 30, 2009; revised June 1, 2009; accepted June 5, 2009)

Abstract. Cyclization of heteroaromatic *o*-aminoester with formamide afforded furo[2,3-d]pyrimidin-4(3*H*)-one which was then chlorinated with thionyl chloride followed by displacement by hydrazine hydrate to furnish hydrazinofuro [2,3-d]pyrimidine. Reaction of hydrazino derivative with formic acid gave furo[3,2-e][1,2,4]triazolo[4,3-c]pyrimidine. Treatment of hydrazino derivative with aromatic aldehydes afforded arylidenehydrazonofuro[2,3-d]pyrimidine derivatives. Reaction of *o*-aminonitrile with carbon disulphide, followed by methylation with methyl iodide and subsequent reaction with hydrazine hydrate afforded hydrazinothieno[2,3-d]pyrimidine. 14 derivatives were synthesized. Some of these derivatives exhibited pronounced antimicrobial activities against *S. typhi, S. aureus, S. dysenteriae, V. cholerae, C. lunata, A. alternata, C. corchori, F. equeseti* and *M. phaseolina*.

Keywords: aminoester, aminonitrile, furo-pyrimidine, thieno-pyrimidine, antimicrobial activity, pyrimidines

Introduction

Among the wide range of heterocycles explored to develop pharmaceutically important molecules, pyrimidine has played an important role in medicinal chemistry. Compounds having a pyrimidine nucleus possess a broad range of biological activities such as antibacterial (Bekhit *et al*., 2003), antiviral (Kumar *et al*., 2002), anticancerous (Haggarty *et al*., 2000), antimalarial (Agarwal *et al*., 2005), antihypertensive (Ismail *et al*., 2006) and anti-inflammatory activities (Sondhi *et al*., 2005; Ferri *et al*., 2003). Some furans are useful for the inhibition of thrombin formation. Furano derivatives are also associated with various biological activities such as antihypertensive, antiallergic, anticonvulsive, anxiolytic, antiamnestic and antidepressant activities (Nalbandyan *et al*., 1999; Sauter *et al*., 1996; Patil *et al*., 1984). In continuation of our search for antimicrobial molecules (Bhuiyan *et al*., 2006; 2005a,b,c; 2004), furano- and thienopyrimidine derivatives were synthesized and evaluated for their anti-microbial activities.

Materials and Methods

Melting points were recorded with electrothermal melting point apparatus and are uncorrected. Evaporation of solvents was performed under reduced pressure on a Buchi rotary evaporator. Thin layer chromatography was performed on Kieselgel GF_{254} and visualization was accomplished by iodine flask or UV Flame. ^{1}H-NMR (500 MHz and 300 MHz) spectrum was recorded for solutions in deuterio chloroform $CDCl_3$ as solvent. Chemical shifts were reported in δ unit (ppm) with reference to TMS as an internal standard and *J* values are given in Hz.

Ethyl 2-amino-4,5-diphenylfuran-3-carboxylate (1). A suspension of ethyl cyanoacetate (2.125 g, 33.3 mmol) and benzoin (5.24 g, 25 mmol) in DMF (7.5 ml) was treated with diethylamine (4 ml). After 12 h standing and 12 h stirring, the mixture was poured onto ice-water (60 ml). The conversion was checked by TLC (*n*-hexane:ethyl acetate; 4:1, v/v) on silica gel which showed complete conversion into the product. The separated solid was collected by filtration and recrystallized from ethanol to give ethyl 2-amino-4,5-diphenylfuran-3-carboxylate **(1)** (75%) as yellow crystals, m.p. 208-210 °C. ^{1}H-NMR(500 MHz, $CDCl_3$): δ_H 9.24 (s, 2H, NH_2), 7.96-7.38 (m, 10H, 2×Ph), 2.66 (q, 2H, CH_2), 1.03 (t, 3H, CH_3).

5,6-Diphenylfuro[2,3-d]pyrimidin-4(3H)-one (2). A solution of **1** (3.85 mmol) in formamide (5 ml) was refluxed for 2 h. The precipitate that formed on cooling was filtered and recrystallized from ethanol to give **2** (70%) as yellow crystals, m.p. 210-212 °C. ^{1}H-NMR (500 MHz, $CDCl_3$): δ_H 7.84 (s, 1H, CH), 7.6-7.4 (m, 10H, 2×Ph), 1.70 (s, 1H, NH).

4-Chloro-5,6-diphenylfuro[2,3-d]pyrimidine (3). A mixture of pyrimidinone **2** (2.28 g, 10 mmol) and thionyl chloride (40 ml) was refluxed at 85 °C for 4 h with continuous stirring. The reaction mixture was then cooled and poured into ice-water. The obtained precipitate was collected and recrystallized from ethanol to give **3** (64%) as yellow needle crystals, m.p. 156-158 °C. ^{1}H-NMR (500 MHz, $CDCl_3$): δ_H 7.84 (s, 1H, CH), 7.6-7.4 (m, 10H, 2×Ph).

*Author for correspondence; E-mail: mosharef65@yahoo.com

4-Hydrazino-5,6-diphenylfuro[2,3-d]pyrimidine (4). A solution of the chloro compound **3** (1.56 g, 74.32 mmol) and hydrazine hydrate (5.5 ml, 76.74 mmol) in dioxane (25 ml) was refluxed for 4 h at 90 ^{0}C with stirring. The separated solid was filtered and recrystallized from dioxane to give **4** (68%) as brown crystals, m.p. 170-172 °C. ^{1}H-NMR(500 MHz, $CDCl_3$): δ_H 8.14 (s, 1H, CH), 7.80-7.45 (m, 10H, 2×Ph), 5.55 (bs, 1H, NH), 4.84 (bs, 2H, NH_2).

8,9-Diphenylfuro[3,2-e][1,2,4]triazolo[4,3-c]pyrimidine (5). A suspension of hydrazino compound **4** (0.74 g, 57.98 mmol) in formic acid (15 ml) was refluxed for 6 h. The solid that precipitated was collected and recrystallized from ethanol to give **5** (65%) as pink crystals, m.p. 120-121 °C. ^{1}H-NMR (500 MHz, $CDCl_3$): δ_H 9.92 (s, 1H, 5-CH), 8.37 (s, 1H, 3-CH), 7.38 (m, 10H, 2×Ph); ^{13}C-NMR ($CDCl_3$): δ_C 158.0, 149.2, 147.1, 140.8, 135.6, 131.2, 129.0, 128.6, 127.3, 103.1.

Arylidene-hydrazono-5, 6-diphenylfuro[2,3-d]pyrimidines. ***General procedure:*** A mixture of hydrazino compound **4** (0.74 g, 57.98 mmol) and aromatic aldehyde (7 ml) in ethanol (25 ml) was refluxed for 8 h. The reaction mixture was then cooled and poured into ice-water. The separated solid was filtered and recrystallized from ethanol to give arylidenehydrazono-5, 6-diphenylfuro[2,3-d] pyrimidine.

4-(Benzylidenehydrazono)-5,6-diphenylfuro[2,3-d] pyrimidine (6). The title compound was prepared from hydrazino compound **4** and benzaldehyde in 70% yield as brown crystals, m.p. 90-92 °C. ^{1}H-NMR (500 MHz, $CDCl_3$): δ_H 8.68 (s, 1H, 2-CH), 7.85 (s, 1H, = CH), 7.59-7.61 (m, 5H, Ph), 7.47-7.34 (m, 10H, 2×Ph), 4.93 (s, 1H, NH); ^{13}C-NMR ($CDCl_3$): δ_C 167.4, 156.8, 154.3, 148.9, 141.0, 136.2, 132.1, 130.4, 129.4, 128.5, 103.5.

4-(4-Hydroxybenzylidenehydrazono)-5,6-diphenylfuro[2,3-d] pyrimidine (7). This compound was prepared from compound **4** and 4-hydroxybenzaldehyde in 68 % yield as pink crystals, m.p. 122-124 °C. ^{1}H-NMR (500 MHz, $CDCl_3$): δ_H 8.61 (s, 1H, 2-CH), 7.98 (s, 1H, =CH), 7.77 (d, 2H, *J*= 8.4 Hz), 7.42 (d, 2H, J= 8.4 Hz), 7.4-7.3 (m, 10H, 2×Ph), 6.21 (s, 1H, OH), 4.93 (s, 1H, NH); ^{13}C-NMR ($CDCl_3$): δ_C 168.0, 159.3, 157.0, 153.7, 149.5, 141.3, 136.0, 131.0, 130.5, 129.0, 128.6, 127.2, 123.8, 115.2, 103.7.

4-(4-Chlorobenzylidenehydrazono)-5,6-diphenylfuro[2,3-d] pyrimidine (8). The title compound was prepared from hydrazino compound **4** and 4-chlorobenzaldehyde in 70% yield as brown crystals, m.p. 130-132 °C. ^{1}H-NMR(500 MHz, $CDCl_3$): δ_H 8.61(s, 1H, 2-CH), 7.98 (s, 1H, =CH), 7.77 (d, 2H, J= 8.4 Hz), 7.42 (d, 2H, J= 8.4 Hz), 7.41-7.38 (m, 10H, 2×Ph), 4.93 (s, 1H, NH); ^{13}C-NMR ($CDCl_3$): δ_C 166.5, 156.8, 154.3, 148.7, 141.5, 136.4, 131.0, 130.1, 120.0, 128.2, 127.2, 103.6.

4-(2-Chloroybenzylidenehydrazono)-5,6-diphenylfuro[2,3-d] pyrimidine (9). The title compound was prepared from hydrazino compound **4** and 2-chlorobenzaldehyde in 65% yield as pink crystals, m.p. 135-138 °C. ^{1}H-NMR(500 MHz, $CDCl_3$): δ_H 9.08(s, 1H, 2-CH), 7.92 (s, 1H, =CH), 7.60-7.49 (m, 4H, Ph), 7.41(m, 10H, 2×Ph), 4.91 (s, 1H, NH); ^{13}C-NMR ($CDCl_3$): δ_C 168.0, 156.8, 153.9, 148.9, 141.5, 135.3, 134.0, 132.1, 131.4, 130.0, 129.0, 128.2, 127.0, 103.1.

2-Amino-4-ethyl-5-methylthiophene-3-carbonitrile (10). Diethyl amine (4 ml) was added dropwise to a mixture of diethylketone (3.2 g, 20 mmol), malononitrile (10.09 ml, 20 mmol) and elemental sulphur (0.64 g, 20 mmol) in 95% ethanol (20 ml). The temperature was maintained below 60 °C by means of ice bath. The mixture was stirred continuously for 8 h and then poured into ice water. The precipitate was filtered, washed with water and recrystallized from ethanol to *o*-aminonitrile **10** as brown crystals, m.p. 80-82 °C. ^{1}H-NMR (300 MHz, $CDCl_3$): δ_H 4.1 (bs, 2H, -NH_2), 2.4 (q, 2H, CH_2), 2.14 (s, 3H, CH_3), 1.36 (t, 3H, CH_3).

5-Ethyl-6-methylthieno[2,3-d]pyrimidine-2,4(1H,3H)-dithione (11). *o*-Aminonitrile **10** (0.4 g, 2.4 mmol) and carbon disulphide (2 ml) in pyridine (5 ml) was refluxed for 8 h. After cooling the reaction mixture was poured into ice-water and the separated solid was filtered and recrystallized from ethanol to give **11** (75%) as pink crystals, m.p. 85-87 °C. ^{1}H-NMR (300 MHz, $CDCl_3$): δ_H 8.67 (s, 1H, 3-NH), 7.93 (s, 1H, 1-NH), 2.83 (q, 2H, CH_2), 1.17 (s, 3H, CH_3), 0.9 (t, 3H, CH_3).

2,4-Dimethylthio-5-ethyl-6-methylthieno[2,3-d]pyrimidine (12). Methyl iodide (2.46 mmol) was added dropwise to a suspension of **11** (0.3 g, 1.23 mmol) in aqueous NaOH (10 ml) and stirred at room temperature for 12 h. The formed yellowish solid was collected and recrystallized from ethanol to give compound **12** (83%) as yellow crystals, m.p. 105-107 °C. ^{1}H-NMR(300 MHz, $CDCl_3$): δ_H 2.85 (q, 2H, CH_2), 2.61 (s, 3H, 4-SCH_3), 2.56 (s, 3H, CH_3), 2.50 (s, 3H, 2-SCH_3), 1.12 (t, 3H, CH_3); ^{13}C-NMR ($CDCl_3$): δ_C 167.4, 165.4, 135.7, 135.0, 129.0, 123.8, 18.6, 17.0, 14.3, 8.0.

4-Hydrazino-2-methylthio-5-ethyl-6-methylthieno[2,3-d]-pyrimidine (13). A mixture of compound **12** (0.3 g, 1.10 mmol) and hydrazine hydrate (1.10 mmol) in dioxane (10 ml) was refluxed for 4 h. The mixture was concentrated in vacuum. The solid was collected and recrystallized from ethanol to give compound **13** (80%) as pink crystals, m.p. 137-139 °C. ^{1}H-NMR(300 MHz, $CDCl_3$): δ_H 4.3 (s, 1H, NH), 3.45 (s, 2H, NH_2), 2.85 (q, 2H, CH_2), 2.15 (s, 3H, 2-SCH_3), 1.14 (s, 3H, CH_3), 0.9 (t, 3H, CH_3); ^{13}C-NMR ($CDCl_3$): δ_C 168.0, 165.2, 135.6, 135.0, 129.1, 123.5, 18.5, 17.0, 14.5, 8.0.

3-Benzoyl-5-ethyl-6-methylthieno[2,3-d]pyrimidin-2,4(1H,3H)-dithione (14). A mixture of compound **11** (0.3 g, 1.23 mmol) and benzoyl chloride (1.8 mmol) in pyridine (4 ml) was stirred at room temperature for 2 h. The mixture was poured into ice-water, neutralized with 10% HCl, washed with saturated sodium bicarbonate and water and extracted with chloroform. The solvent was removed under reduced pressure and the separated solid was recrystallized from ethanol to give compound **14** (80%) as white crystals, m.p. 140-142 °C. ^{1}H-NMR(300 MHz, $CDCl_3$): δ_H 7.54 (m, 5H, Ph), 4.93 (s, 1H, NH), 2.80 (q, 2H, CH_2), 1.20 (s, 3H, CH_3), 0.88 (t, 3H, CH_3); ^{13}C-NMR ($CDCl_3$): δ_C 165.5, 152.3, 147.4, 133.7, 132.0, 131.5, 129.5, 128.6, 127.0, 125.1, 16.9, 10.2, 7.3.

Antibacterial and antifungal screening. Some of the synthesized compounds (**5-9, 11-14**) were screened for antibacterial activity against pathogenic organisms; *Bacillus cereus* (BTCC 19), *Salmonella typhi* (AE 14612), *Staphylococcus aureus* (ATCC 6538), *Shigella dysenteriae* (AE 14396) and *Vibrio cholerae* (Table 1) and antifungal activity against C*urvularia lunata*, *Alternaria alternata* (Fr.) Kedissler, *Colletotrichum corchori* Ikata (Yoshida), *Fusarium equiseti* (Corda) Sacc and *Macrophomina phaseolina* (Tassi) Goid (Table 2). The disc diffusion method (Bauer *et al*., 1966) and poisoned-food technique (Grover and Moore, 1962) were used for antibacterial and antifungal activities, respectively.

The tested compounds were dissolved in *N*,*N*-dimethyl formamide (DMF) to get a solution of 1 mg/ml. The inhibition zones were measured in mm at the end of an incubation period of 48 h at 28 °C. DMF alone showed no inhibition zone.

Table 1. Antibacterial activity of the synthesized compounds

Comp. No.	Diameter of zone of inhibition in mm (100 µg(dw)/disc)				
	Bacillus cereus	*Salmonella typhi*	*Staphylococcus aureus*	*Shigella dysenteriae*	*Vibrio cholerae*
5	6	7	8	-	-
6	-	6	-	-	6
7	-	6	8	-	-
8	6	8	6	-	-
9	6	-	7	-	-
11	10	7	-	6	-
12	-	10	10	7	6
13	10	8	-	6	10
14	-	10	-	13	12
Ampicillin 25µg(dw)/disc	21	24	13	30	17

Table2. Antifungal activity of the synthesized compounds

Comp. No.	Percentage inhibition of mycelial growth (100 µg(dw)/ml PDA)				
	Curvularia lunata	*Alternaria alternata*	*Colletotrichum corchori*	*Fusarium equiseti*	*Macrophomina phaseolina*
5	20.70	31.04	2.00	21.20	-
6	20.70	27.00	20.00	22.11	17.60
7	30.00	6.89	20.40	21.40	-
8	32.00	34.00	26.53	28.00	25.50
9	15.00	12.00	26.60	13.00	33.30
11	31.00	100.00	20.00	26.00	27.77
12	29.00	27.00	28.57	19.50	-
13	23.00	7.00	32.65	36.00	11.11
14	50.00	44.82	36.70	11.00	22.20
Nystatin 25µg(dw)/ ml PDA	75.00	51.55	40.51	44.70	71.78

Nutrient agar (NA) and potato dextrose agar (PDA) were used as basal media, respectively, to test the bacteria and fungi. Commercial antibacterial Ampicillin and antifungal Nystatin were also tested under similar conditions for comparison.

Results and Discussion

The starting material, ethyl 2-amino-4,5-diphenylfuran-3-carboxylate (**1**) was prepared from benzoin and ethyl cyanoacetate according to the procedure of Gewald *et al*. (1966). Refluxing of *o*-aminoester **1** with formamide afforded 5,6-diphenylfuro [2,3-d]pyrimidin-4(*3H*)-one (**2**) (Scheme-1). The structural assignment of compound **2** was confirmed by spectroscopic analysis. Its ^{1}H-NMR spectrum exhibited signal a one-proton singlet at δ 7.84 for CH proton at 2-position. Other peaks were in accordance with the structure. Chlorination of compound **2** with thionyl chloride gave 4-chloro-5,6-diphenylfuro [2,3-d] pyrimidine (**3**).

The chlorine group of **3** underwent nucleophilic displacement by reflux with hydrazine hydrate in dioxane to produce 4-hydrazino-5,6-diphenylfuro[2,3-d]pyrimidine (**4**). Upon boiling with formic acid, hydrazino compound **4** cyclized to produce 8,9-diphenylfuro[3,2-e][1,2,4]triazolo[4,3-c] pyrimidine (**5**). Its ^{1}H-NMR spectrum exhibited signals a one-proton singlet at δ 9.92 for CH proton at 5-position and another one-proton singlet at δ 8.37 for CH proton at 3-position.

The hydrazino compound **4** was condensed with aromatic aldehydes, benzaldehyde, 4-hydroxybenzaldehyde, 4-chlorobenzaldehyde and 2-chlorobenzaldehyde to give 4-(benzylidenehydrazono)-5,6-diphenylfuro[2,3-d]pyrimidine (**6**), 4-(4-hydroxybenzylidenehydrazono)-5,6-diphenylfuro[2,3-d] pyrimidine (**7**), 4-(4-chlorobenzylidenehydrazono)-5, 6-diphenylfuro[2,3-d]pyrimidine (**8**) and 4-(2-chlorobenzylidene-hydrazono)-5,6-diphenylfuro[2,3-d]pyrimidine (**9**), respectively. Assignments of the structures **6-9** to the proposed reaction products are based on spectral data.

o-Aminonitrile **10** was readily cyclized to the corresponding 5-ethyl-6-methylthieno[2,3-d]pyrimidin-2,4(*1H,3H*)-dithione (**11**) upon treatment with carbon disulphide in refluxing pyridine (Scheme-2). Methylation of dithione **11** with methyl iodide in aqueous NaOH afforded compound 2,4-dimethylthio-

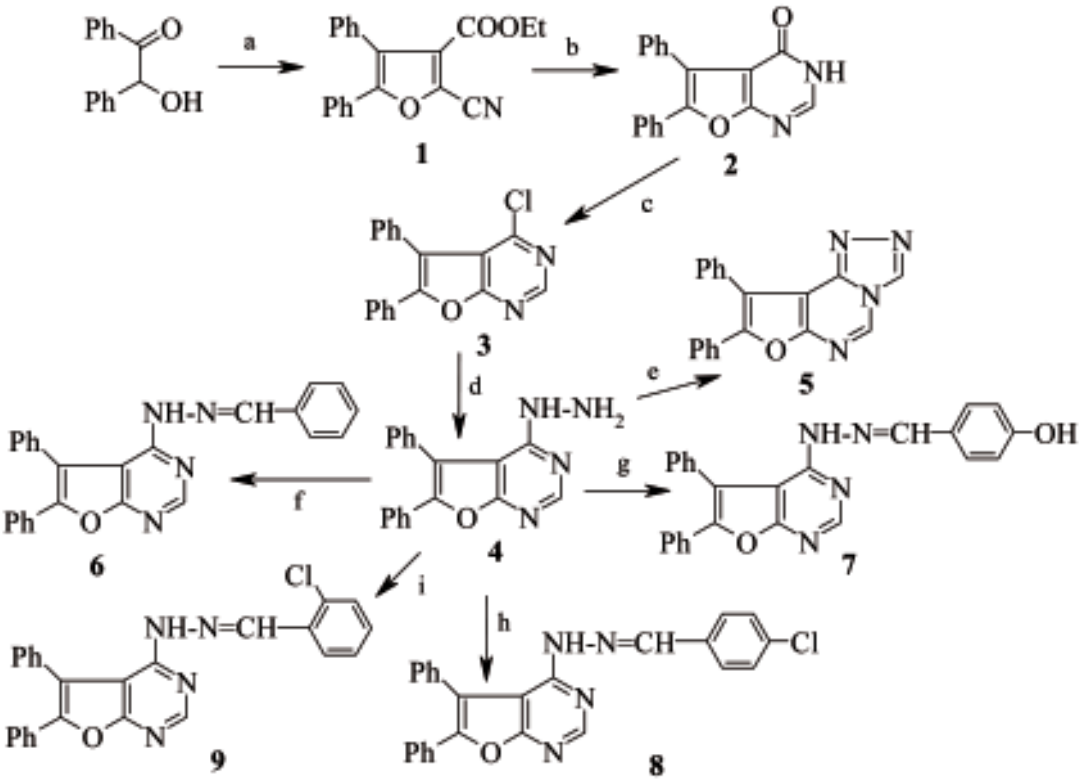

Scheme-1

Reagents: a) $NCCH_2COOEt$, Et_2NH, DMF; b) $HCONH_2$, reflux; c) $SOCl_2$; d) $NH_2NH_2.H_2O$; e) HCOOH; f) benzaldehyde, EtOH, reflux; g) 4-hydroxybenzaldehyde, EtOH, reflux; h) 4-chlorobenzaldehyde, EtOH, reflux; i) 2-chlorobenzaldehyde, EtOH, reflux.

5-ethyl-6-methylthieno[2,3-d]pyrimidine (**12**). Treatment of compound **12** with hydrazine hydrate furnished 4-hydrazino-2-methylthio-5-ethyl-6-methylthieno[2,3-d]pyrimidine (**13**) in good yield. Acylation of **11** with benzoyl chloride afforded 3-benzoyl-5-ethyl-6-methylthieno[2,3-d]pyrimidin-2,4(1*H*,3*H*)-dithione (**14**). The structures of **11-14** were established from their spectral data.

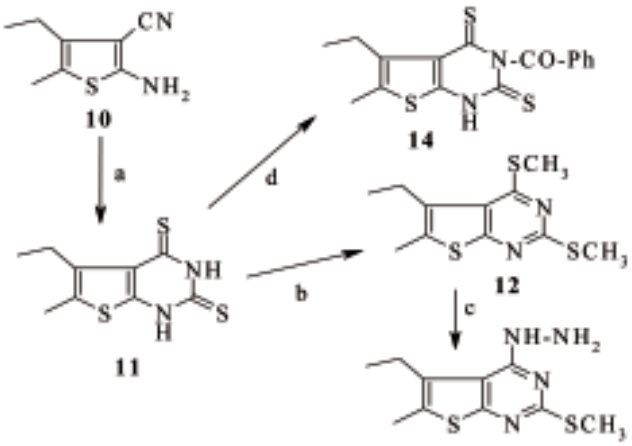

Scheme-2

Reagents: (a) CS_2, pyridine; (b) CH_3I, aq. NaOH; (c) $NH_2NH_2.H_2O$; (d) benzoyl chloride.

Most of the synthesized compounds showed moderate antibacterial activity whereas some did not show inhibition (Table 1). Most of the tested compounds exhibited good to excellent results against all the fungi (Table 2).

Acknowledgements

Authors wish to thank Dr. M. Shafiqur Rahman, Department of Microbiology, University of Chittagong, Bangladesh for his cooperation in determining the antimicrobial activity of the synthesized compounds. Authors also highly acknowledge the Research Cell, University of Chittagong, for the financial support to carry out this project work.

References

Agarwal, A., Srivastava, K., Puri, S.K., Chauhan, P.M.S. 2005. Antimalarial activity and synthesis of new trisubstituted pyrimidines. *Bioorganic and Medicinal Chemistry Letters* **15:** 3130-3132.

Bauer, A.W., Kirby, W.M.M., Sherris, J.C., Turck, M. 1966. Antibiotic susceptibility testing by a standerdized single disc method. *American Journal of Clinical Pathalogy* **45:** 493-496.

Bekhit, A.A., Fahmy, H.T.Y., Rostam, S.A.F., Baraka, A.M. 2003. Design and synthesis of some substituted-1H-pyrazolyl-thiazolo[4,5-d]pyrimidines as anti-inflammatory-antimicrobial agents. *European Journal of Medicinal Chemistry* **38:** 27-36.

Bhuiyan, M.M.H., Rahman, K.M.M., Hossain, M.K., Rahim, M.A., Hossain, M.I., Naser, M.A. 2006. Synthesis and antimicrobial evaluation of some new thienopyrimidine derivatives. *Acta Pharmaceutica* **56:** 441-450.

Bhuiyan, M.M.H., Rahman, K.M.M., Hossain, M.K., Rahim, M.A. Hossain, M.I. 2005a. Fused pyrimidines. Part II: Synthesis and antimicrobial activity of some furo[3,2-e]imidazo[1,2-c]pyrimidines and furo[2,3-d]pyrimidines. *Croatica Chemica Acta* **78:** 633-636.

Bhuiyan, M.M.H., Rahman, K.M.M., Hossain, M.I., Naser, M.A., Shumi, W. 2005b. Fused Pyrimidines. Part III: Synthesis and antimicrobial activity of some furopyrimidines and imidazopyrazolopyrimidine. *Journal of Applied Sciences Research* **1:** 218-222.

Bhuiyan, M. M. H., Rahman, K. M. M., Hossain, M. K., Rahim, M. A. 2005c. Synthesis and antimicrobial activity of some heterocycles: Part V. *Pakistan Journal of Scientific and Industrial Research* **48:** 318-321.

Bhuiyan, M.M.H., Rahman, K.M.M., Hossain, M.K., Fakhruddin, M. 2004. Fused pyrimidines. Part I: Synthesis of imidazo[1,2-a]thieno[2,3-d]pyrimidin-5(1*H*)-imine and pyrimido[1,2-a]thieno[2,3-d]pyrimidin-6(1*H*)-imine. *Pakistan Journal of Scientific and Industrial Research* **47:** 256-258.

Ferri, P.F., Ubeda, A., Guillen, I., Lasri, J., Rosende, M.E.G., Akssira, M. Arques, J.S. 2003. Synthesis and evaluation of 2-tosylamino and 2-tosyliminopyrimidine derivatives as inhibitors of some leukocyte functions. *European Journal of Medicinal Chemistry* **38:** 289-296.

Gewald, K., Schinke, E., Bottcher, H. 1966. 2-Amino-thiophene aus methylenaktiven Nitrilen, Carbonyl verbindungen und schwefel. *Chemische Berichte* **99:** 94-100.

Grover, R.K., Moore, J.D. 1962. Toximetric studies of fungicides against the brown rot organisms, *Sclerotinia fructicola* and *S. laxa*. *Phytopathology* **52:** 876-880.

Haggarty, S.J., Mayer, T.U., Miyamoto, D.T., Fathi, R., King, R.W., Mitichison, T.J., Schreiber, S.L. 2000. Dissecting cellular processes using small molecules: identification of colchicine-like, taxol-like and other small molecules that perturb mitosis. *Chemistry and Biology* **7:** 275-286.

Ismail, M.M., Al-Sayed, N.A., Rateb, H.S., Ellithey, M., Ammar, Y.A. 2006. Synthesis and evaluation of some 1,2,3,4-tetrahydropyrimidine-2-thione and condensed pyrimidine derivatives as potential antihypertensive agents.

Arzneimittel-Forschung **56:** 322-327.

Kumar, R., Nath, M., Tyrrell, D.J. 2002. Design and synthesis of novel 5-substituted acyclicpyrimidine nucleosides as potent and selective inhibitors of hepatitis B virus. *Journal of Medicinal Chemistry* **45:** 2032-2040.

Nalbandyan, G.K., Mkrtchyan, A.P., Noravyan, A.S., Dzhagatspanyan, I.A., Melikyan, G.G., Sukasyan, R.S. 1999. Condensed furopyrimidine derivatives. Part III: Synthesis and psychotropic activity of pyrano [4',3':4,5] furo[3,2-a]-1,2,4-triazolo-(tetrazolo)[4,3-a]pyrimidines. *Pharmceutical Chemistry Journal* **33:** 74-77.

Patil, V.M., Sangapure, S.S., Agasimuddin, Y.S. 1984. Studies in benzofurans: Part XV-Curtius rearrangement and other reactions of ethyl3-carbethoxyamino-2-carboxylate. *Indian Journal of Chemistry* **23B:** 132-135.

Sauter, F., Frohlich, J., Chowdhury, A.Z.M.S. 1996. Reagents for new heteroannelation reactions. Part I: Isocyanatedithioketal reagents. *Science Pharm*acy **64:** 647-653.

Sondhi, S.M., Singh, N., Johar, M., Kumar, A. 2005. Synthesis, anti-inflammatory and analgesic activities evaluation of some mono, bi and tricyclic pyrimidine derivatives. *Bioorganic Medicinal Chem*istry **13:** 6158-6166.

Pak. J. Sci. Ind. Res. 2009 **52** (4) 186-190

In vitro Analysis and Data Comparison of Market Brands of Ciprofloxacin, Ofloxacin and Levofloxacin

Muhammad Zaheer*, Salma Rahman, Shahid Mahmood and Muhammad Saleem
Applied Chemistry Research Centre, PCSIR Laboratories Complex, Shahrah-e-Jalaluddin Romi, Lahore-54600, Pakistan

(received December 3, 2008; revised June 22, 2009; accepted June 30, 2009)

Abstract. In the evaluation of three different groups of 12 brands of locally manufactured Quinolone tablets available in the market i.e. ciprofloxacin HCl, ofloxacin and levofloxacin hemihydrate, it was found that composition of active ingredients were within the range of pharmacoepial limits but their disintegration time and rate of dissolution were different, some being very close to the lower pharmacoepial limit. One product was substandard having high disintegration time and very low rate of dissolution.

Keywords: flouroquinolone, ciprofloxacin, ofloxacin, levofloxacin

Introduction

The spread of fake and substandard drugs is a major problem in both the developed and the developing countries. The existence of counterfeit and substandard drugs particularly antibiotics and antiparasitic agents (Frankish, 2003; WHO, 1999; Wondemagegnehu, 1999; Shakoor *et al*., 1998; Anon, 1993) have been increasingly reported in the developing countries where drug regulations are ineffective (Newton *et al*., 2001; WHO, 1999). Drugs that treat serious diseases such as malaria, tuberculosis, AIDS or other infections are more often the object of counterfeit (Ahmad 2004; Pincock, 2003). Consistent with the recommendations of the WHO (1999) the World Health Organization launched the International Medical Products Anti-Counterfeiting Taskforce (IMPACT) in February 2006, to stop the production and trading of fake medicines.

In Pakistan, although Drug Regularity Authority and drug laws are in function, the problem exits and the extent of problem is not known due to unavailability of data. Aim of the present study is to evaluate various market brands of antiinfective drugs to provide a data base as a ground for better implementation of drug laws in the country. Fluoroquinolones are synthetic anti-bacterial agents derived from the first pyrridone-beta-carboxylic derivative, nalidixic acid (Bryskier and Lowther, 2002). Fourteen brands of three types of quinolone derivatives are the focus of the present evaluation study.

Materials and Methods

Three types of quinolone derivatives were selected for the study: ciprofloxacin, ofloxacin and levofloxacin. Four brands of each type i.e. total of twelve samples were collected from local market and reference standards of USP grade were used. After identification, the drugs were analyzed for their disintegration time, dissolution rate and assay by spectrophotometer and HPLC.

*Authror for correspondence; E-mail: mzaheevchem@yahoo.com

Identification of active ingredient. E1% solution of the ingredients were prepared in 0.1M HCl and absorbance was measured by UV-Vis spectrophotomer Perkin Elmer Lambda 35. $\ddot{e}_{max}$ for ciprofloxacin was 276 nm and for ofloxacin and levofloxacin, it was 294 nm.

I. Evaluation of Ciprofloxacin

Disintegration time. Test was carried out according to the specifications of British Pharmacoepoeia (2007).

Dissolution test. Test was carried out according to United States Phamacopoeia (2004) with 900 ml of 0.01N HCl in each basket; temperature was adjusted at 37±1°C. The rotation of the paddle was adjusted at 50 rpm and the run time of the apparatus was 30 min.

Sample preparation. Sample was drawn after 30 min, filtered and cooled down to room temperature. 9 ml of this solution was taken in a 100 ml flask and diluted with 0.01N HCl to 25μg/ml concentration.

Standard preparation. For preparation of the working standard, 291 mg ciprofloxacin HCl, equivalent to 250 mg ciprofloxacin, was weighed in 100 ml volumetric flask and dissolved in 0.01N HCI till the volume was up to the mark. 1ml of this solution was further diluted up to 100 ml with 0.01N HCl (25 μg/ml).

Absorbance of the standard and the sample solution was measured at 276 nm taking 0.01N HCl as blank.

Assay by UV: ***Standard preparation.*** For preparation of working standard, ciprofloxacin HCl, 116.4 mg equivalent to 100 mg of ciprofloxacin, was weighed in 100 ml volumetric flask, dissolved in 0.1 N HCl till the volume was upto the mark. 1 ml of this solution was diluted upto 100 ml with the same solvent for preparing a solution of 0.3 mg/ml concentration.

Sample preparation. Twenty (20) tablets were weighed and ground. The powder equivalent to 100 mg of ciprofloxacin was taken in 100 ml volumetric flask and dissolved in 0.1 N HCl. The solution was fltered and diluted. 1 ml of this solution was diluted up to 100 ml with 0.1 N HCl.

The absorbance of the sample and the standard were measured at 276nm taking 0.1N HCl as blank.

Assay by HPLC. The assay was carried out by the method of United States Pharmacopoeia (2004) using high performance liquid chromatography. A Schimadzu LC-9 was used with UV detector set at 278 nm having ODS column (25 cm × 4.6 mm). Temperature was adjusted at 30 ± 1 °C.

The mobile phase was prepared by mixing 0.025 M phosphoric acid of pH 3.0 and acetonitrile (87:13). Flow rate was kept at 1.5 ml/min.

Standard preparation. For preparation of working standard, 349.2 mg of ciprofloxacin HCl, equivalent to 300 mg of ciprofloxacin, was weighed in 100 ml volumetric flask, dissolved in water and the volume was made upto the mark. 10 ml of this solution was diluted to 100 ml with the same solvent to prepare a solution of 0.3 mg/ml.

Sample preparation. Twenty (20) tablets were weighed and ground. The powder equivalent to 5 tablets was taken in 500 ml volumetric flask, about 400 ml water was added and sonicated for 20 min. The volume was made upto the mark with water; 10 ml of this solution was diluted to 100 ml with the same solvent to prepare a solution of 0.25 mg/ml.

Ciprofloxacin contents expressed in mg/tablet were calculated using the following formula:

$$\text{Amount of ciprofloxacin (mg)} = \frac{331.35 \times C \times L \times ru}{367.81 \times D \times rs}$$

where:

331.35 = Molecular weight of ciprofloxacin HCl.
367.81 = Molecular weight of anhydrous ciprofloxacin HCl.
C = Concentration (mg/ml) of USP grade ciprofloxacin HCl RS in the prepared standard.
L = Labelled amount (mg) of ciprofloxacin in each tablet.
D = Concentration (mg/ml) of ciprofloxacin in the prepared sample.
ru = Ciprofloxacin peak response obtained from the prepared sample.
rs = Ciprofloxacin peak response obtained from the prepared standard.

II. Evaluation of Ofloxacin

Disintegration time. Test was carried out according to specifications of British Pharmacoepoeia (2007).

Dissolution test. Test was carried out according to USP (2004) with 1000 ml of 0.1N HCl in each basket; temperature was kept at 37±1°C. Rotation of the paddle was adjusted at 50 rpm; run time of the apparatus was 30 min.

Sample preparation. Sample was drawn after 30 min, filtered and cooled down to room temperature; 10 ml of this solution was taken in 100 ml volumetric flask and diluted with 0.1 N HCl to get a solution of 20 µg/ml concentration.

Standard preparation. For preparing reference standard, ofloxacin equivalent to 200 mg was weighed in 100 ml volumetric flask, dissolved in 0.01 N HCl and the volume was made upto the mark; 1 ml of this solution was diluted with the same solvent to get a solution of 20 µg/ml concentration.

Absorbance of the standard and the sample solution was measured at 294 nm, taking 0.1 N HCl as blank.

Assay by UV. ***Standard preparation.*** For preparing working standard, ofloxacin equivalent to 100.0 mg was weighed in 100 ml volumetric flask, dissolved in 0.1 N HCl and the volume was made up to the mark; 1 ml of this solution was diluted to 100 ml with the same solvent.

Sample preparation. Twenty (20) tablets were weighed and ground. Powder equivalent to 100 mg of ofloxacin was taken in 100 ml volumetric flask, dissolved in 0.1N HCl and the volume was made upto the mark. The solution was filtered and 1 ml of this solution was diluted up to 100 ml with the same solvent.

Absorbance of the sample and the standard was measured at 294 nm taking 0.1 N HCl as blank.

Assay by HPLC. The assay was carried out by the method of USP (2004) using high performance liquid chromatography. A Schimadzu LC-9 was used with UV detector set at 294 nm having ODS column (25 cm × 4.6 mm), temperature was adjusted at 35 ± 1°C.

The mobile phase used was mixture of dodecyl sodium sulphate (0.24% aqueous solution), acetonitrile, and glacial acetic acid (580:400:20) with flow rate of 1.5 ml/min.

Standard preparation. For preparing working standard, ofloxacin, equivalent to 60 mg, was weighed in 100 ml

volumetric flask, dissolved in 0.05 N HCI and the volume was made upto the mark; 10 ml of this solution was diluted to 100 ml with the same solvent so as to prepare a solution of 0.06 mg/ml.

Sample preparation. Twenty (20) tablets were weighed and ground. Powder equivalent to 60 mg of ofloxacin was taken in 100 ml volumetric flask, dissolved in 0.05 N HCI and the volume was made up to 100 ml; 10 ml of this solution was diluted to 100 ml with the same solvent so as to prepare a solution of 0.06 mg/ml.

Percentage amount of ofloxacin expressed in mg/tablet was calculated by the following formula.

Percentage of ofloxacin = (ru/rs) × 100,

where:

ru = Ofloxacin peak response obtained from the sample preparation and
rs = Ofloxacin peak response obtained from the standard preparation.

III. Evaluation of Levofloxacin

Disintegration time. Test was carried out according to the specifications of British Pharmacopoeia (2007) using one tablet.

Dissolution test. Dissolution test was carried out by the same procedure as used for ofloxacin tablets.

Sample preparation. Sample was drawn after 30 min, filtered and cooled down to room temperature; 08 ml of this solution was diluted with 0.1N HCl in a 100 ml flask to get a solution of 20 µg/ml concentration.

Standard preparation. For reference standard, levofloxacin equivalent to 250 mg was weighed in 100 ml volumetric flask, dissolved and the volume was made upto the mark with 0.01 N HCl; 0.8 ml of this solution was further diluted with 0.1 N HCl to get a solution of 20 µg/ml concentration.

Absorbance of the standard and the sample solution were measured at 294 nm taking 0.1 N HCl.

Assay by UV. *Standard preparation.* For preparing working standard, levofloxacin equivalent to 100.0 mg was weighed in a 100 ml volumetric flask, dissolved in 0.1N HCl and the volume was made up to the mark; 1 ml of this solution was diluted to 100 ml with the same solvent.

Sample preparation. Twenty (20) tablets were weighed and ground. Powder equivalent to 100 mg of levofloxacin was taken in 100 ml volumetric flask and dissolved in 0.1 N HCl. The solution was filtered and 1ml of this solution was diluted with 0.1 N HCl upto 100 ml.

Absorbance of the sample and the standard were measured at 294 nm taking 0.1 N HCl as blank.

Assay by HPLC. The assay was carried out by high performance liquid chromatography. A Schimadzu LC-9 was used with UV detector set at 294 nm having ODS Column (25cm × 4.6 mm) and temperature was adjusted at 35 ± 1°C.

The mobile phase used was mixture of dodecyl sodium sulphate (0.24% aqueous solution), acetonitrile, and glacial acetic acid (580:400:20) with flow rate of 1.5 ml/min.

Standard preparation. For preparing the working standard, levofloxacin equivalent to 60 mg was weighed in 100 ml volumetric flask, dissolved in 0.05 N hydrochloric acid and the volume was made upto the mark; 10 ml of this solution was diluted to 100 ml with the same solvent to prepare a solution of 0.06 mg/ml.

Sample preparation. Twenty (20) tablets were weighed and ground. Powder equivalent to 60 mg levofloxacin was taken in 100 ml volumetric flask, dissolved in 0.05 N HCl and the volume was made upto the mark; 10 ml of this solution was diluted to 100 ml with the same solvent to prepare a solution of 0.06 mg/ml.

For expressing the percentage amount of levofloxacin in mg/tablet, formula is the same as used for ofloxacin.

Results and Discussion

For evaluation of four brands of ciprofloxacin, ofloxacin and levofloxacin each, only tablet form of the drugs was selected. Physical and chemical analysis and *in vitro* bioavailability through dissolution were carried out; results are reported in Tables 1-3.

Table 1. Analysis of ciprofloxacin tablets

Formulations	Assay by UV-Vis spectrophotometer (%)	Assay by HPLC (%)	Dissolution assay (%)	Disintegration time (min)
C1	100.62	98.59	88.38	9-10
C2	102.01	103.15	85.316	5-6
C3	96.74	97.15	99.31	2-3
C4	103.10	101.80	95.89	3-4

Table 2. Analysis of ofloxacin tablets

Formulations	Assay by UV-Vis spectro-photometer (%)	Assay by HPLC (%)	Dissolution assay (%)	Disintegration time (min)
O1	97.29	97.68	96.80	0 - 1
O2	96.30	95.84	93.93	10 - 11
O3	96.59	95.76	81.91	2 - 4
O4	98.90	98.12	89.75	11 - 12

Table 3. Analysis of levofloxacin tablets

Formulations	Assay by UV-Vis spectro-photometer (%)	Assay by HPLC (%)	Dissolution assay (%)	Disintegration time (min)
L1	102.71	102.23	102.71	2-3
L2	98.61	100.14	97.51	9-10
L3	97.30	96. 87	24.18	34-35
L4	99.92	99.50	100.11	5-6

Physical tests of all the samples show the physical stability of compounds in different formulations. UV absorption of the sample and the reference standard of ciprofloxacin showed absorption $ë_{max}$ at 276 nm and that of ofloxacin and levofloxacin showed $ë_{max}$ at 294. It was found that the active compounds in all the samples were chemically stable and there were no significant impurities present in the tablets.

Quantitative estimation of the active ingredients was also confirmed by HPLC according to the standard procedure of United State Pharmacopoeia (2004). Percentage composition of all the compounds was determined by using reference standards (USP grade) of the same concentration. Retention time of the sample and the reference standard of ciprofloxacin was 7.230 (Fig. 1), of ofloxacin was 9.880 (Fig. 2) and of levofloxacin was 10.570 (Fig. 3). Variations and differences of the active ingredients in all the formulations were within the US pharmacopoeial limit i.e. (90- 110%).

For evaluating the efficacy of the tablets, apart from the amount of drug per tablet, capacity of the tablet to release the drug is to be determined. For this purpose the bioavailability of the tablets was ascertained *in vitro*. A generally accepted maxim for a drug to be readily available to the body is that it must be in the form of solution. For tablets, the first important step towards dissolution is breakdown of the tablet into smaller particles or granules. This disintegration takes place naturally in the stomach.

The disintegration time of all the tablets was determined (Tables 1-3). The standard time for disintegration by the film coated tablet is not more than 30 min (British Pharmacopoeia, 2007).

The disintegration time of ciprofloxacin sample tablets (Table 1) ranged from 2-10 min which complies with the standard values. The disintegration time of ofloxacin tablets (Table 2) ranged from 1-12 min which also complies with the standard values. However, the disintegration time of levofloxacin sample tablets (Table 3) ranged from 2- 35 min which does not follow the standard values. Although the maximum disintegration time is a little above the maximum standard limit of 30 min for film coated tablets, but disintegration time of 35 min is not desirable in life saving medicines.

The disintegration time, however, simply identifies the time required for the tablet to break up under the condition of test and for all particles to pass through a 10-mesh screen. The test offers no assurance that the resultant particles will

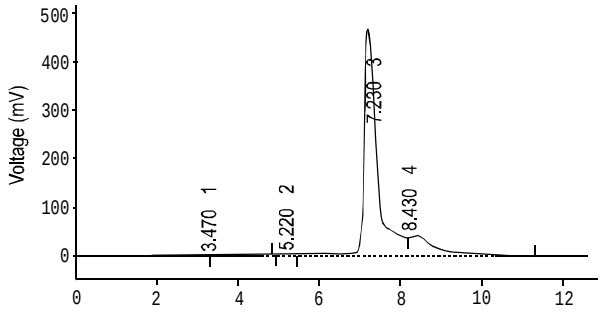

Fig. 1. The HPLC chromatogram of ciprofloxacin.

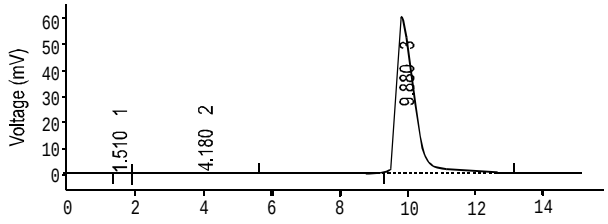

Fig. 2. The HPLC chromatogram of ofloxacin.

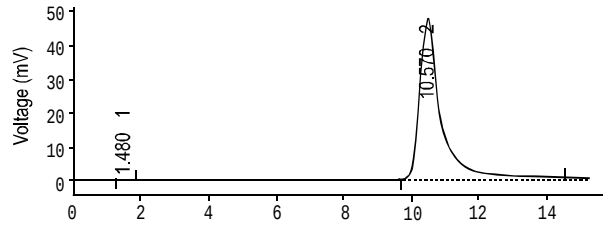

Fig. 3. The HPLC chromatogram of levofloxacin.

release the active ingredient in solution at an appropriate rate. For this purpose the test for the dissolution rate was performed.

The dissolution rate is critically important for the tablets. The standard values for these tablets are not less than 80% (United State Pharamacopoeia, 2004).

The results (Table 1) show that the dissolution rate for the ciprofloxacin tablets ranged from 85-99%, which complies with the standard value. The dissolution rate for ofloxacin tablets (Table 2) ranged from 81-87%. Dissolution rate of 81% though close to the standard values is not a desirable one. Dissolution rate of levofloxacin tablets (Table 3) ranged from 24-102%, which does not comply with the standard value and indicates the substandard criteria of the product. Dissolution rate of 24% is quite below the minimum standard limit. It was observed that the disintegration time also correlated with the dissolution rate.

Thus it may be concluded that the active ingredients in all the tablets were present in appropriate quantities. Products were chemically stable according to their shelf life but the bioavailability of these tablets was considerably different which need to be improved through making improvements in the formulations.

References

Ahmad, K. 2004. Antidepressants are sold as antiretrovirals in DR Congo. *Lancet* **363:** 713.

Anon, 1993. Counterfeit drugs. *Bulletin of World Health Organization* **71:** 464-470.

British Pharmacopoeia, 2007. *British Pharmacopoeia*, The Stationery Office, UK.

Bryskier, A., Lowther, J. 2002. Fluoroquinolones and tuberculosis. *Expert Opinion on Investigational Drugs* **11:** 233.

Frankish, H. 2003. WHO steps up campaign on counterfeit drugs. *Lancet* **362:** 1730.

Newton, P., Proux, S., Green, M., Smithuis, F., Rozendaal, J., Prankongpan, S., Chotivanich, K., Mayxay, M., Looareesuwan, S., Farrar, J., Nosten, F., White, N.J. 2001. Fake artesunate in southeast Asia. *Lancet* **357:** 1948-1950.

Pincock, S. 2003. WHO tries to tackle problem of counterfeit medicines in Asia. *British Medical Journal* **327:** 1126.

Shakoor, O., Taylor, R.B., Behrens, R.H., Verduin-Muttiganzi, G. 1998. Assessment of the incidence of substandard drugs in developing countries. *Tropical Medicine and International Health* **3:** 602.

United States Pharmacopoeia (USP) 2004. *United States Pharmacopoeia (USP 27). The National Formulary (NF 22)*, 27th edition. USP, Washington DC, USA.

WHO 1999. *Counterfeit Drugs: Guidelines for the Development of Measures to Combat Counterfeit Drugs*, 60 pp. Department of Essential Drugs and Other Medicines, World Health Organization, Geneva, Switzerland.

Wondemagegnehu, E. 1999. *Counterfeit and Substandard Drugs in Myanmar and Vietnam*, 55 pp. Report of a study carried out in cooperation with the Government of Myanmar and Vietnam - EDM Research Series No.29. WHO Department of Essential Drugs and Other Medicines, Geneva, Switzerland.

Biological Sciences

Pak. J. Sci. Ind. Res. 2009 **52** (4) 191-199

Purification and Characterization of Bacteriocin Like Substance Produced from *Bacillus lentus* with Perspective of a New Biopreservative for Food Preservation

Nivedita Sharma*, Ambika Attri and Neha Gautam

Department of Basic Sciences, Microbiology Research Laboratory, Dr. Y.S. Parmar Univerisy of Horticulture and Forestry, Nauni-Solan (H.P.) 173 230, India

(received January 24, 2009; revised June 8, 2009; accepted June 16, 2009)

Abstract. Molecular weight of bacteriocin like substance (BLIS) of a new strain of *Bacillus lentus* 121 was found to be approximately 11 kDa. Purification of BLIS was attained by single step gel exclusion chromatography. BLIS was characterized by studying the inhibitory spectrum. It was active at broad pH range, high temperature and high NaCl concentration and showed sensitivity to proteolytic enzymes like trypsin, α-chymotrypsin and papain, the characters desirable for food preservation. BLIS extended the shelf stability of milk upto 21 days as a biopreservative.

Keywords: bacteriocin like inhibitory substance, BLIS, *B. lentus,* antimicrobial activity, biopreservative

Introduction

Food products get easily contaminated with spoilage/ pathogenic bacteria, which not only causes public health problems but is also associated with great economical losses (Sharma and Kapoor, 2004). Several processes have been developed to enhance the safety and shelf life of perishable foods with chemical preservatives. However, experiencing the adverse side effects of chemical preservatives on human health, efforts are currently underway on the search for safe products of natural origin; ultimately, biopreservation has emerged as an attractive approach for food preservation.

Biopreservatives are biologically derived antimicrobial substances which arrest/retard growth of spoilage-causing microorganisms thus contributing preservative potential to foods (Marekova *et al.,* 2007). Among biopreservatives, bacteriocins are catching rapid attention and believed to be safe for human consumption since these become inactive when treated with protease. These are mostly heat stable and wider pH tolerant, thus can withstand heat,acidity/alkalinity of food during storage conditions. In recent years, several new bacteriocins have been obtained from different species of *Bacillus* and purified (Sharma and Gautam, 2008). Important bacteriocins, purified so far, are nisin, diplococcin, acidophilin, bulgaricin, helviticin, enterocin, lacticin and plantaricin (Xiaomei *et al.,* 2006; Ogunbanwo *et al.,* 2003).Out of all bacteriocins, only nisin has got the GRAS (Generally Recognized as Safe) status and is used commercially to preserve various dairy products (Jeevaratham, *et al.,* 2005) while others are still in the process for commercialization. Nisin, though very effective, has limitations in its use due to narrow pH specificity. Thus, consistent efforts are being made for isolating bacteria capable of producing novel bacteriocin-like-substances (BLIS) for food preservation at wider scale. *Bacillus lentus* isolated from fermented dough was reported for the first time to produce BLIS having characteristics desirable for food preservation (Sharma *et al*., 2006). The BLIS of *B.lentus* has been found to withstand heat and acidity/alkalinity of foods during storage conditions, to be stable for longer period and to express inhibition against a broad range of selected food pathogens. Thus, keeping in mind these attributes, an effort has been made to purify and characterize it with the aim of using it as a high profile food biopreservative.

Materials and Methods

Isolate used. *Bacillus lentus,* BLIS producer, showing very high activity units was isolated from dough, a traditional food of Himalayan states of India (Sharma *et al*., 2006), and used in the study.

Test indicators. Test indicators, used for analyzing the pattern of antimicrobial activity, were: *Escherichia coli, Staphylococcus aureus, Salmonella typhimurium, Aeromonas hydrophila, Listeria monocytogens* MTCC 1143, *Leuconostoc mesenteroides* MTCC107, *Enterococcus faecalis* MTCC 2729, *Pseudomonas aeruginosa* and *Lactobacillus* sp.

*Author for correspondence; E-mail: niveditashaarma@yahoo.co.in

Well diffusion method. The antimicrobial activity of BLIS was tested by well diffusion method (Kimura *et al*., 1998) as follows. One ml of inoculum of each indicator bacteria (1.0 OD) was swabbed properly on pre-poured sterilized nutrient agar plates with the help of sterilized cotton bud. Wells of 7 mm diameter and 5mm depth were cut on the lawns of indicators and 300 µl of BLIS was poured into each well. The plates were incubated at 37 °C for 24 h and zones of clearance formed around the wells were measured.

Production of BLIS. The culture of *B. lentus* (1.0 OD_{540}) was added to 1000 ml of nutrient broth @10%. The inoculated flasks were kept at 37 °C at 150 rpm for 72 h.

Partial purification of BLIS. Partial purification of BLIS was carried out through ammonium sulphate precipitation using salt saturation method (Sharma *et al.*, 2006). *B. lentus* culture (1.0 OD_{540}) was saturated with different concentrations of ammonium sulphate i.e. 10, 20, 40, 50, 60, 70, and 80% with subsequent constant stirring. Precipitation occurred at 80% saturation level of ammonium sulphate in culture supernatant of *B. lentus*. This preparation was kept at 4 °C for 24 h. After 24 h, centrifugation was repeated at 20,000 × g at 4 °C for 30 min. This led to separation of pellets and supernatant. The pellets were suspended in 0.1 M PO_4 buffer, pH 7.0 and stored at 4 °C.

Purification of BLIS. ***Column chromatography (Gel exclusion)*.** For carrying out gel exclusion column chromatography, BLIS sample (5 ml) was loaded on Sephadex G-100 column which was packed according to the recommended procedure of Kumar and Vadhera (1980) as follows: Sephadex G-100 (5 g) was weighed and suspended in 500 ml of phosphate buffer for overnight. It was swollen for 5 h in boiling water bath, deaerated next day for 1h and brought to room temperature before packing the column of dimension 75x1.5 cm. Packing was done to avoid entrapment of any air bubbles in the gel bed. Column was then eluted with phosphate buffer (pH 7.0, 0.1M) and 3 ml fractions of the sample were collected in each of a total of 30 tubes. A flow rate of 15 ml/h of the sample was maintained. The fractions were analyzed for protein contents by taking OD at 280 nm.

Protein estimation. Protein concentration of BLIS of *B. lentus* was measured using the Lowry's method (Lowry *et al.*,1951). Following reagents were used for protein estimation:

A. Alkaline sodium carbonate (2 % Na_2CO_3 in 0.1 N NaOH),
B. 1 % copper sulphate,
C. 2 % sodium potassium tartarate,
D. Alkaline copper reagent (prepared afresh by mixing A + B + C in the ratio of 100 : 1 : 1) and
E. 1 N folin-ciocalteu phenol reagent, and prepared afresh.

0.1 ml BLIS sample was added to 0.9 ml of distilled water in the test tubes. 3 ml of reagent D was added and the tubes were allowed to stand at room temperature for 10 min. Then 0.3 ml of 1N folin's reagent was added to each test tube. The test tubes were incubated at 37 °C for 30 min and OD was measured at 670 nm against the reagent blank. The blank reagent contained all the reagents except for the BLIS. The amount of protein samples were worked out from standard curve prepared by using bovine serum albumin (10-100 µg/ml) and the estimated protein was expressed in mg/ml.

Sodium dodecyl sulphate polyacrylamide gel electrophoresis (SDS-PAGE). SDS PAGE was performed following the method of Laemmli (1970). Purification of BLIS was monitored, using 12% acrylamide gel. Standard molecular weight marker (Sigma) was run along with the sample.

Staining of gel. The gel was stained using silver staining method of Merril *et al*. (1981). Gel was kept in fixing solution for overnight, then put in 30% (50 ml) ethanol for 30 min and later kept in Farmers reagent for 5 min. Three washings of 10 min each were given with autoclaved distilled water ; 0.1% $AgNO_3$ solution (100 ml) was added and the gel was kept in dark for 30 min. Three washings were given again with distilled water for 20 sec each. Developing solution (100 ml) was added and gel was gently shaken in gel rocker until brown colour bands appeared in it. The reaction was brought to an end with 1% acetic acid and the gel was stored in plastic bags at refrigerated temperature.

Calculation of activity units (arbitrary units-AU/ml) of BLIS. The activity units of culture supernatant, partially purified and purified BLIS of *B. lentus* were calculated by serial two fold dilution method of Barefoot and Klaenhammer (1983).The culture supernatant, partially purified and purified BLIS were serially diluted and the reciprocal of smallest detectable zone of inhibition was marked for calculation of AU/ml.

Arbitrary units (AU/ml) were calculated as follow:

a) for culture supernatant of BLIS
0.3 µl = 200
1 ml = 6.6 x 10^5 AU/ml

b) for partially purified bacteriocin of BLIS
0.3 µl = 600
1 ml = 20 x 10^5 AU/ml

c) for purified bacteriocin of BLIS
0.3 µl = 1200
1 ml = 4 x 10^6 AU/ml

Characterization of purified BLIS. ***Effect of temperature on activity of BLIS.*** BLIS (0.5 ml) aliquot was added to 4.5 ml of nutrient broth in a test tube. Each test tube was then overlaid with paraffin oil to prevent evaporation and then kept for 10 min at different temperatures *viz.* 40, 50, 60, 70, 80, 90, and 100 °C on a water bath and moist heat treatment at 121°C was given in autoclave for the same time. Activity of heat treated BLIS was analyzed by the following methods.

1) Well diffusion method: as described earlier.

2) Optical density (OD) method: BLIS, treated at various temperatures for 10 min, was mixed with 0.5 ml indicator strains (*L. monocytogenes*, *S. aureus* and *A. hydrophila*) and incubated at 37 °C for 24 h. Their OD was measured at 540 nm. Minimum OD exhibited maximum inhibition of the sensitive strain by that particular fraction of heat treated BLIS.

Effect of pH on activity of BLIS. BLIS (0.5 ml) was added to 4.5 ml of nutrient broth, at pH, 3.0, 4.0, 5.0, 6.0, 7.0, 8.0, 9.0, 10.0 and 11.0. The test tubes were incubated for 30 min at 37 °C. Each pH treated BLIS was assayed by well diffusion and optical density methods as already mentioned.

Effect of salt (NaCl) concentration on activity of BLIS. To check the effect of salt concentration on activity of BLIS, different salt concentration viz., 0.1, 0.5, 1.5, 2.5, 3.5, 4.5, 5.5% were prepared in distilled water (100 ml). BLIS (0.5 ml) was added to 0.5 ml of each NaCl concentration; controls were run in parallel. Effect of various salt concentrations on BLIS activity was assayed using well diffusion assay and optical density methods.

Effect of stability on activity of BLIS. The potency of purified BLIS was checked at regular intervals *viz*. 0.5, 1.0, 1.5, 2.0, 3.0, 4.5, 5.0 and 5.5 months. Purified BLIS was stored in a clean sterilized glass bottle in frozen state. BLIS activity was recorded against three indicator strains *viz. L. mono-cytogenes*, *S. aureus* and *A. hydrophila* by well diffusion method, noting the size of individual zones.

Effect of proteolytic enzymes on activity of BLIS. Proteolytic enzymes namely trypsin, α-chymotrypsin, and papain were selected for the study. Lawns of *L. monocytogenes*, *S. aureus* and *A. hydrophila* were prepared.

EC_1 i.e. Enzyme control I as 0.3 ml phosphate buffer, EC_2 i.e. Enzyme control II as 0.15 ml bacteriocin of each isolate + 0.15 ml of phosphate buffer and ER i.e. enzyme reaction as 0.25 mg of enzyme trypsin/α chymotrypsin or papain were dissolved separately in 1ml each of 0.1 M phosphate buffer and then added to BLIS in the ratio of 1:1.

The preparations EC_1, EC_2 and ER were incubated for 1 h at 37 °C. Enzyme reaction and both enzyme control were assayed by well diffusion method against corresponding indicators.

Application as biopreservative for milk. Fresh cows milk procured locally was taken in sterilized glass flask and boiled at 100 °C for 2 min, followed by cooling at room temperature. Milk sample, 10 ml each, were put in three clean and sterilized bottles. Mixed inoculum of *L. monocytogens* and *S. aureus* in the ratio of 1:1 (8.80 log cfu/ml, 1OD) was used for inoculating the sample.

To one set of milk, BLIS was added @ 2000 ppm (Lucke,2000) while the standard chemical preservative, benzoic acid, was added to another set of milk at the same concentration for comparative study. The third set of milk was kept as control without any addition. These tubes, after proper plugging and sealing with hot wax, were kept in refrigerator (4 °C). Colony count was made by pour plate method and log cfu/ml was calculated on day 0, 7, 14, 21 and 28 for mixed inoculum. Morphological changes were also observed simultaneously. Experiments were conducted in triplicate and results were analyzed statistically; factorial CRD was used for comparative study of the biopreservative with the chemical preservative, against indicators, to enhance storage of milk.

Results and Discussion

BLIS of *B. lentus* showed a broad range antagonistic spectrum against *L. monocytogens*, *S. aureus*, *A. hydrophila*, *Lactobacillus* sp., *P. aeroginosa* and *E. coli*. BLIS was found to be effective against gm +ve as well as gram -ve bacteria whereas generally other BLIS were found active against only closely related gram +ve strains (Chen and Williams, 2003; Osmangaoglu *et al.*, 2001). However, there are a few reports of bacteriocin of LAB isolated from different food sources capable of inhibiting the growth of both gram +ve and gram -ve bacteria (Sharma and Gautam, 2008; Ivanova *et al.*, 2000). BLIS secreted by *B. lentus* were partially purified by salt saturation method. Final purification of BLIS was attained by column chromatography. Single gel exclusion chromatography step was used subsequently after ammonium sulphate precipitation. So far, this is the first time that any BLIS has been purified through only one chromatographic step. Other BLIS have been purified in 2 or 3 steps. Protein activity was observed in fractions 12-20 at 280 nm (Fig.1a), which was found to be 0.45, 0.62, 0.70, 0.91, 1.20, 0.92, 0.81, 0.65 and 0.32 OD, respectively. Fraction 16 showed the highest activity of OD 1.20, confirmed by well diffusion method as well. Fractions 2-20 were pooled for further studies. Inhibitory activity of pooled fractions were observed against the three tested strains i.e. *L. monocyto-genes*,

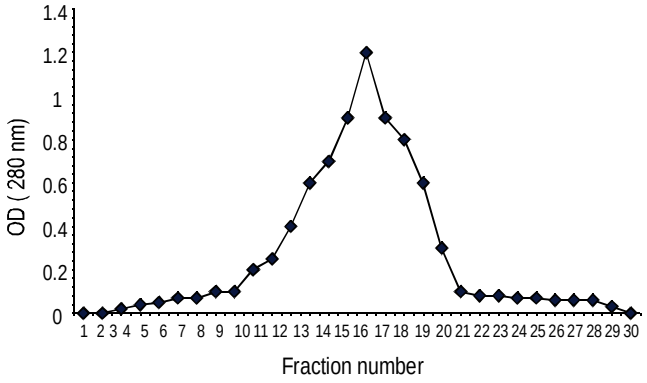

Fig. 1(a). Protein activity of BLIS fractions in terms of OD at 280 nm.

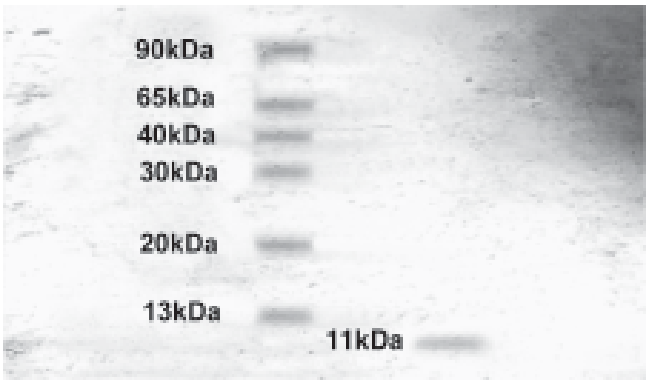

Fig. 1(b). SDS-polyacrylamide gel electrophoresis of purified BLIS of *B. lentus.*

S. aureus and *A. hydrophila,* and zones of 36 mm, 32 mm and 30 mm, respectively, were measured. The purity of bioactive fraction was checked by SDS PAGE and the molecular weight of BLIS was found to be approximately 11 kDa (Fig 1b).

BLIS exhibited very high activity ($4x10^6$ AU/ml) which reflected its strong potential against the tested spoilage-causing and food-borne pathogens thus proving its efficacy as preservative for enhancing the shelf life of food items. There was a consistent increase in activity of BLIS at each step of purification ranging from $6.6 x10^5$ AU/ml for culture supernatant, $20 x 10^5$ AU/ml for partially purified BLIS to $4x10^6$ AU/ml for purified BLIS (Table 1). The purified preservative showed 50 fold activity as compared to the crude BLIS. After purification, a spectacular increase in inhibition zone size was noticed as compared to the zone size of partially purified BLIS. There was 50% increase in zone size of purified BLIS against *L. monocytogenes,* and *A. hydrophila* over partially purified BLIS while 45.5% increase against *S. aureus* was observed.

Further characterization was done on the basis of temperature and pH in terms of inhibition zone and OD. BLIS was found active at 121°C against *L. monocytogenes* and *S. aureus* while it lost activity against *A. hydrophila* at 121°C. It showed high thermostability w.e.f. 40 to 100 °C for all the three indicators tested though inhibition zone size decreased with the increase in temperature (Fig. 2). It is clear from Fig 3 that optical density was low at 40 °C and 50 °C for the three test strains and as the temperature increased, there was an increase in OD indicating lesser activity of the preservative. Similar studies have been reported about bacteriocin of *L. brevis, L. plantarum* and *L. lactis* to be heat stable at high temperature *viz.*, 121°C (Ogunbanwo *et al*., 2003) while others lost their activity even at 50 °C (Gharairi *et al.*, 2005; Vanghan *et al*., 1992).

For studying the effect of pH, purified BLIS was exposed to pH ranging from 2 to 11. Well diffusion assay was used with test indicators revealing maximum inhibition zone of 36, 32 and 30 mm against *L. monocytogens, S. aureus* and *A. hydrophila,* respectively, at pH 7.0 thus showing its highest activity at neutral pH. BLIS was also found active on shift of pH towards acidic (pH 3.0) as well alkaline side (pH 10/11) though partial loss in its activity was indicated by decreasing zone sizes against the specific test strains (Fig. 4). OD_{540} for

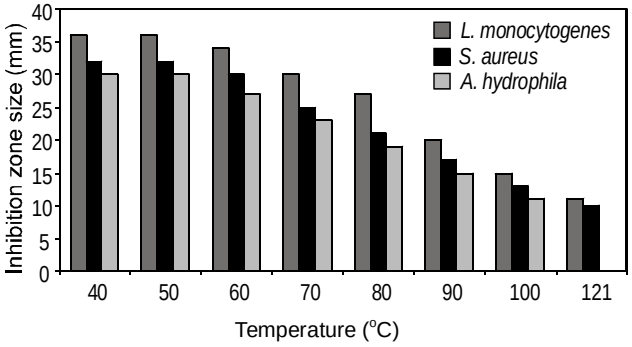

Fig. 2. Effect of temperature on activity of purified BLIS (in terms of inhibition zone).

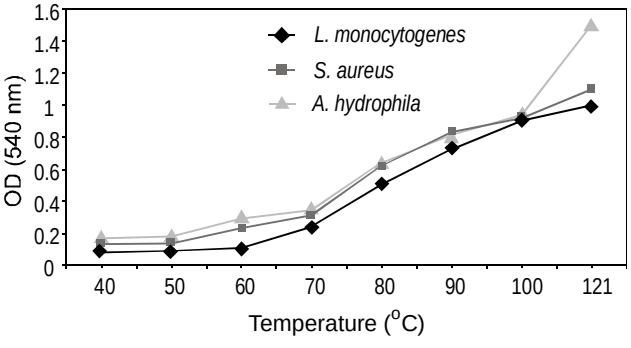

Fig. 3. Effect of temperature on activity of purified BLIS (in terms of OD at 540 nm).

Table 1. Profile of culture supernatant, partially and wholly purified BLIS produced by *B. lentus.*

Purification status	Volume (ml)	Activity unit (AU/ml)	Total activity	Protein (mg/ml)	Specific activity (AU/mg)	Purification fold	Recovery (%)
Culture supernatant	500	6.6×10^5	3.3×10^8	13.2	5×10^4	1	100
Partially purified BLIS (ammonium sulphate ppt.)	20	20×10^5	4.0×10^7	8.9	2.3×10^5	4.5	67
Purified BLIS	10	4.0×10^6	4.0×10^7	1.6	2.5×10^6	50	12

Total activity = volume x activity; protein concentration was determined by Lowry's method; specific activity = the activity unit/protein concentration; purification fold is increased in specific activity; recovery (%) = concentration of the remaining protein as % of the initial concentration of protein.

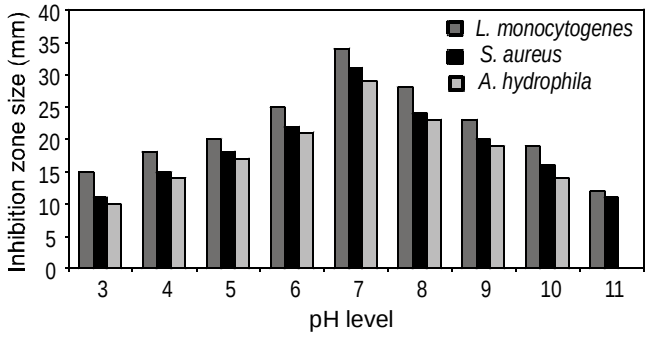

Fig. 4. Effect of pH on activity of purified BLIS (in terms of inhibition zones).

L. monocytogens, *S. aureus* and *A. hydrophila* was the lowest at neutral pH indicating highest activity of BLIS. pH range of 3.0-4.0 and 10.0-11.0 showed maximum OD expressing minimum activity of BLIS (Fig 5). In this respect, BLIS has an edge over nisin for food preservation since it can remain stable in all acidic, alkaline or neutral types of foods (Periago and Moezelaar, 2001).

The bacteriocin pediocin PA1 when used against *L. monocytogens* was found effective at a pH range of 5.5 to 6.5

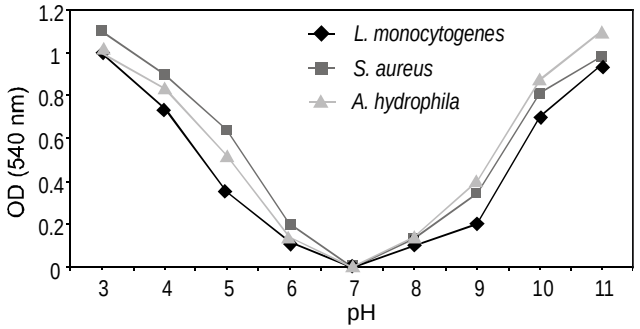

Fig. 5. Effect of pH on activity of purified BLIS (in terms of OD at 540 nm).

(Gravesen *et al.*, 2002). Nisin, the only commercially available bacteriocin, has its use limited to acidic foods only. Bacteriocin of *Bacillus cereus* was reported to be active at pH 3.0 to 12.0 (Naclerio *et al.*, 1993).

Effect of salt (NaCl) concentration *viz* 0.5% to 5.5% on BLIS activity was observed by well diffusion assay (inhibition zone) and OD method against *L. monocytogenes*, *S. aureus* and *A. hydrophila* while controls were run in parallel. BLIS retained its activity till 3.0% concentration of salt but as the concentration increased to 3.5% there was a slight decrease in zone size and increase in OD, which further enhanced with increase in concentration of salt upto 4.5% and 5.5%. The controls run in parallel showed no zone formation against the indicators. The results reveal that a very high salt concentration partially inhibit the BLIS activity (Fig. 6 & 7). Bacteriocin activity in some LAB was enhanced in the presence of low NaCl concentration of 1-2 percent but was lost at a slight higher concentration of 3 percent or more. Bacteriocin of *L. curvatus* LTH 1174 showed decrease in activity at low salt concentration of 2 per cent (Vignolo *et al.*, 1995) while that of *Carnobacterium piscicola* A9b was not affected by 0-10

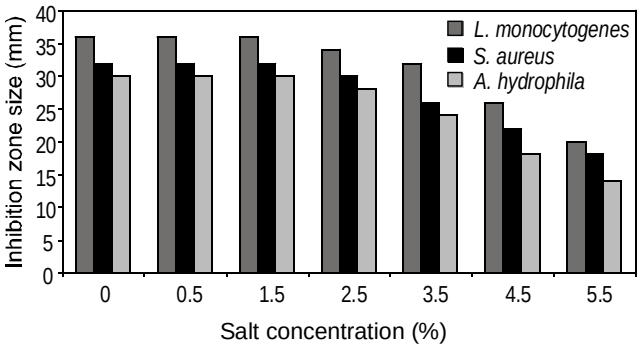

Fig. 6. Effect of salt (NaCl) concentration on activity of purified BLIS (in terms of inhibition zone).

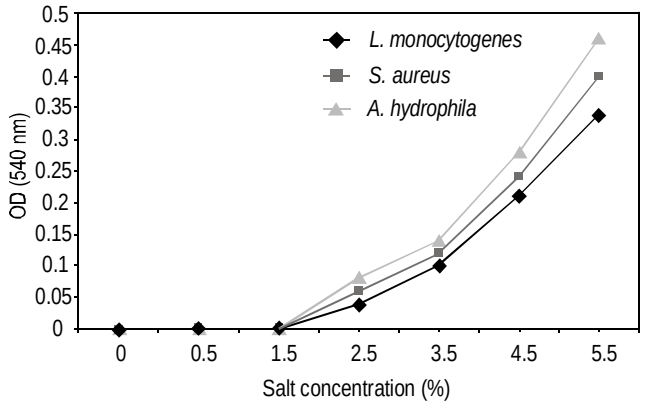

Fig. 7. Effect of salt (NaCl) concentration on activity of purified BLIS (in terms of inhibition zone).

per cent NaCl against *L. monocytogenes.* Himelbloom *et al*. (2001) found that bacteriocion stability remained unaltered for one month at 4 °C at low salt concentration.

When the effect of three proteolytic enzymes *viz*. trypsin, α-chymotrypsin and papain on the activity of purified BLIS of *B. lentus* was studied, no zones were found against *L. monocytogenes*, *S. aureus* and *A. hydrophila*. However, when BLIS was treated with phosphate buffer (EC_2) and then reacted with their respective sensitive indicators, zones of 36 mm, 32 mm were formed against *L. monocytogenes*, *S. aureus* and *A. hydrophila*, respectively. Phosphate buffer in which trypsin, α-chymotrypsin and papain were diluted had nil effect towards activity of BLIS. The inactivation of BLIS with proteolytic enzymes proved that BLIS is proteinaceous in nature. This further adds to the fact that BLIS can be broken down by the proteolytic digestive juices when consumed thus rendering it completely harmless in human system. Ivanova *et al.* (2000) showed that bozacin 14 produced by *Lactococcus lactis* subsp. *lactis* was sensitive to proteinase K, pronase E and pepsin indicating it to be proteinaceous in nature and thus it may be considered as a bacteriocin. Ogunbanwo *et al.* (2003) showed that bacteriocin produced by *Lactobacillus plantarum* F1 lost its activity after treatment with all the proteolytic enzymes. Bacteriocin lactococcin R 9/2, lactococcin R 10/1 were inactivated by only proteinase K and α-chymotrypsin. Lactococcin R 9/2 was inactivated by α-amylase as well (Elotmani *et al*., 2002).

Effect of storage on the activity of purified BLIS. Purified-BLIS showing activity of 4 x 10^6 AU/ml was stored at freezing temperature and periodically checked at interval of 0.5 months, i.e. after 0.5, 1.0, 1.5, 2.0, 3.0, 4.5, 5.0 and 5.5 months. The zone size of 36 mm, 32 mm and 30 mm against *L. monocytogenes, S. aureus* and *A. hydrophila* was maintained, retaining the full potency, till one month after purification. After 1.5 months of storage, there was a slight decrease in zone size being 32 mm for *L. monocytogenes,* 28 mm for *S. aureus* and 26 mm for *A. hydrophila* which was maintained for 2.0 months. There was further decrease in zone size *viz.* 30 mm, 26 mm and 24 mm for the three strains, respectively, at the end of 3.0 months. After 4.5 months of storage of purified BLIS the zones of inhibition showed further decrease being 22 mm, 18 mm and 16 mm for the respective indicators showing partial loss of activity of the bio-preservative. After 5.0 months of storage of BLIS in frozen state, the zone size reduced to 18 mm, 14 mm and 12 mm respectively, and after 5.5 months of storage, to 14 mm, 12 mm and 10 mm, respectively, for *L. monocytogenes, S. aureus* and *A. hydrophila*.

BLIS was fully stable for all the three hosts for a month after its purification while there was a slight decrease in the activity at three months of storage at refrigerated temperature. After 4.5 months of storage there was 61.1%, 56.3% and 53.3% decrease in the activity against the three microbes in the same order, while the loss of stability of BLIS reached to 38.9%,37.5% and 33.3% after 5.5 months of storage. This study proved that BLIS of *B.lentus* could be stored as purified fraction for approximately three months at refrigeration temperature with minimal loss in its activity.

Yildrim and Johnson (1998) observed that bacteriocin lactococcin R produced by *Lactococcus lactis* subsp. *cremoris* remained active at -20 °C and -70 °C for 3 months after storage. A bacteriocin isolated from group B-*Streptococcus* was found extremely stable when stored in its crude form at 4 °C for at least 6 months with no loss of activity while there was loss of activity in purified bacteriocin after 1 week at 4 °C (Tagg *et al*., 1975). A bacteriocin JF426, isolated from *Serratia marcescens* having molecular weight of 6.4 kDa, was stable when stored in frozen condition showing biological activity for at least 3 months (Foulds, 1972).

The storage studies of milk inoculated with mixed inoculum of *L. monocytogens* and *S. aureus* with addition of lenticin, benzoic acid and control showed initial log cfu/ml of 8.80 and initial pH value of 6.8. There was a decrease in log cfu/ml of BLIS samples till the 7th day. The log cfu/ml for benzoic acid and control was 8.40 and 8.90, respectively. On the 14th day, values of log cfu/ml of BLIS, chemical preservative and control were respectively 6.90, 7.50 and 9.00. Mean value was 7.80 while log values changed to 7.40, 8.10 and 10.80 for BLIS benzoic acid and control, respectively, on the 21st day onward. The mean value was 8.77 which increased further on 28 days of preservation being 8.0, 9.8 and 9.92 in the same

order and the final pH was 6.7,5.9 and 5.5. The calculated mean for BLIS was 7.58, for benzoic acid 8.52 and for control, 9.92. CD value was 0.05, T value was 0.07 and D value was 0.09. The T×D value was calculated to be 0.16 (Table 2). Graphical representation of log cfu/ml against days showd that BLIS is a better preservative than benzoic acid for milk inoculated with *L.monocytogenes* and *S.aureus* (Fig 8). The results show higher stability of the sample till day 21 and better activity of BLIS as compared to benzoic acid when used commercially for preservation of milk. Morphological changes were also recorded which showed no curdling, colour change or offensive smell of milk in case of the biopreservative and the chemical preservative containing samples while control showed curdling from the 1st week onwards. Concentration of BLIS was kept below 5000 ppm in milk sample which is the permissible limit for food (Ray, 2001). Xiaomei *et al*. (2006) reported that *Bacillus subtilis fmbJ* was found to produce an antimicrobial substance, which exhibited inhibitory activity against food spoilage microbes and pathogens. The inhibitory effect of antimicrobial extracts against two gram +ve, seven gram -ve and five moulds was identified.

Table 2. Comparative study of activity of BLIS and chemical preservative (sodium benzoate) against mixed inoculum *(L. monocytogenes + S. aureus)* for storage of milk at 4 °C.

Days	Biopreservative (BLIS) (log cfu/ml)	Chemical preservative (sodium benzoate) (log cfu/ml)	Control (no preservative) (log cfu/ml)	Mean
0	8.80	8.80	8.80	8.80
7	6.80	8.40	8.90	8.03
14	6.90	7.50	9.00	7.80
21	7.40	8.10	10.80	8.77
28	8.00	9.80	12.10	9.97
Mean	7.58	8.52	9.92	

$CD_{0.050}$; treatment (T) = 0.07; days (D) = 0.09; T x D = 0.16.

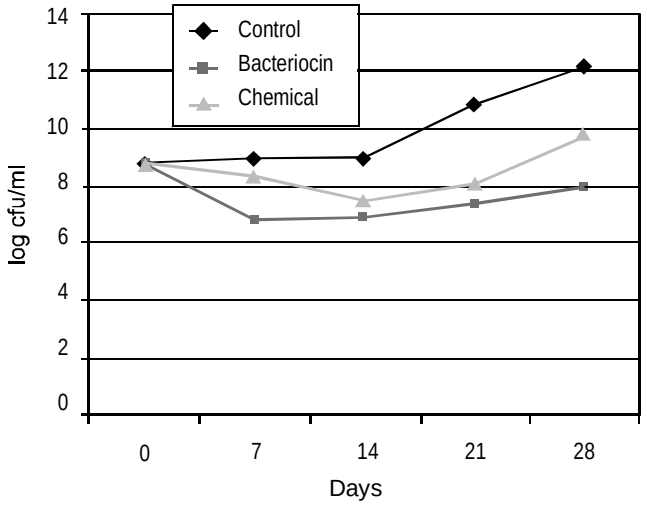

Fig. 8. Comparative study of activity of BLIS and chemical preservative (sodium benzoate) against mixed inoculum (*L. monocytogenes* + *S. aureus*) to enhance storage of milk at 4 °C.

Conclusion

Purified BLIS obtained from *B. lentus*, an isolate of sour dough, a traditional fermented food, had low molecular weight, high thermostability and salt tolerance. It had activity over a broad pH range, long storage life and was proteinaceous in nature. Considering these characteristics, desirable for a food preservation, BLIS of *B.lentus* is recommended for use as a potential biopreservative in different food items. It could enhance the shelf stability of milk upto 21 days and could delay spoilage better than other standard chemical preservatives.

Acknowledgement

Financial assistance provided by DRDO, GoI to carry out this work is highly acknowledged.

References

Barefoot, S.F., Klaenhammer, T.R. 1983. Detection and activity of lactacin B, a bacteriocin produced by *Lactobacillus acidophilus*. *Applied and Environmental Microbiology* **45:** 1808-1815.

Chen, H., Williams, J. 2003. Bacteriocin offer enormous promise in food packaging safety advances. *Research on-line Technical Bulletin* **1**(2).

Elotmani, F., Junelles, A.M.R., Assobai, O., Milliere, J.B. 2002. Characterization of anti *Listeria monocytogenes* bacteriocins from *Enterococcus faecalis*, *Enterococcus faecium* and *Lactococcus lactis* strain isolated from raib–a Moroccan traditional fermented milk. *Current Microbiology* **44:** 10-17.

Fitzgerald, G.F. Vaughan, E.V., Daly, C., 1992. Identification, characterization of helviticin V-1829 a bacteriocin produced by *Lactobacillus helveticus* 1829. *Journal of Applied Bacteriology* **73:** 299-308.

Foulds, J. 1972. Purification and partial characterization

of a bacteriocin from *Serratia marcescens. Journal of Bacteriology* **10:** 1001-1009.

Gharairi, T., Frere, J.J., Berjeaud, M., Manai, M. 2005. Lactococcin MMT24, a novel two-peptide bacteriocin produced by *Lactococcus lactis* isolated from rigouta cheese. *International Journal of Food Microbiology* **105:** 389-398.

Gravesen, A., Axelsen, A.M.J., DaSilva, J.M, Hansen, T.B., Knochal, S. 2002. Frequency of bacteriocin resistance development and associated fitness costs in *Listeria monocytogenes*. *Applied and Environmental Microbiology* **68:** 756-764.

Himelbloom, B., Nilsson, L., Gram, L. 2001. Factors affecting production of an antilisterial bacteriocin by *Carnobacterium piscicola* strain A9b in laboratory media and model fish systems. *Journal of Applied Microbiology* **91:** 506-513.

Ivanova, I., Kabadjova, P., Pantev, A., Danova, S., Dousset, X. 2000. Detection, purification and partial characterization of a novel bacteriocin substance produced by *Lactococcus lactis* subsp. *lactis* B14 isolated from boza–a Bulgarian traditional cereal beverage. *Biocatalysis Fundamentals and Applications* **41:** 47-53.

Jeevaratnam, K., Jammuna, M., Bawa, A. S. 2005. Biological preservation of foods - Bacteriocins of lactic acid bacteria. *Indian Journal of Biotechnology* **4:** 446-454.

Kimura, H., Sashihara, T., Matsusaki, H., Sonomoto, K., Ishizaki, A. 1998. Novel bacteriocin of *Pediococcus* sp. ISK-1 isolated from well-aged bed of fermented rice bran. *Annals of the New York Academy of Science* **864:** 345-348.

Kumar, R., Vadhera, D.V. 1980. Gel permeation and ion exchange chromatography. In: *Analytical and Purification Techniques in Microbilogy. Lab Manual*, 91 p. Department of Microbiology, Punjab University, Chandigarh, India.

Lucke, F.K. 2000. Utilization of microbes to process and preserve meat. *Meat Science* **56:** 105-115.

Laemmli, U.K. 1970. Cleavage of structural proteins during the assembly of the head of bacteriophage T4. *Nature* **227:** 680-685.

Lowry, O. H, Rosebrough, N.J, Farr A.L., Randall, R J. 1951. Protein measurement with folin phenol reagent. *Journal of Biological Chemistry* **193:** 265-275.

Marekova, M., Laukova, A.,Skaugen M., Nes, I. 2007. Isolation and characterization of a new bacteriocin termed enterocin M, produced by environmental isolate *Enterococcus faecium* AL41. *Journal of Industrial Microbiol and Biotechnology* **34:** 533-537.

Merril, C.R., Goldman, D., Sedman, S.A., Elbert, M.H. 1981. Ultrasensitive stain for proteins in polyacrylamide gels show regional variations in cerebrospinal fluid proteins. *Science* **211:** 1437-1438.

Naclerio, G., Ricca, E., Sacco, M., DeFelice, M. 1993. Antimicrobial activity of a newly identified bacteriocin of *Bacillus cereus*. *Applied and Environmental Microbiology* **59:** 4313-4316.

Ogunbanwo, S.T., Sanni, A.I., Onilude, A.A. 2003. Characterization of bacteriocin produced by *Lactobacillus plantarum* F1 and *Lactobacillus brevis* OG1. *African Journal of Biotech* **2:** 219-227.

Osmanagaoglu, O., Beyatli, Y., Gunduz, U. 2001. Isolation and characterization of pediocin producing *Pediococcus pentosaceus* Pep1 from vacuum-packed sausages. *Turkish Journal of Biology* **25:** 133-143.

Periago, P.M., Moezelaar, R. 2001. Combined effect of nisin and carvacrol at different pH and temperature levels on the viability of different strains of *Bacillus cereus*. *International Journal of Food Microbiology* **68:** 141-148.

Ray, B. 2001. Sublethal injury bacteriocins and food microbiology. *ASM (*American Society for Microbiology) *News* **59:** 285-291.

Sharma, N.,Gautam, N.2008. Antimicrobial activity and characterization of bacteriocin of *Bacillus mycoides* from whey. *Indian Journal of Biotechnology* **7:** 117-121.

Sharma, N., Kapoor, G., Neopaney, B. 2006. Characterization of a new bacteriocin produced from a novel isolated strain of *Bacillus lentus* NG121. *Antonie van Leeuwenhoek* **89:** 337-343.

Sharma, N., Kapoor, G. 2004. Production of food biopreservative bacteriocin from traditional fermented food of H.P. In: *Intellectual Property Rights in Horticulture*, K.K. Jindal and R. Baba (eds.), pp. 175-179. S. Publishers, Dehradun, India.

Tagg, J.R., Dajani, A.S., Wannamaker, L.W. 1976. Bacteriocin of gram positive bacteria. *Bacteriology Review* **40:** 722-756.

Vignolo, G.M., Kairuz, M.N., Holgado, A.A.P., Oliker, G. 1995. Influence of growth conditions on the production of lactocin 705, a bacteriocin produced by *Lactobacillus casei* CRL 705. *Journal of Applied Bacteriology* **78:** 5-10.

Xiaomei, B., Zhaoxin, L., Fengxia, L. 2006. Preservation effect of an antimicrobial substance from *Bacillus subtilis* fmbj on pasteurized milk during storage. *Food Science and Technology International* **12:** 189-194.

Yildrim, Z., Johnson, M.G.1998. Detection and characterization of a bacteriocin produced by *Lactococcus lactis* Subsp. *cremoris* R isolated from radish. *Letters in Applied Microbiology* **26:** 297-304.

Pak. J. Sci. Ind. Res. 2009 **52** (4) 200-207

Karyomorphological and Morphometric Studies of Ploidy Levels in Some Wheat (*Triticum aestivum* L.) Genotypes

E. A. Kamel*[a], A. Arminian[b] and S. Houshmand[b]

[a]Department of Biological Sciences and Geology, Faculty of Education, Ain Shams University, P.C. 11341, Roxy, Cairo, Egypt
[b]Department of Crop Production, Faculty of Agriculture, Shahrekord University, P.O. Box 115, Shahrekord, Iran

(received September 2, 2008; accepted June 15, 2009)

Abstract. Karyomorphological and morphometric investigations of different ploidy levels of 14 genotypes of *Triticum aestivum* L. and one genotype of *Triticum durum* Desf. showed that, total chromosomal length (TCL) varied between genotypes. The highest value (56.21 μm) was recorded with mean chromosomal length of 8.03 ± 0.81 μm, while the lowest value of TCL (31.65 μm) was found with mean chromosomal length (MCL) of 4.52 ± 0.41 μm. Simple Pearson correlation coefficient (r) between TCL and MCL was the highest (r = 1.0 and P = 0.000). While the correlation coefficients between mean arm ratio (MAR) and parameters: total form (TF), intrachromosomal asymmetry index (A_1) and m (karyotype; metacentric region chromosome) as well as the coefficients between TF and m and between A_1 and m were the only significant (P<0.01) ones. Intrachromosomal asymmetry had a significant (P = 0.000) effect of total form percent than interchomosomal index. TCL and MCL were the most important karyological features influencing the principal component analysis and had 81.7 % variation, while in combination with MAR revealed 94% variation. Cluster dendrogram revealed close association and adjacent phylogenetic relatedness of tri- and hexaploid and also tetra- and hexaploid genotypes.

Keywords: cluster analysis, karyotype features, principal component analysis, wheat (*Triticum aestivum* L.), genotypes

Introduction

The genus *Triticum*, both wild and cultivated, has been one of the most intensively studied groups of plants. Hexaploid wheat (2*n* = 6*x* = 42, *Triticum aestivum* L.) (~600 million tons is produced annually) is the most widely adapted of the major crops, thus offering potential for increased food production. It includes domesticated diploid and tetraploid wheats as well as rye (*Secale cereale*) and barley (*Hordeum vulgare*) (Huang *et al*., 2002).

Cytogenetical investigation is one of the best documented experimental proofs for the elucidation of the mode of speciation on different groups of plants (Zohary, 1984; Kumar and Rai, 2007).

The morphological and chromosomal studies are necessary for inducing genetic variations, transfer of useful characters and for study of genetic and cytogenetic variations using cluster analysis between genotypes (Siahsar *et al*., 2005). Studies of the morphology of chromosomes in hexaploid wheat have been made by many workers (Jahan and Vahidy, 1989; Kimber, 1971; Khan, 1963; Schulz-Schaeffer and Haun, 1961).

Karyotype analysis has played an important role in the identification and designation of chromosomes in many plant species. Among others, morphometric investigation of the karyological data can be studied through multivariate procedures including principal component and cluster analysis. Principal component analysis (PCA) is a multivariate statistical technique for exploration and simplifying complex data sets through transforming a number of possibly correlated variables into a smaller number of variables called principal components (Everitt and Dunn, 1992).

Cluster analysis can be used to identify variables which can be classified into main groups and subgroups based on similarity and dissimilarity. This technique is useful for parental selection in breeding programs (El-Deeb and Mohamed, 1999) and crop modeling (Leilah and Al-Khateeb, 2005; Siahsar *et al*., 2005; Jaynes *et al*., 2003; Morphy, *et al*., 1992; Souza and Sorvells, 1991).

In this experiment, we performed karyological and morphometric evaluations in a population of diplo-tetra- and hexaploid wheat genotypes to estimate the best parameters interpreting the genetic diversity using karyological features.

Materials and Methods

Plant materials. The experiment consisted of five F_8 double-haploid lines, obtained as somaclones *via* regeneration of

Author for correspondence: E-mail: ehabk63@yahoo.com

plants from callus derived from immature inflorescences/ embryos of three hexaploid bread wheat genotypes and two d11887825 generations up to F_8 derived from a single R_0 doubled-haploid plant through selfed progeny for each line. These five lines were compared with nine bread wheat and one durum wheat (ID-10) genotypes. Features of the studied 15 genotypes are given in Table 1. Wheat genotypes were grown at Siwa Oasis, Tegzerty Experimental Farm of Desert Research Center during 2004 - 2005 winter seasons. Soil of the experimental site was characterized to be of sandy loam texture, saline (ECe 12.3 dS/m), calcareous ($CaCO_3$, 18.1 %) with 0.7 % organic matter. Deep artesian well irrigation water of EC about 4.1 dS/m was used for supplying nine irrigations throughout the growing seasons.

Methodology. Cytological preparations were carried out on root tips obtained from seeds germinated on sterile moist filter paper in petri dishes at 25 °C. Roots were pretreated with 0.05 % colchicine solution for 2-3 h, fixed in Carnoy for 24 h and stored in 70 % ethanol at 4 °C. Cytological preparations were made using the Feulgen squash method. The well-spread c-metaphase chromosomes were photographed from temporary preparations at magnification, 2000×. Slides of the original karyotypes are preserved in the Laboratory of Cytogenetics of Biological Sciences and Geology Department, Faculty of Education, Ain Shams University, Roxy, Cairo, Egypt. A karyogram for each genotype was constructed by arranging the chromosomes in homologous pairs by order of their length and arm ratio as measured from the photographic prints. The number of chromosome types was determined as described by Levan *et al.* (1965). Measurement of chromosomal length was taken on the same photographs of the karyogram. Variation in mean chromosomal length (MCL) and chromosome arm ratio (MAR) within the karyotype had been estimated by calculating the standard error (SE) of these parameters. Karyotype asymmetry deduced from the ratio between the short arms of the chromosomes and their total length was expressed as total form percent (TF %) as proposed by Huzwara (1962). Karyotype asymmetry expressed by the ratio between chromosome arms has also been estimated as the intrachromosomal asymmetry index (A_1) (Romero-Zarco, 1986). The value of A_1 was considered close to zero if all chromosomes were metacentric and approx. one if all chromosomes are telocentric. Karyotype asymmetry due to the ratio between sizes of different chromosomes was also estimated as the interchromosomal asymmetry index (A_2) using Pearson's dispersion coefficient, which is the ratio between the standard deviation and the mean chromosome length (Romero-Zarco 1986).

Table 1. Name, source, pedigree and selection history of the wheat genotypes used in the study

Genotype no.	Genotype	Source	Pedigree/selection history
1	Mexipak 65	ICARDA	II 8156-OPAK
2	Sahel - 1	Egypt	Ns. 732/Pima//Veery "S" #5 Sd735-4Sd-1Sd-1Sd-0Sd
3	Mar – 3	Egypt*	Cham 4/Sakha 8//2* Sakha 8 Su74-3Mr-32Mr-5Sw-13Sw-0Sw
4	ID - 10	ICARDA	ICD88-1233-ABL-8AP-0AP-3AP-0AP
5	Gem - 7	Egypt	CMH74A-630/Xs//Seri82/3/Agent/C Gm4611-2Gm-3Gm-16Gm-0Gm
6	Giza - 168	Egypt	MRL/BUC//SERI CM93046-8M-0Y-0M-2Y-0B-0GZ
7	Mar- 5	Egypt*	Giza 162//Bch'S/4/PI-ICW79 Su5-11Mr-38Mr-1Mr-0Mr
8	Cham - 4	Syria	CM 39816-1S-1AP-0AP
9	S_8 / 17	Egypt	R_8 tissue culture regenerated double haploid plant
10	LR / 1	Egypt	R_8 tissue culture regenerated double haploid plant
11	LR / 2	Egypt	R_8 tissue culture regenerated double haploid plant
12	Giza - 160 / 1	Egypt	R_8 tissue culture regenerated double haploid plant
13	Giza - 160	Egypt	L.2188/1131 – Chenab 70/ Giza 155
14	Lerma Rojo - 64	Spain	Long – term check
15	L R / 3	Egypt	R_8 tissue culture regenerated double haploid plant

*Newly bred line released through Desert Research Center, Wheat Breeding Program; ICARDA = International Center of Agricultural Research in the Dry Areas.

Table 2. Karyological features of the studied genotypes of *Triticum aestivum* L

Genotype	*x*	*2n*	TCL (μm)	MCL ± SE (μm)	MAR ± SE (*r*-value)	TF %	A_1	A_2	SAT	Chromosome type		
										M	m	sm
1	7	21	37.59	5.37 ± 0.30	1.30 ± 0.07	43.76	0.22	0.15	-	-	7	-
2	7	28	56.21	8.03 ± 0.81	1.35 ± 0.13	43.50	0.23	0.27	-	-	6	1
3	7	28	51.40	7.34 ± 0.41	1.42 ± 0.08	41.67	0.29	0.15	+	-	6	1
4	7	14	45.82	6.55 ± 0.79	1.63 ± 0.11	38.02	0.37	0.32	+	-	5	2
5	7	42	42.41	6.06 ± 0.51	1.45 ± 0.06	41.19	0.30	0.22	+	-	7	-
6	7	28	33.48	4.78 ± 0.35	1.30 ± 0.07	43.79	0.22	0.19	-	1	6	-
7	7	42	32.38	4.63 ± 0.45	1.28 ± 0.04	43.45	0.22	0.26	-	-	7	-
8	7	42	31.65	4.52 ± 0.41	1.23 ± 0.06	44.49	0.18	0.24	-	-	7	-
9	7	42	40.44	5.78 ± 0.42	1.32 ± 0.06	43.18	0.23	0.19	-	-	7	-
10	7	28	35.02	5.00 ± 0.38	1.33 ± 0.04	42.89	0.24	0.20	-	-	7	-
11	7	28	47.95	6.85 ± 0.48	1.24 ± 0.05	44.75	0.18	0.18	+	-	7	-
12	7	42	38.53	5.50 ± 0.48	1.48 ± 0.08	40.85	0.31	0.23	+	-	6	1
13	7	21	38.67	5.52 ± 0.40	1.51 ± 0.13	40.29	0.31	0.19	+	-	4	3
14	7	42	40.51	5.79 ± 0.43	1.22 ± 0.04	45.40	0.17	0.20	+	-	7	-
15	7	42	37.71	5.39 ± 0.52	1.38 ± 0.08	41.69	0.26	0.26	+	-	7	-

NS = Non-significant at 0.05 of statistical level; ** = significant at 0.05 of statistical level; *** = significant at 0.001 of statistical level. TLC = mean chromosome length; MCL = mean chromosome length; MAR = mean arm ratio; SE = standard error; M = metacentric chromosome; m = metacentric region chromosome; sm = submetacentric chromosome; TF% = total form percent; SAT = satellite; A_1 = intrachromosomal asymmetry index; A_2 = interchromosomal asymmetry index.

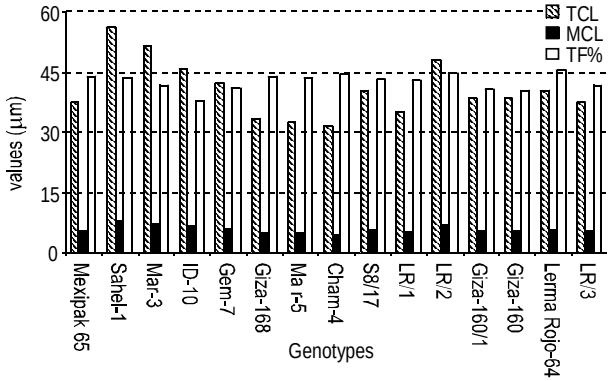

Fig. 1. Comparison of 15 genotypes on the basis of total chromosome length (TCL), mean chromosome length (MCL) and total form percentage (TF %).

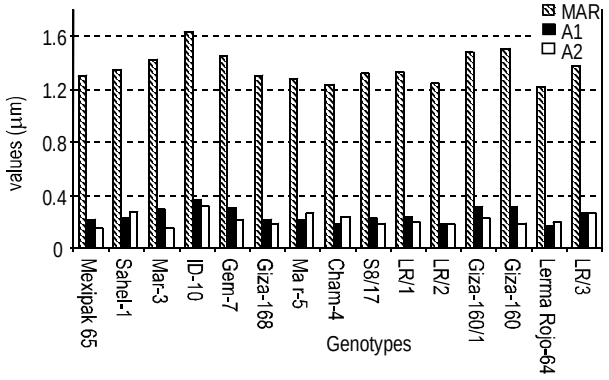

Fig. 2. Comparison of 15 genotypes on the basis of total chromosome arm ratio (MAR), intrachromosomal asymmetry index (A_1) and interchromosomal asymmetry index (A_2).

For the numerical characterization of the karyotypes, the following parameters were calculated (Seijo and Fernandez, 2003): (1): total chromosomal length of the haploid complement (TCL); (2) mean chromosome length (MCL); (3) intrachromosomal asymmetry index (A_1) = 1 - [$\sum(b/B)/n$]; where *b* and *B* are the mean length of short and long arms of each pair of homologues, respectively, *n* is the number of homologues, (4) interchromosomal asymmetry index (A_2) = *s*/*x*, were *s* is the standard deviation and *x* the mean chromosome length. Karyotype asymmetry was determined using A_1 and A_2 indices (Romero-Zarco, 1986) and the categories of Stebbins (1971) and (5) total form percentage (TF %) which measures the symmetry of the chromosomes over the whole karyotype (El-Bakatoushi and Richards, 2005).

Statistical analysis. In order to determine the association of the karyotype features, simple Pearson coefficient of correlation (r) and also the linear regression analysis between MAR and A_1 and A_2 were applied. For grouping the lines showing similar karyotype characteristics, clustering method

ward as well as ordination based on principal components analysis (PCA) were performed (Sheidai *et al*., 2006). Statistical analysis was performed using Minitab V.15 statistical software (Minitab Inc, 2008).

Results and Discussion

A summary of the karyological features of the studied genotypes of *Triticum aestivum* L. is given in Table 2 and Fig. 1 and 2. Among the 15 genotypes studied different ploidy levels appeared including a diploid (genotype 4), two triploid (genotypes 1 and 13), five tetraploid (genotypes 2, 3, 6, 10 and 11) and seven hexaploid (genotypes 5, 7, 8, 9, 12, 14 and 15). It is well known that the mode of chromosome pairing in triploid ($2n = 3x = 21$) and pentaploid ($2n = 5x = 35$) hybrids helped Kihara (1944) to uncover the ancestral species of allopolyploid wheats.

The genotypes had different total chromosomal lengths (TCL) (Table 2; Fig. 1 and 2) ranging from 56.21 (in genotype 2) to 31.65 μm (in genotype 8). The karyotypes of the examined genotypes are considerably symmetrical with regard to chromosomal length. The most similar chromosomes are scored in genotype (1) (SE of MCL = 0.30 μm). The degree of karyotype asymmetry as indicated by TF (%) value ranges between 38.02 % in genotype 4 and 45.40 % in genotype 14. In general, A_1 and A_2 values show high degree of karyotype symmetry in the majority of the genotype studied (Table 2). Eight of the studied genotypes (3, 4, 5, 11, 12, 13, 14 and 15) are characterized by the presence of SAT in their chromosome arms (Table 2).

Hexaploid wheat ($2n = 6x = 42$) is an allohexaploid and contains three genomes. Karp and Maddock (1984) studied chromosomes of 192 regenerated plants derived from immature embryo callus of hexaploid wheat cultivars. A total of 71 % of the regenerants carried the expected $2n = 42$ chromosomes and 29 % of the plants were aneuploid ($2n = 38$ to 45). It is thought that somaclonal variation possibly occurs during the process of plant tissue culture which is considered to provide a source of new germplasm. Polyploidy is one of the most frequent incidents among the somaclonal variations (Sangthong *et al*., 2004).

Cytological investigations revealed that the number of chromosomes varied highly in anther-derived calli and in their regenerants (Nishibayashi *et al*., 1989); high variability was also reported in chromosomal number during callus induction and plant regeneration from mature barley embryos (Lupotto, 1984). In an experiment, González *et al.* (1996) determined chromosomal number in calli of barley plants cultures regenerated from two kinds of explants, immature embryos and seedling leaves. They pointed out diploid cells were predominant in all cases; although in leaf-derived cultures, tetraploid cells ($2n = 4x = 28$) showed a tendency to increase as duration of culture increased and after more than six months in culture, diploid cells decreased down to almost 70 %. Aneuploid cells were generally infrequent in all cases. The source of explant had been more important than the genotype (cultivar) and the type of callus (morphogenic *vs.* non-morphogenic) in the chromosomal stability of cultures as time increased. From short term cultures, only 1.85% of the regenerated plants were tetraploid; the remaining were diploids.

Brasileiro *et al.* (1999) reported that in anther derived tomato plant cultures, the regenerated plants presented tetraploid cells and rare diploid cells. These tetraploid plants could be used as source of further trisomic lines, for the purpose of genetic localization studies and analysis of protein compound.

The pair-wise simple Pearson correlation coefficients between all karyotype features is given in Table 3. Significant correlation may be observed between total chromosomal length (TCL) and mean chromosomal length ($r = 1.0$ and $P < 0.001$). This relationship is well expected because total and mean chromo-

Table 3. Simple pair-wise Pearson correlation coefficients between karyotype features

	TCL	MCL	MAR	TF(%)	A_1	A_2
MCL	1.00000***					
MAR	0.27831^{NS}	0.27802^{NS}				
TF %	-0.17402^{NS}	-0.17391^{NS}	-0.98475***			
A_1	0.22976^{NS}	0.22946^{NS}	0.98891***	-0.98691***		
A_2	0.04543^{NS}	0.04688^{NS}	0.38636^{NS}	-0.42095^{NS}	0.34446^{NS}	
m	-0.23761^{NS}	-0.23646^{NS}	-0.72690**	0.66574**	-0.66292**	0.16694^{NS}

NS = Non-significant at 0.05 of statistical level; ** = significant at 0.05 of statistical level; *** = significant at 0.001 of statistical level.
TLC = mean chromosome length; MCL = mean chromosome length; MAR = mean arm ratio; SE = standard error; M = metacentric chromosome; m = metacentric region chromosome; sm = submetacentric chromosome; TF% = total form percent; SAT = satellite; A_1 = intrachromosomal asymmetry index; A_2 = interchromosomal asymmetry index.

somal lengths are associated positively. So the karyological features function in the same direction, each of which could be applied to the karyological studies. The next significant correlation coefficients include a negative value for mean arm ratio (MAR) with TF % ($r \sim -0.98$ and $P<0.001$), a positive value for MAR with A_1 ($r \sim -0.99$ and $P<0.001$) and a negative coefficient for MAR with m ($r \sim -0.73$ and $P<0.01$). It is presumably logical that intrachromosomal asymmetric index (A_1) is well related to mean arm ratio. The same holds for MAR and m (chromosome type). There are also negative significant correlation coefficients between total form percentage (TF %) and A_1 ($r \sim -0.99$ and $P<0.001$) and A_1 and m ($r \sim -0.66$ and $P<0.01$). The other pair-wise correlation coefficients between other karyotype features were not significant ($P>0.05$). Interestingly, the interchromosomal asymmetry (A_2) in this study showed no relation to individual chromosomal characteristics.

The results of stepwise regression revealed that among six karyotype features (TCL, MCL, MAR, A_1, A_2 and m), the first four features had the most effect on total form (TF %) and A_2 had not any special effect. The multiple linear regression analysis showed a significant causative relationship between the four predicting features and TF percentage. The simple regression analysis individually showed significant relationships between MAR, A_1 and m and TF %. Other features individually did not have significant effect on total form percentage. So the contributions of these three features are more notable and effective in determining total form of chromosomes and can be definitely applied in the karyological studies.

Though the MAR, A_1 and m indicated that they determine the total form of a chromosomal set, but according to morphometric investigations (principal component analysis and cluster categorization) they cannot be applied in interpretation of all aspects of the karyotype studies. The reason is that, though these three parameters visually depict the karyotype, but there remains the problem of grouping and classifying different genotypes in the diversity studies. Applying principal component analysis (PCA) of some of the features, this problem can be solved. For evaluating and grouping 15 wheat genotypes of various ploidy levels, principal component analysis of this experiment has been performed, standardizing the data of karyotype features and using correlation coefficient matrix for PCA as shown in Table 4.

PCA results indicated that the first principal component had variance (eigenvalue) of 3.915 and accounted for 55.9 % of the total variance. This data (Table 4), graphically shown in Fig. 3, demonstrated that an increase in the number of components was associated with a decrease in the eigenvalue. This trend reached its maximum at three factors. Accordingly, it is reasonable to assume that the principal components analysis had grouped the estimated wheat variables into three main components which all together accounted for 94.0 % of the total variation of karyotype features. The coefficients listed under PC_1 show how to calculate the principal component scores. Results showed that PC_1 correlated moderately well with MAR, TF %, A_1 and m. Meanwhile, the PC_2 correlated moderately with TCL and MCL. The third component i. e. PC_3 had a moderate correlation with 'm' and and the highest correlation with 'A_2' karyotype features. Variables which significantly correlated with the first three eigenvectors were the variables with the greatest variability. The factor loadings (Fig. 2) refer to the coefficients in each principal component or the correlation between the component and the variables. A high correlation between PC_1 and a variable indicates that the

Table 4. (a) Principal component analysis: (b) Eigenanalysis of the correlation matrix

(a) Principal component analysis

Variable	PC_1	PC_2	PC_3	PC_4	PC_5	PC_6	PC_7
TCL	-0.226	-0.664	-0.079	-0.024	-0.025	0.023	0.707
MCL	-0.226	-0.664	-0.081	-0.025	-0.033	0.019	-0.707
MAR	-0.492	0.128	0.074	-0.177	0.272	-0.794	0.000
TF %	0.476	-0.207	-0.030	0.270	0.802	-0.117	-0.004
A_1	-0.478	0.158	0.102	-0.336	0.527	0.587	-0.004
A_2	-0.220	0.174	-0.919	0.270	0.056	0.038	0.001
m	0.390	-0.062	-0.356	-0.842	0.009	-0.094	0.001

(b) Eigen analysis of the correlation matrix

Eigenvalue	3.9150	1.8032	0.8602	0.4090	0.0083	0.0043
Proportion	0.559	0.258	0.123	0.058	0.001	0.001
Cumulative	0.559	0.817	0.940	0.998	0.999	1.000

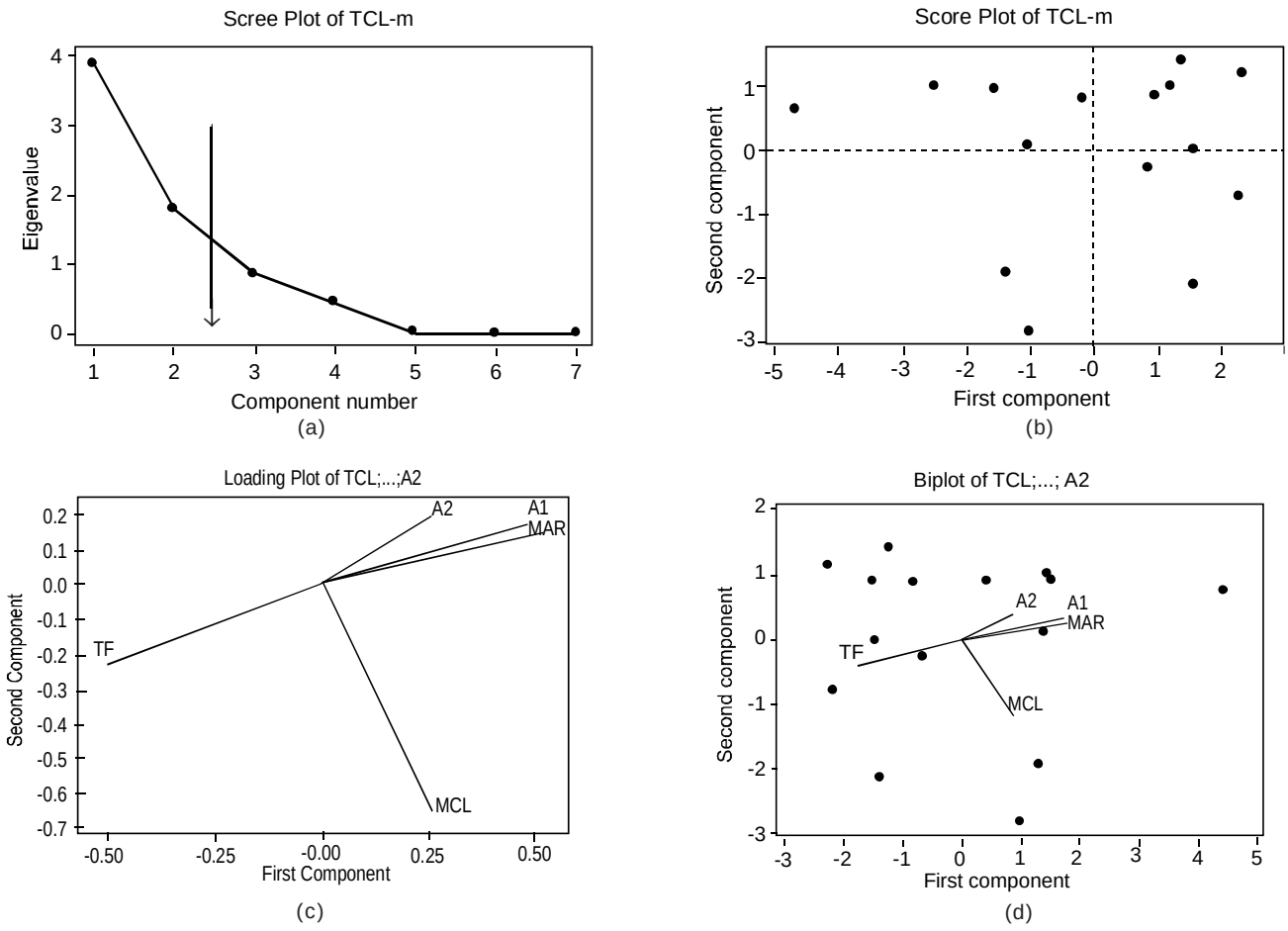

Fig. 3. (a) Scree plot showing eigenvalues in response to number of components for the estimated variables of wheat. (b) Score plot of the PCA. (c) Loading plot of the PCA. (d) Biplot of the PCA.

variable is associated with the direction of the maximum amount of variation in the data set (Leilah and Al-Khateeb, 2005).

$$PC_1 = -0.226\,(TCL) - 0.226\,(MCL) - 0.492\,(MAR) + 0.476\,(TF\,\%) - 0.478\,(A_1) - 0.220\,(A_2) + 0.390\,(m)$$

It should be noted that the interpretation of the principal components is subjective; however, obvious patterns emerge quite often. For instance, one could think of the first principal component as representing total chromosomal length, mean chromosomal length, mean arm ratio and total form percentage in the karyotype studies for grouping different genotypes, because the coefficients of the first three terms have the same sign and are not close to zero. This case could be followed for the second principal component which has variance 1.8032 and accounts for 25.8 % of the data variability, which has been calculated from the original data using the coefficients listed under PC_2. This component could be thought of as an important alternative to the first component for grouping. Together, the first two and the first three principal components represent 81.7 % and 94 %, respectively, of the total variability. Thus, most of the data structure can be captured in two or three underlying dimensions. The remaining principal components account for a very small proportion of the variability and are probably unimportant. The eigenvalue (scree) plot provides this information visually (Fig. 3 (b-d)) (Minitab Inc., 2008).

The next important part of the study is classifying 15 genotypes using multivariate schedule cluster analysis wherein the Ward method was utilized and cluster tree was drawn (Fig. 4) using Minitab software (Minitab Inc., 2008). The cluster analysis of karyological data and ordination of taxa on the first three PCA axes are given in Fig. 3 (A-D). Grouping by ordination of taxa based on the first three PCA axes supports the clustering results. Briefly, cluster methods start with the calculation of the distance of each variable in relation to other variables. Groups are then formed by the process of agglomeration division. In this process, all variables start individually. Close groups then gradually merge until

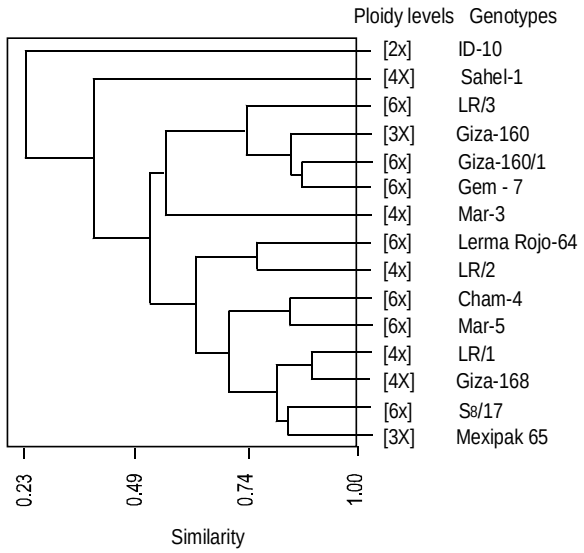

Fig. 4. Cluster categorization of 15 wheat (*T. aestivum* L.) genotypes of different ploidy levels obtained *via* Ward method. Similarity levels of the estimated 7 wheat characters (variables) using Ward cluster analysis, showing cluster 1 (ID-10, diploid genotype), cluster 2 (including Sahel-1, tetraploid genotype) and cluster 3 (including other genotypes without diploid, including triploids.

finally all variables form a single group (Leilah and Al-Khateeb, 2005).

As is apparent (Fig.4), 15 genotypes were classified in three major categories, so that ID-10, a diploid, and Sahel-1, a tetraploid genotype, were located in 2 discrete categories and LR/3, Giza-160, Giza-160/1 and Gem-7 in the next category. The tetraploid Mar-3 genotype was located in another separate cluster. The other category identified Lerma Rojo-64 and LR/2. And finally the last cluster belonged to Cham-4, Mar-5, LR/1, Giza-168, S8/17 and Mexipak 65. The most important finding, derived from the callus culture, is that these genotypes showed various ploidy levels ranging from diploid to hexaploid. It was found that the diploid and other ploidy levels especially triploid had never been placed adjacent to one another in a common category, i.e. the triploid and hexaploid genotypes were always in the same categories which may be due to their remotely different chromosomal set.

Moreover, tetraploid-tetraploid, hexaploid-hexaploid and even tetraploid-hexaploid genotypes were put in the same categories. Interestingly, the results showed that the closeness of triploid and hexaploid genotypes may prove a close evolutionary relationship between these two ploidy levels. Thus the hexaploid wheat plant could be obtained simpley through doubling the chromosomal set (diploidization) of a triploid plant, regenerated from endosperm-derivation.

Acknowledgement

The authors thank Dr. Kamel Zaki Ahmed, Director, MCGEB, (Minia Centre for Genetic Engineering and Biotechnology, Faculty of Agriculture, Minia University, Iran) for providing five F_8 double haploid lines of *Triticum aestivum* L. for the study.

References

Brasileiro, A.S.R., Willadino, L., Carvalheira, G.G., Guerra, M. 1999. Callus induction and plant regeneration of tomato (*Lycopersicon esculentum* cv. IPA 5) *via* anther culture. *Ciência Rural*, Santa Maria **29:** 619-623.

El-Bakatoushi, R., Richards, A.J. 2005. Karyological variation between two taxa of *Plantago major* L., ssp. *major* and ssp. *intermedia* (Gilib.) Lange. *Cytologia* **70:** 365-372.

El-Deeb, A.A., Mohamed, N.A. 1999. Factor and cluster analysis for some quantitative characters in sesame (*Sesamum indicum* L.). The Annual Conference ISSR, Cairo University, 4-6 December,vol. **34**, Part (II).

Everitt, B.S., Dunn, G. 1992. *Applied Multivariate Data Analysis.* Oxford University Press, New York, USA.

González, A.I., Peláez, M.I., Ruiz, M.L. 1996. Cytogenetic variation in somatic tissue cultures and regenerated plants of barley (*Hordeum vulgare* L.) *Euphytica* **91:** 37-43.

Huang, S., Sirikhachornkit, A., Su, X., Faris, J., Gill, B., Haselkorn, R., Gornicki, P. 2002. Genes encoding plastid acetyl-CoA carboxylase and 3-phosphoglycerate kinase of the *Triticum/Aegilops* complex and the evolutionary history of polyploid wheat. *Proceedings of National Academy of Science* **99:** 8133-8138.

Huzwara, Y. 1962. Karyotype analysis in some genera of Compositae VIII. Further studies on the chromosomes of Aster. *American Journal of Botany* **49:** 116-119.

Jahan, Q., Vahidy, A.A. 1989. Karyotype analysis of hexaploid wheat, *Triticum aestivum* L. cv. 'Sarsabz'. *Journal of Islamic Academy of Sciences* **2:** 179-181.

Jaynes, D.B., Kaspar, T.C., Colvin, T.S., James, D.E. 2003. Cluster analysis of spatiotemporal corn yield pattern in an Iowa field. *Agronomy Journal* **95:** 574-586.

Karp, A., Maddock, S.E.1984. Chromosome variation in wheat plants regenerated from cultured immature embryos. *Theoretical and Applied Genetics* **67:** 249-255.

Khan, S.I. 1963. Karyotype analysis of Holdfast: a cultivar of *Triticum aestivum* L. *Cellule* **63:** 291-305.

Kihara, H. 1944. The discovery of DD analyzer, one of the ancestors of common wheat (preliminary reports). *Aric.*

Hort. **19:** 889-890.

Kimber, G. 1971. The rationale of measuring chromosomes. *Seiken Ziho* **22:** 5-8.

Kumar, G., Rai, K.P. 2007. EMS induced karyomorpholo-gical variations in maize (*Zea mays* L.) Inbreds. *Turkish Journal of Biology* **31:** 187-195.

Leilah, A.A., Al-Khateeb, S.A. 2005. Statistical analysis of wheat yield under drought conditions. *Journal of Arid Environments* **61:** 483-496.

Levan, A., Fredga, K., Sanders, A.A. 1965. Nomenclature for centromeric position on chromosomes. *Hereditas* **52:** 201-220.

Lupotto, E. 1984. Callus induction and plant regeneration from barley mature embryos. *Annals of Botany* **54:** 523-530.

Minitab Inc. 2008. Minitab User's Guide. Available at: http://www.Minitab.com

Morphy, D.P.L., Cox, T.S., Rodgers, D.M. 1992. A multivariate approach to the analysis of cereal crops structure at harvest. *European Society for Agronomy* **23:** 194-195.

Nishibayashi, S., Hayashi, Y., Kyozuka, J., Shimamoto, K. 1989. Chromosome variations in protoplast-derived calli and in plants regenerated from the calli of cultivated rice (*Oryza sativa* L.). *Dengaku Zasshi* **64:** 355-361. .

Romero-Zarco, C. 1986. A new method for estimating karyotype asymmetry. *Taxon* **35:** 526-530.

Sangthong, R., Mii, M., Soonthornchainaksaeng, P., Supaibulwatana, K. 2004. Characteristics of the tetraploid plant derived as a somaclonal variation in *Lilium longiflorum*. *IX International Symposium on Flower Bulbs*. Available at: http://www.actahort.org

Schulz-Schaeffer, J., Haun, C.R. 1961. The chromosomes of hexaploid common wheat, *Triticum aestivum* L.Z. *Pflanzenzuchtg* **46:** 112-124.

Seijo, J.G., Fernandez, A. 2003. Karyotype analysis and chromosome evolution in South American species of *Lathyrus* (Leguminosae). *American Journal of Botany* **90:** 980-987.

Sheidai, M., Mehdigholi, K., Ghahreman, A., Attar, F. 2006. Cytogenetic study of the genus *Cousinia* (Asteraceae, section *Serratuloideae*) in Iran. *Genetic Molecular Biology* **29:** 117-121.

Siahsar, B.A., Ghaffari Pour, S., Karimzadeh, G., Sahebi, M., Akbari-Moghadam, H. 2005. Karyotypic and Morphologic Variations in some Hull-less Barley (*Hordeum vulgare* L.) Genotypes. *Proceedings of 9th ICABR International Conference on Agricultural Biotechnology Research (ICABR):* July 6 to July 10, 2005, Ravello (Italy).

Souza, E., Sorvells, M.E. 1991. Relationships among 70 North American oat germplasms. I. Cluster analysis using quantitative characters. *Crop Science* **31:** 599-605.

Stebbins, G.L. 1971. *Chromosomal Evolution in Higher Plants*. Addison-Wesley, London, UK.

Zohary, D. 1984. Modes of Evolution in Plants under Domestication. In: *Plant Biosystematic*, W.F. Grant, (ed.), p. 579-596. Academic Press, Canada.

Pak. J. Sci. Ind. Res. 2009 **52** (4) 208-216

Ameliorative Effect of Ethanolic Extract of *Cichorium intybus* on Cisplatin - Induced Nephrotoxicity in Rats

Shafaq Noori and Tabassum Mahboob*
Department of Biochemistry, Clinical Biophysics Research Unit, University of Karachi, Karachi - 75270, Pakistan

(received February 24, 2009; revised April 28, 2009; accepted June 05, 2009)

Abstract. In the study of the possible ameliorative effect of the *Cichorium intybus vs.* cisplatin-induced nephrotoxicity, no sign of toxicity was observed in rats on administration of ethanolic extract of *C. intybus* (500 mg/kg) with cisplatin (3 mg/kg). Oral administration of *C. intybus* extract reduced cisplatin-induced nephrotoxicity and also prevented elevated plasma creatinine, urea and nitrate, plasma and tissue MDA levels and restored antioxidant enzymes.

Keywords: cisplatin, *Cichorium intybus*, nephrotoxicity, antioxidant enzymes

Introduction

Cisplatin, or cis-diamminedichloroplatinum (II) (CDDP) is extensively used for the management of oncological disorders, particularly of ovary, testis, bladder, head and neck (Hamers *et al*., 1991). Although higher doses of cisplatin are more efficacious for cancer chemotherapy, but such therapy manifests non-haematological toxicities like nephrotoxicity (Bodenner *et al*., 1986). Formation of free radicals by CDDP (Matsushima *et al*., 1998), leading to oxidative stress, has been shown to be one of the main pathogenic mechanisms of these toxicities and side effects of nephrotoxicants (Greggi *et al*., 2001).

Antioxidant-based drugs/formulations for the prevention and treatment of complex diseases like atherosclerosis, stroke, diabetes, Alzheimer's disease and cancer have appeared during the last 3 decades (Devasagayam *et al*., 2004) attracting a great deal of interest in research on natural antioxidants. Subsequently, a worldwide trend has increased towards the use of natural phytochemicals present in berry crops, tea, herbs, oilseeds, beans, fruits and vegetables (Jiao and Wang, 2000). Several herbs and spices have been reported to exhibit antioxidant activity, including rosemary, sage, thyme, nutmeg, turmeric, white pepper, chilly pepper, ginger and several Chinese medicinal plants extracts (Ali *et al*., 2008; Lee and Shibamoto, 2000; Jiao and Wang, 2000; Deiana *et al*., 1999). The majority of the active antioxidant compounds are flavonoids, isoflavones, flavones, anthocyanins, coumarins, ligands, catechins and isocatechins. In addition to the above compounds found in natural foods, vitamins C and E, carotene, α-tocopherol are known to possess antioxidant potential (Maliakel *et al*., 2008; Lee *et al*., 2003; Kikuzaki and Nakatani, 1993; Jitoe *et al*., 1992; Kikuzaki *et al*., 1991).

*Author for correspondence; E-mail: tab60@hotmail.com

Cichorium intybus Linn. (chicory) is a medicinally important plant that belongs to the family Asteraceae. (Nandagopal and Ranjitha, 2007; Varotto *et al*., 2000). The root of the chicory has been used as folk medicine in Pakistan for treating liver diseases and hepatic system disorders. A group of clinical researchers recently isolated a phenolic compound called esculetin from the extract of *C. intybus* root and further confirmed that it is a hepatoprotectant compound. This extract inhibited the oxidative degradation of DNA in the tissue debris of mice liver (Gilani *et al*., 1998). Ahmed *et al*. (1998) reported antiulcerogenic effect of the aqueous extract of *C. intybus*.

A decoction of dried root is a noted treatment for stomach acidity. The tonic property of *C. intybus* makes it an excellent mild bitter tonic for the liver, gall-bladder, digestive tract and is also used for cleaning the urinary tract (Khan and Aslam, 2004) and in fever, vomiting and as diuretic (Hussain *et al*., 2008). This herb is used for rheumatic conditions and gout as well. The leaves and flowers can aid in digestion. The bruised leaves are used externally as a poultice for the relief of swellings, skin lacerations and inflammations (Rehmat *et al*., 2006). Moreover, *C. intybus* reduces extra heat of various organs and acts as deobstruent, tonic and febrifuge (Aslam, 2006).

C. intybus extract has high antioxidant potential as reported previously by Nandagopal and Ranjitha (2007). Despite the above described role of *C.intybus* in the treatment of various diseases, no attempt has been as yet made to investigate its role as an antioxidant in prevention of drug-induced nephrotoxicity. The present study was designed to evaluate the role of altered antioxidant enzymes in the ameliorative effect of *C. intybus* on cisplatin-induced nephrotoxicity, using rat models.

Materials and Methods

Animals and diet. 24 Wistar male albino rats (200-260 g b.w.) were purchased from the animal house of International Center for Chemical and Biological Sciences (ICCBS), Karachi, Pakistan for the study. Animals were acclimatized to the laboratory conditions one week before the start of experiment and caged in a temperature controlled room (23±4 °C). Rats had free access to water and standard rat diet. The experiments were conducted in accordance with ethical guidelines of internationally accepted principles for laboratory use and care in animal research (Health Research Extension Act, 1985).

Crude extraction of *C. intybus* Linn. *C. intybus* Linn plant was collected from the Northern area of Pakistan and identified by experts. 10 kg of dried aerial parts of *C. intybus* plant was powdered, screened and soaked in ethanol (10 litre) for one week. The filtrate was separated and concentrated under vacuum using a rotary evaporator, as a dark green semisolid (yield 44.4%). The extract was standardized by quantification of a reference standard with HPLC system. The reference standard was gallic acid.

Study design. The animals were divided into four experimental groups (n=6). Each group received the following treatment:

Group I, control, remained untreated

Group II received cisplatin i.p. (3 mg/kg b.w.) for 5 alternate days

Group III received *C. intybus* extract orally (500 mg/kg b.w.) for 10 days

Group IV received *C. intybus* extract orally (500 mg/kg b.w.) for 10 days + cisplatin i.p. (3 mg/kg b.w.) for 5 alternate days (the extract was administered orally, 30 min prior to administration of cisplatin).

Sample collection. After 48 h of administration of the last dose to the treated groups, animals were anesthetized, decapitated and blood was sampled from head wounds in lithium heparin coated tubes. A portion of blood was used to get plasma. Kidneys were excised, trimmed of connective tissues, rinsed with saline to eliminate blood contamination, dried by blotting with filter paper and weighed. The tissues were then kept in freezer at 70 °C until used for analysis.

Histological examination. Left kidney was quickly removed, immersed in 10% formaline, dehydrated and embedded in paraffin, sectioned at 3 µm, stained with hematoxylin and eosin (H&E) and examined by light microscopy.

Biochemical Assay. *Assessment of renal functions*. Plasma samples were assayed for urea and creatinine, spectrophotometrically by Oxime method (Butler *et al*., 1981) and Jeff's method (Spierto *et al*., 1979), respectively.

Assessment of oxidative stress. Plasma sample was assayed for nitrate and MDA.

Plasma nitrate estimation by ion selective electrode (ISE) method. Plasma nitrate was estimated by ion selective electrode using ion meter 3345 (Jenway) which detected free ionic nitrate (NO_3^{-2}) in plasma/serum sample. In a clean glass test tube, 1.7 ml of deionized water was taken; 0.2 ml of ISAB(4M KCl) (ionic strength adjusting buffer) and 0.1 ml of plasma were added and mixed well. The electrode was rinsed, blotted dry and the result was recorded in mg/l.

Kidney homogenate preparation. Kidney homogenate was obtained by using a tissue homogenator, Ultra Taurax T-25 Polytron, at 4 °C. The homogenates (1:10 w/v) were prepared by using a 100 mmol KCl buffer pH 7 containing EDTA 0.3 mmol. All homogenates were centrifuged at 600 g for 60 min at 4 °C and the supernatant was used for biochemical assays.

Assessment of tissue lipid peroxides. 10 µl of BHT (butylated hydroxytoluene) (0.5 M in acetonitrile) was added to prevent homogenate from oxidation and the homogenate was stored at -70 °C until analysis was made for malonyldialdehyde (MDA) and 4-hydroxy-2-nonenal (4-HNE).

Estimation of MDA. The MDA content, a measure of lipid peroxidation, was assayed in the form of thiobarbituric acid reacting substances (TBARS) by the method of Ohkawa *et al*. (1979). Briefly, the reaction mixture, consisting of 0.2 ml of 8.1% sodium dodecyle sulphate, 1.5 ml of 20% acetic acid solution adjusted to pH 3.5 with sodium hydroxide and 1.5 ml of 0.8% aqueous solution of thiobarbituric acid, was added to 0.2 ml of 10% (w/v) of the homogenate. The mixture was brought up to 4.0 ml with distilled water and heated at 95 °C for 60 min. After cooling with tap water, 1.0 ml distilled water and 5.0 ml of the mixture of *n*-butanol and pyridine (15:1 v/v) was added and the mixture was centrifuged. The organic layer was taken out and its absorbance was measured at 532 nm and compared with those obtained from MDA standards (1,1,3,3- tetramethoxy-propane). The concentration values were calculated by measurement of absorption against standard absorption.

Estimation of 4-HNE. The 4-HNE content was measured by the method of Kinter (1996). Briefly, the assay mixture consisted of 2 ml of filtrate with 1 ml of 2,4-dinitrophenyl hydrazine which was kept for 1 h at room temperature. Sample was extracted with hexane, and the extract was evaporated at 40 °C. Cooled sample was measured at 350 nm against methanol blank. The standard was 4-HNE-DMA (dimethyle acetal).

Assessment of antioxidant status. *Estimation of catalase*. Catalase activity was assayed by the method of Sinha (1972). Briefly, the assay mixture consisted of 1.96 ml phosphate buffer (0.01 M, pH 7.0), 1.0 ml hydrogen peroxide (0.2 M) and 0.04 ml (10%) homogenate in a final volume of 3.0 ml. 2 ml dichromate acetic acid reagent was added to 1 ml of reaction mixture, boiled for 10 min, cooled and changes in the absorbance were recorded at 570 nm.

Estimation of SOD. Levels of SOD in the cell free supernatant were measured by the method of Kono (1978). Briefly, 1.3 ml of solution A (0.1 mm EDTA containing 50 mM Na_2CO_3, pH 10.0), 0.5 ml of solution B (90 µm NBT i.e. nitro blue tetrazolium dye), 0.1 ml of solution C (0.6% TritonX-100 in solution A) and 0.1 ml of solution D (20 mmol hydroxylamine hydrochloride, pH 6.0) were mixed and the rate of NBT reduction was recorded for one min at 560 nm. 0.1 ml of the supernatant was added to the test and reference cuvette, which did not contain solution D. Finally, the percentage inhibition in the rate of reduction of NBT was recorded as described above. One enzyme unit was expressed as inverse of the amount of protein (mg) required for inhibiting the reduction rate by 50% in one minute.

***Statistical analysis*.** Results are presented as mean± SE. Statistical significance of the differences between the control and the test values were evaluated by Student's t-test. Statistical probability of P <0.01, <0 .05 was considered to be significant.

Results and Discussion

In the evaluation of effect of *C. intybus* on cisplatin-induced nephrotoxicity in rats, observations were made of four groups of rats i.e. control, cisplatin treated, *C. intybus* treated and *C. intybus* treated with cisplatin pretreated rats. Results are given as under:

Effects on body weight, kidney weight and relative kidney weight. Table 1 and Fig. 1 show effects of cisplatin, *C. intybus* extract and pretreatment of *C. intybus* extract with cisplatin on kidney and body weight, respectively. A marked decrease in rats body weight was observed in cisplatin-treated rats and CDDP + *C. intybus* group on the 10th day. Alone *C. intybus* extract also showed decrease in body weight but the decrease was less than that in cases of cisplatin treatment and CDDP + *C. intybus* pretreatment groups. Kidneys of rats treated with cisplatin were enlarged with significantly increased kidney weight ($P < 0.05$) and relative kidney weight; however, the results, were not significant as compared to the control. Sole treatment and pretreatment with *C. intybus* extract showed significantly increased relative kidney weight ($P < 0.05$).

Table 1. Effect of treatments on kidney weight and relative kidney weight of the study groups

Parameters	Control	Cisplatin (3mg/kg)	*C. intybus* (500mg/kg)	*C. intybus* +cisplatin
Mean kidney weight (g)	0.672 ±0.132	0.861** ±0.118	0.791 ±0.070	0.863 ±0.177
Mean relative kidney weight 10^{-3}	2.516 ±0.784	3.551 ±0.881	3.452** ±0.191	3.696** ±0.269

Values are mean±SE; significant difference between various groups by t-test; **P<0.05

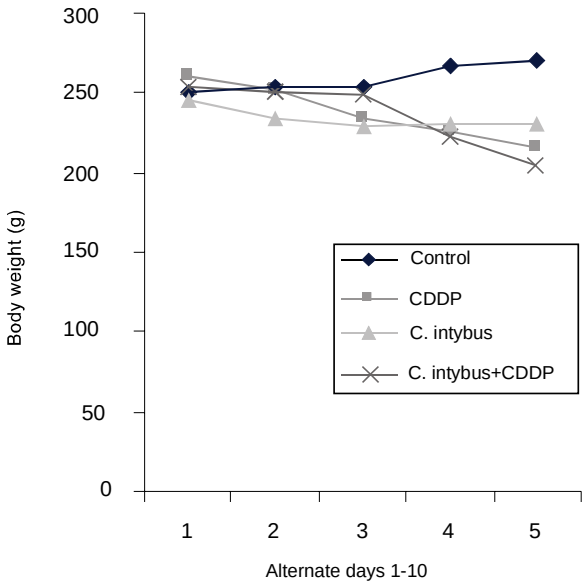

Fig. 1. Effect of treatments on body weight in the study groups.

Histology of kidney. After treatment for alternate days, cisplatin-treated rats showed glomeruli congestion, marked ATN in proximal and distal tubules, decrease in the height of epithelial cells, shedding of atypical cytoplasm and loss of brush boarder Fig. (2b). Wide opening of lumen and marked congestion in vessels (++++) were also seen. Pretreatment with *C. intybus* extract markedly prevented congestion in glomeruli and vessels (+) and other alterations Fig. 2(d). Treatment with *C. intybus* extract alone showed slight congestion in vessels and glomeruli (Fig. 2(c)). Histology of kidney of control group is given in Fig. 2(a) and histological activity index (HAI), in Table 2.

Plasma urea level. Cisplatin treated rats showed marked increase in level of plasma urea (35.7±3.46, P<0.01) as compared to the control (Fig. 3). *C. intybus* extract alone showed slightly increased urea level but the result was not significant. *C. intybus* extract partially prevented increase in urea level

in CDDP + *C. intybus* group (27.0±3.60, P<0.01) as compared to the control.

Plasma creatinine level. Figure 4 shows a significant effect on plasma creatinine level in cases of cisplatin and pretreatment with *C. intybus* extract. Creatinine level was significantly increased (1.03 ± 0.13, P < 0.01) in cisplatin-treated rats as compared to the control. Pretreatment with *C. intybus* extract partially prevented increase in plasma creatinine level in CDDP + *C. intybus* group(0.36±0.28, P<0.05). *C. intybus* extract alone produced no significant change.

Plasma MDA level. Increased level of plasma MDA was observed in cisplatin treated rats but the result was not significant. A significant decrease in plasma MDA was noted after only *C. intybus* extract treatment (3.26 ± 0.91, P< 0.01). The increased MDA level was prevented by pretreatment with *C. intybus* (10.03 ± 4.71, P < 0.05) in CDDP + *C. intybus* group (Fig. 5) as compared to control.

Table 2. Histological activity index (HAI)

Groups	Congestion in vessels	Congestion in glomeruli	Congestion in tubules	Interstitial inflammation	Interstitial edema
Control	-	-	-	-	-
Cisplatin	+4	+3	+4	+1	-
C. intybus	+1	+1	-	-	-
Cisplatin +*C. intybus*	+1	+1	-	-	-

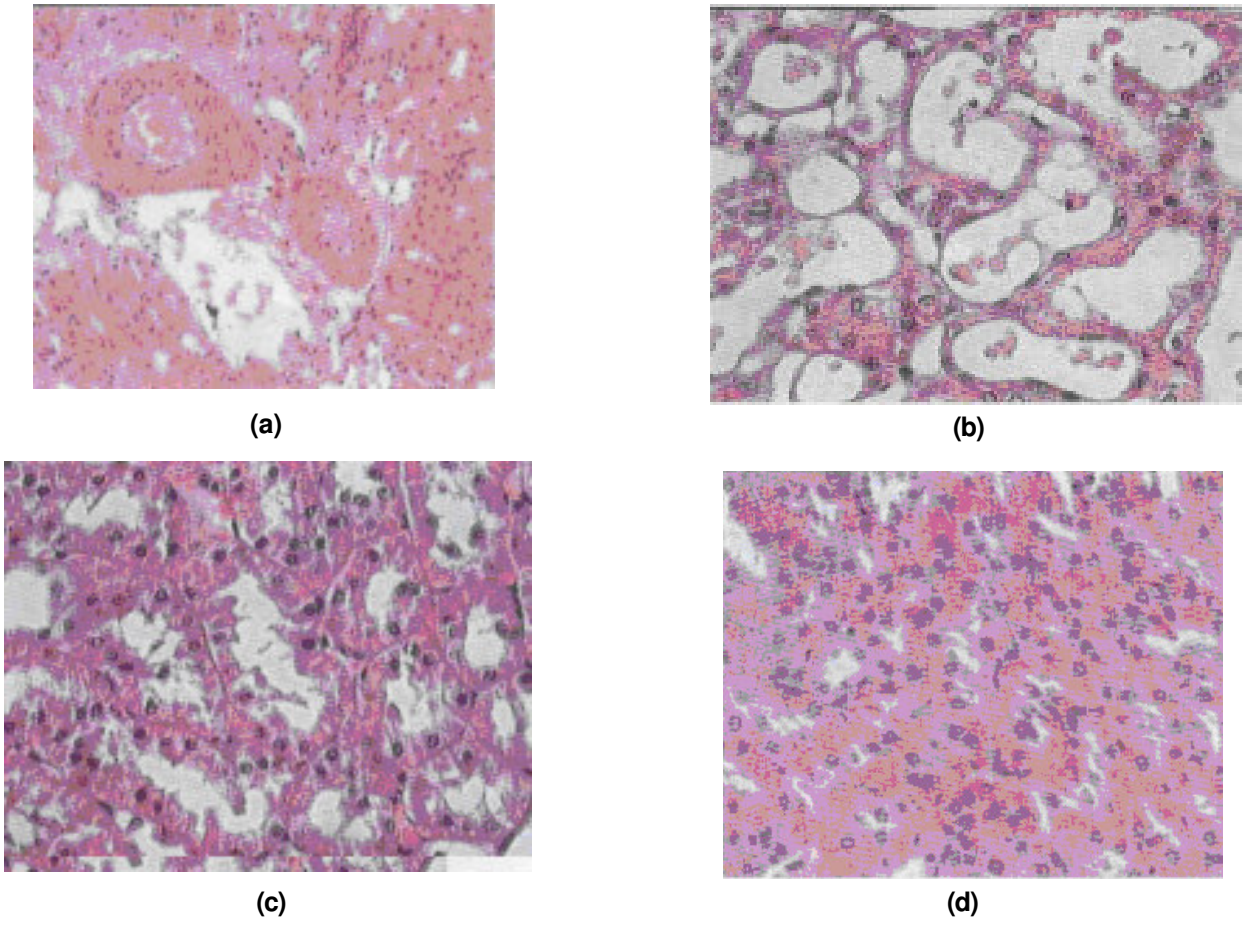

Fig. 2. (a-d) Histology of kidney in (a) control; (b) cisplatin treated rats; (c) *C. intybus* treated rats; (d) cisplatin + *C. intybus* pretreated rats.

(a) Normal kidney histology of control rats; (b) histological abnormalities after cisplatin administration for 5 alternate days; (c) *C. intybus* extract did not produce any histological alterations; (d) histological abnormalities and their prevention by *C. intybus* extract

Tissue MDA level. Figure 6 shows oxidative status in rat kidney after cisplatin treatment, *C. intybus* extract treatment and cisplatin with *C. intybus* extract treatment. Tissue MDA level increased in cisplatin treated rats. The correction of stress was indicated in CDDP + *C. intybus* group. *C. intybus* extract treatment alone showed significant decrease in MDA level ($1.20 \pm 0.35, P < 0.01$).

Tissue 4-HNE level. A significant increase in tissue 4-HNE was observed in cisplatin treated rats ($412.13 \pm 69.09, P < 0.01$) as compared to the control, indicating oxidative stress (Fig. 7). In CDDP + *C. intybus* group, 4-HNE level was not different as compared to the control group. *C. intybus* extract alone treatment produced no significant result.

Plasma nitrate level. Nitrate level in plasma was increased ($23.49 \pm 1.97, P < 0.01$) (Fig. 8) in cisplatin treated rats, indicating nitrosative stress. CDDP + *C. intybus* group showed slightly decreased nitrate level but results were not significant. *C. intybus* extract treatment solely showed no significant effect.

Tissue catalase level. Tissue catalase level decreased significantly ($25.8 \pm 2.5, P < 0.01$) in cisplatin treated group as compared to the control (Fig. 9). *C. intybus* extract prevented decrease in catalase level in CDDP + *C. intybus* group but results were not significant, while only *C. intybus* extract produced no significant effect.

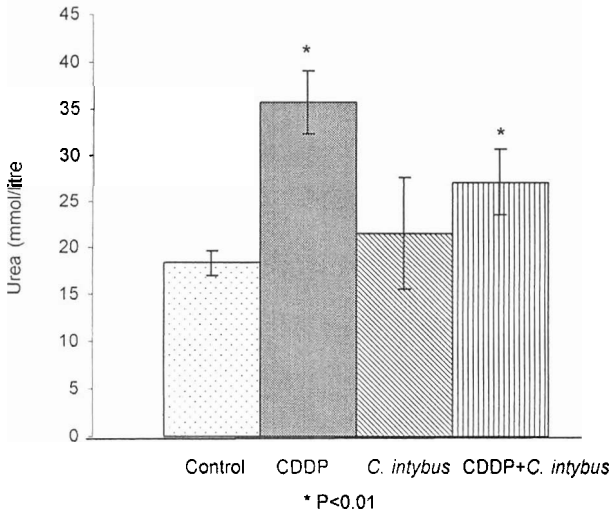

Fig. 3. Plasma urea level in the study groups.

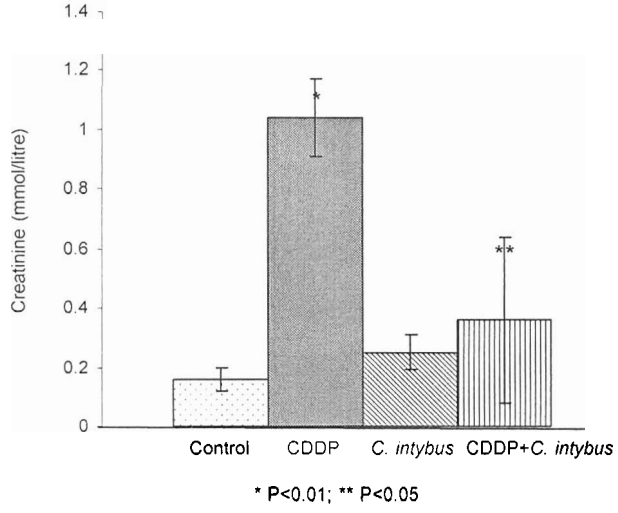

Fig. 4. Plasma creatinine level in the study groups.

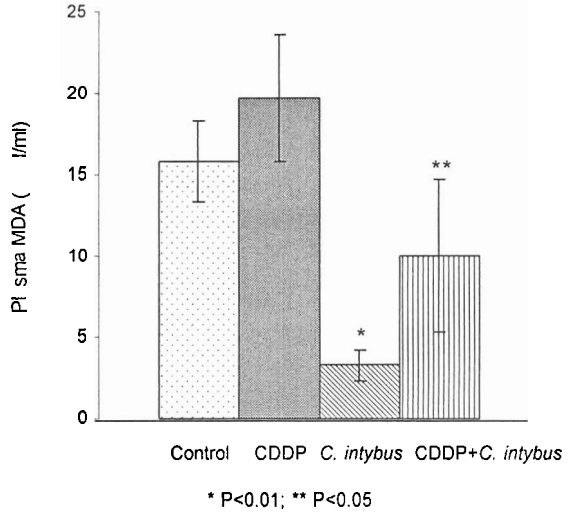

Fig. 5. Plasma MDA level in the study groups.

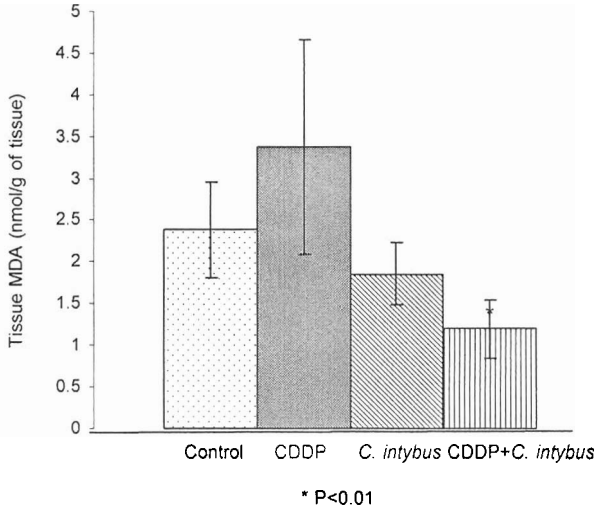

Fig. 6. Tissue MDA level in the study groups.

Tissue SOD level. Figure 10 shows a significant effect on cisplatin treated (17.61 ± 4.19, $P < 0.05$) rats. Cisplatin treatment decreased the SOD level significantly. In CDDP + *C. intybus* group the results were not different as compared to the control group. *C. intybus* extract alone produced no significant effect.

Reactive oxygen species (ROS) are constantly generated in our body. Production of ROS is essential for a number of biochemical reactions involved in the synthesis of prostaglandins, hydroxylation of proline and lysine, oxidation of xanthine and other oxidative processes. Excessive oxidation leads to impairment of cell functions and development of morbid conditions (Ames *et al*., 1993).

There is evidence that indigenous antioxidants may be useful in preventing the deleterious consequences of oxidative stress and there is increasing interest in the protective biochemical functions of natural antioxidants contained in spices, herbs and medicinal plants (Noda *et al*., 1997).

In the present study, the rats treated with cisplatin showed a decrease in body weight (Fig. 1). Mora *et al*. (2003) suggested that CDDP-induced weight loss might be due to gastrointestinal toxicity and reduced ingestion of food.

Plasma urea and creatinine levels significantly increased after administration of cisplatin (3 mg/kg) on 5 alternate days (Fig. 2(b), 3, 4), showing insufficiency of renal function.

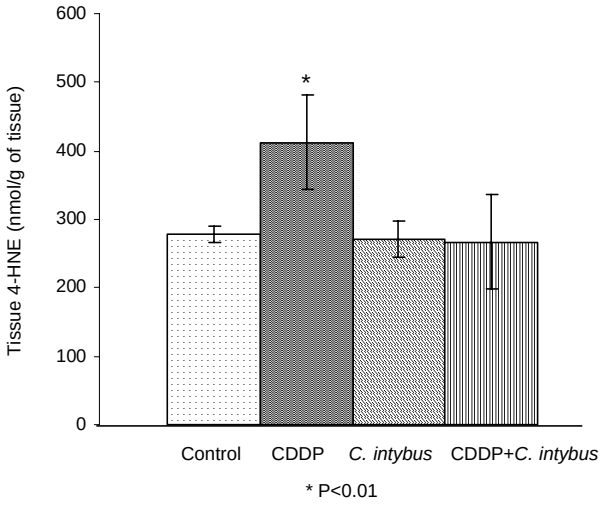

Fig. 7. Tissue 4-HNE level in the study groups.

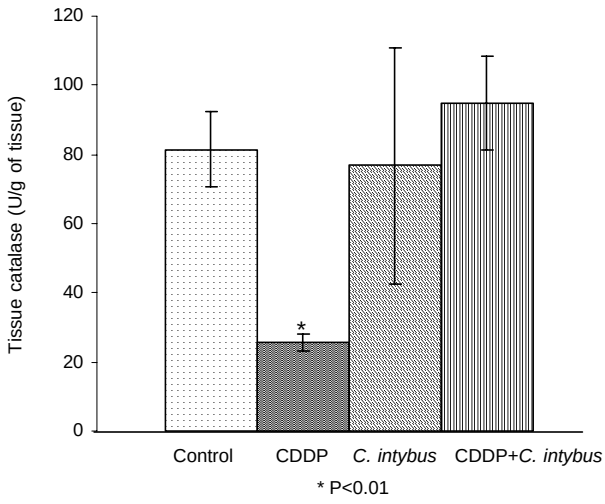

Fig. 9. Tissue catalase level in the study groups.

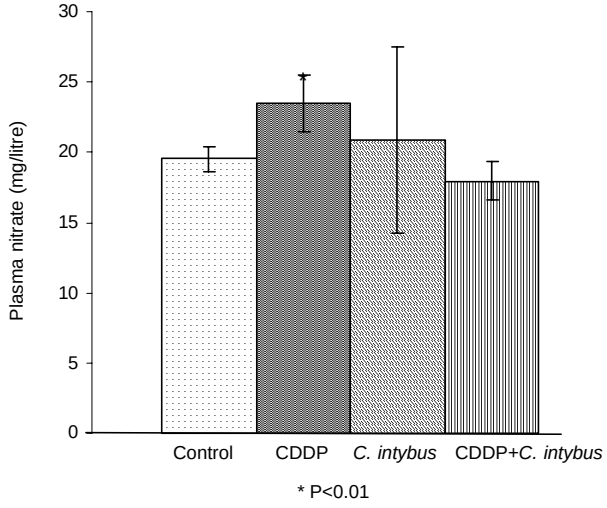

Fig. 8. Plasma Nitrate level in the study groups.

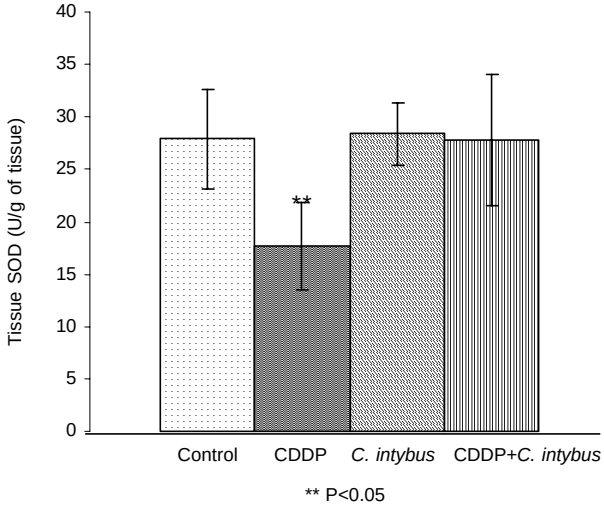

Fig. 10. Tissue SOD level in the study groups.

Studies in animals have established that tubular injury plays a central role in the reduction of glomerular filtration rate in acute tubular necrosis. Two major tubular abnormalities could be involved in the decrease in the glomerular function in cisplatin treated rats through obstruction and backleak of glomerular filtrate (Ozen *et al*., 2004).

Alterations in glomerular function in cisplatin-treated rats may also be secondary to reactive oxygen species (ROS) (Leena and Alaraman, 2005), which induce mesangial cells contraction, altering the filtration surface area and modifying the ultrafiltration coefficient factors that decrease the glomerular filtration rate (Ozen *et al*., 2004). In accordance with the previous findings, our result confirmed increased level of urea and creatinine in cisplatin treated group. A significant change in urea and creatinine levels, after pretreatment with *C. intybus* in cisplatin treated rats, provided an evidence of prevention of toxicity developed by cisplatin treatment (Fig. 2d, 3, 4).

Cisplatin induced oxidative stress is associated with increased level of MDA, 4-HNE and NO_3^{-2} (Fig. 5-8). Free radicals are known to play an important role in cisplatin-induced nephrotoxicity. The free radicals and reactive oxygen species induce oxidative stress in kidneys (Uslu and Bonavida, 1996).

MDA and 4-HNE (4-hydroxy-2-nonenal) are the end products produced by the decomposition of w_3 and w_6 polyunsaturated fatty acids (Yildirim *et al*., 2003). Due to cisplatin administration, platinum sulphydryl group complexes formed are taken up by renal cells and stabilized by intracellular GSH for several hours. In case of intracellular GSH depletion the complexes undergo rapid transformation to receive metabolites. This depletion seems to be the prime factor that permits lipid peroxidation and impairs antioxidant enzymes (Ban *et al*., 1994).

NO is able to react with O_2^- to produce $ONOO^-$, which is a powerful oxidant, more reactive than its precursors, and has been implicated in an increasing, acute renal ischemia (Ganther and Lawrence, 1997). The increase in renal $ONOO^-$ induced by cisplatin may be secondary to the increase in NO and O_2^- production. The O_2^- increase in nephrotoxicity due to cisplatin may be simply the consequence of the mitochondrial dysfunction (Chirino *et al*., 2004; Ozen *et al*., 2004) and the decrease in superoxide dismutase activity (Kadikoylu *et al*., 2004). The present investigation indicate that *C. intybus* extract produced no sign of toxicity in rats. Survival rate of rats in CDDP + *C. intybus* group showed protective effect of *C. intybus*. Alone *C. intybus* lead to marked decrease in tissue MDA level and slight decreased plasma MDA level. High intake of *C. intybus* may be responsible for less production of ROS.

Decreased antioxidant enzymes levels (SOD, catalase) observed in this study after cisplatin administration (Fig. 9-10), might be due to the loss of copper and zinc, which are essential for enzyme activity (Sharma, 1985). The decrease in SOD activity is insufficient to scavenge the superoxide anion produced during the normal metabolic process. The superoxide anion can cause initiation and progression of lipid peroxidation (Sheena *et al*., 2003).

Similarly, decreased catalase activity in cisplatin treated rats decreases the activity of kidney to scavenge the toxic H_2O_2 and lipid peroxides. Restoration of renal oxidative enzymes by pretreatment with *C. intybus* extract suggests the extract is capable of protecting the antioxidant enzymes.

The data discussed in this study shows that cisplatin treatment increased the MDA, 4-HNE and NO^-_3 and decreased SOD and catalase level, which implicated the nephrotoxic effect and produced the imbalance between oxidative status and antioxidant enzymes in kidney. Pretreatment with *C. intybus* counteracted these deleterious effects. The active phytochemicals other than gallic acid may have been responsible for antioxidant activity. However, alone *C. intybus* showed less production of ROS and decreased body weight, which intimates that high doses of *C. intybus* could interfere with the important biological functions. It is, therefore, suggested that the therapeutic doses of *C. intybus* could be adjusted for preventing cisplatin-induced nephrotoxicity. Moreover, combined therapy of *C. intybus* extract offers protective effect.

Acknowledgement

Financial grant from HEC is gratefully acknowledged.

References

Ahmad, K.D., Gilani, S.N., Akhtar, A.H., Khan, L. 1998. Antiulcerogenic evaluation of aqueous extracts of *Cichorium intybus* and *Phyllanthus emblica* in normal and aspirin treated rats. *Pakistan Journal of Scientific and Industrial Research* **41:** 92-96.

Ali, B.H., Al-Moundhri, M., Eldin, M.T., Nemmar, A., Al-Siyabi, S., Annamalai, K. 2008. Amelioration of cisplatin-induced nephrotoxicity in rats by tetramethylpyrazine, a major constituent of the Chinese herb *Lingusticum wallichi*. *Experimental Biology and Medicine* (Maywood) **233:** 891-896.

Ames, B.N., Shigenaga, M.K., Hagen, T.M. 1993. Oxidants, antioxidants and the degenerative diseases of aging. *Proceedings of National Academy of Sciences USA* **90:** 7915-7922.

Aslam, M. 2006. *Guidelines for Cultivation, Collection, Conservation and Propagation of Medicinal Herbs*, pp. 61. Ministry of Food, Agriculture and Livestock, Economic Division, Govt. of Pakistan, Islamabad.

Ban, M., Hettich, D., Huguet, N. 1994. Nephrotoxicity mechanism of *cis*-platinum(II) diamine dichloride in mice. *Toxicology Letters* **71:** 161-168.

Bodenner, D.L., Dedon, P.C., Keng, P.C., Katz, J.C., Borch, R.F. 1986. Selective protection against cis-diamminedichloroplatinum(II)-induced toxicity in kidney, gut and bone marrow by diethyldithiocarbamate. *Cancer Research* **46:** 2751-2755.

Butler, A.R., Hussain, I., Leitch, E. 1981. The chemistry of the diacetyl monoxime assay of urea in biological fluids. *Clinica Chimica Acta* **112:** 357-360.

Chirino, Y.I., Hernandez-Pando, R., Pedraza-Chaverri, J. 2004. Peroxynitrite decomposition catalyst ameliorates renal damage and protein nitration in cisplatin-induced nephrotoxicity in rats. *BMC Pharmacology* **4:** 20.

Deiana, M., Arouma, O.I., Bianchi, M.P.L.P., Spencer, J.P.E., Kaur, H., Hallivell, B., Aeschbach, R., Banni, S., Dessi, M.A., Chorongiu, F.P. 1999. Inhibition of peroxinirite dependent DNA base modification and tyrosine nitration by the extra virgin olive oil-derived antioxidant hydroxytyrosol-A reinvestigation. *Free Radical Biology and Medicine* **26:** 762-769.

Devasagayam, T.P.A., Tilak, J.C., Boloor, K.K. 2004. Review: Free radicals and antioxidants in human health; Current status and future prospects. *Journal of the Association of Physicians of India* **52:** 794-804.

Ganther, H.E., Lawrence, J.R. 1997. Chemical transformations of selenium in living organisms. Improved forms of selenium for cancer prevention. *Tetrahedron* **53:** 12299-12310.

Gilani, A.H., Janbaz, K.H., Shah, B.H. 1998. Esculetin prevents liver damage induced by paracetamol and CCl4. *Pharmacological Research* **37:** 31-35.

Greggi Antunes, L.M., Darin, J.D.C., Bianchi, M.deP. 2001. Effects of the antioxidants curcumin or selenium on cisplatin-induced nephrotoxicity and lipid peroxidation in rats. *Pharmacological Research* **43:** 145-150.

Hamers, F.P.T., Gispen, W.H., Neijt, J.P. 1991. Neurotoxic side effects of cisplatin. *European Journal of Cancer* **27:** 372-376.

Health Research Extension Act 1985. *Animals in Research*. Public Law 99-158, November 20, 1985. U.S. Department of Health and Human Services.

Hussain, K., Shahzad, A., Hussnain, S.Z. 2008. An ethnobotanical survey of important wild medicinal plants of Hattar District Haripur, Pakistan. *Ethnobotanical Leaflets* **12:** 29-35.

Jiao, H., Wang, S.Y. 2000. Correlation of antioxidant capacities to oxygen radical scavenging enzyme activities in blackberry. *Journal of Agricultural and Food Chemistry* **48:** 5672-5676.

Jitoe, A., Masuda, T., Tengah, I.G.P., Suprapta, D.N., Gara, I.W., Nakatani, N. 1992. Antioxidant activity of tropical ginger extracts and analysis of the contained curcuminoids. *Journal of Agricultural and Food Chemistry* **40:** 1337-1340.

Khan, A.M., Aslam, M. 2004. *Medicinal Plants of Balochistan*, pp. 3-44. Project on Introduction of Medicinal Herbs and Species as Crop. Ministry of Food, Agriculture and Livestock, Government of Pakistan.

Kikuzaki, H., Nakatani, N. 1993. Antioxidant effects of some ginger constituents. *Journal of Food Science* **58:** 1407-1410.

Kikuzaki, H., Usuguchi, J., Nakatani, N. 1991. Constituents of Zingiberaceae I. Diarylheptanoids from the rhizomes of ginger (*Zingiber officinale* roscoe). *Chemical and Pharmaceutical Bulletin* **39:** 120-122.

Kinter, M. 1996. *Free Radicals-A Practical Approach*, N. A. Punchard and G. J. Kelly (eds.), 136 p. Oxford University Press, Oxford, UK.

Kadikoylu, G., Bolaman, Z., Demir, S., Balkaya, M., Akalin, N., Enli, Y. 2004. The effects of desferrioxamine on cisplatin-induced lipid peroxidation and the activities of antioxidant enzymes in rat kidneys. *Human and Experimental Toxicology* **23:** 29-34.

Kono, Y. 1978. Generation of superoxide radical during autooxidation of hydroxyalamine and an assay for superoxide dismutase. *Archives of Biochemistry and Biophysics* **186:** 189-195.

Lee, S.E., Hwang, H.J., Ha, J.S., Jeong, H.S., Kim, J.H. 2003. Screening of medicinal plant extracts for antioxidant activity. *Life Science* **73:** 167-179.

Lee, K.G., Shibamoto, T. 2000. Antioxidant properties of aroma compounds isolated from soybeans and mung beans. *Journal of Agricultural and Food Chemistry* **48:** 4290-4293.

Leena, P., Alaraman, B.R. 2005. Effect of green tea extract on cisplatin induced oxidative damage on kidney and testes of rats. *ARS Pharmaceutica* **46:** 5-18.

Maliakel, D.M., Kagiya, T.V., Nair, C.K. 2008. Prevention of cisplatin-induced nephrotoxicity by glucosides of ascorbic acid and alpha -tocopherol. *Experimental Toxicology and Pathology* **60:** 521-527.

Matsushima, H., Yonemura, K., Ohishi, K., Hishida, A. 1998. The role of oxygen free radicals in cisplatin-induced acute renal failure in rats. *Journal of Laboratory and Clinical Medicine* **131:** 518-526.

Mora, L.deO., Antunes, L.M., Francescato, H.D., Bianchi, M., deL. 2003. The effects of oral glutamine on cisplatin-induced nephrotoxicity in rats. *Pharmacological Research* **47:** 517-522.

Nandagopal, S., Ranjitha Kumari, B.D. 2007. Phytochemical and antibacterial studies of Chicory (*Cichorium intybus* L) - A multipurpose medicinal plant. *Advances in Biological Research* **1:** 17-21.

Noda, Y., Anzai Kmori, A., Kohono, M. 1997. Hydroxyl and superoxide anion radical scavenging activities of natural source antioxidants using the computerized JES-FR30 ESR spectrometer system. *Biochemistry and Molecular Biology International* **42:** 35-44.

Ohkawa, H., Ohishi, N., Yagi, K. 1979. Assay for lipid peroxides in animal tissues by thiobarbituric acid reaction. *Analytical Biochemistry* **95:** 351-358.

Ozen, S., Akyol, O., Iraz, M., Sogut, S., Ozugurlu, F., Ozyurt, H., Odaci, E., Yildirim, Z. 2004. Role of caffeic acid phenethyl ester, an active component of propolis, against cisplatin-induced nephrotoxicity in rats. *Journal of Applied Toxicology* **24:** 27-35.

Rehmat, S., Shah, U., Hassan, G., Rehman, A., Ahmed, I. 2006. Ethnobotanical studies of the flora of district Musakhel and Barkhan in Balochistan, Pakistan. *Pakistan Journal of Weed Science Research* **12:** 199-211.

Sharma, R.P. 1985. Interactions of cisplatinum with cellular zinc and copper in liver and kidney tissues. *Pharmacological Research Communication* **17:** 197-206.

Sheena, N., Ajith, T.A., Janardhanan, K.K. 2003. Prevention of nephrotoxicity induced by the anticancer drug cisplatin, using *Ganoderma lucidum*, a medicinal mushroom occuring in south India. *Current Science* **85:** 478-482.

Sinha, K.A. 1972. Colorimetric assay of catalase. *Analytical Biochemistry* **47:** 389-394.

Spierto, F.W., Macneil, M.L., Burtis, C.A. 1979. The effect of temperature and wavelength on the measurement of creatinine with the Jaffe's procedure. *Clinical Biochemistry* **12:** 18-21.

Uslu, R., Bonavida, B. 1996. Involvement of the mitochondrion respiratory chain in the synergy achieved by treatment of human ovarian carcinoma cell lines with both tumour necrosis factor-alpha and cis-diamminedichloroplatinum. *Cancer* **77:** 725-732.

Varotto, S., Lucchin, M., Parrini, P. 2000. Immature embryos culture in Italian red chicory (*Cichorum intybus*). *Plant Cell Tissue and Organ Culture* **62:** 75-77.

Yildirim, Z., Sogut, S., Odaci, E., Iraz, M., Ozyurt, H., Kotuk, M., Akyol, O. 2003. Oral erdosteine administration attenuates cisplatin-induced renal tubular damage in rats. *Pharmacological Research* **47:** 149-156.

Technology

Pak. J. Sci. Ind. Res. 2009 **52** (4) 217-227

Effects of Biodiesel from Soybean Oil on the Exhaust Emissions of a Turbocharged Diesel Engine

Asad Naeem Shah[ab]*, G. E. Yun-shan[a], TAN Jian-wei[a] and He Chao[c]

[a]School of Mechanical and Vehicular Engineering, Beijing Institute of Technology, Beijing 100081, P.R. China
[b]Department of Mechanical Engineering, University of Engineering and Technology, Lahore 54000, Pakistan
[c]School of Transportation, Mechanical and Civil Engineering, Southwest Forestry College, Kunming, 650224, P.R. China

(received August 23, 2008; revised June 2, 2009; accepted June 8, 2009)

Abstract. This paper presents the regulated emissions in the light of cylinder pressure and heat release rate (HRR) from a 4-stroke direct injection (DI) diesel engine fuelled with neat soybean oil-based biodiesel, commercial diesel and 20% biodiesel-diesel blend. The engine was run using electrical dynamometer at four different engine conditions. The experimental results revealed that brake power (BP) of the engine decreased but brake specific fuel consumption (BSFC) increased with biodiesel as compared to diesel. Relative to diesel, the maximum combustion pressure (MCP) was higher; however, HRR curves were not much deeper in the ignition delay (ID) periods and the premixed combustion peaks were lower with biodiesel. Carbon monoxide (CO), total hydrocarbons (HC), smoke opacity, and particulate matter (PM) emissions decreased by 3% to 14%, 32.6% to 46%, 56.5% to 83%, and 71% to 87.8%, respectively; however, oxides of nitrogen (NO_x) increased by 2% to 10% with biodiesel, compared to the commercial diesel. Both smoke and NO_x pollutants were greatly influenced by the MCP. CO, HC, and PM emissions were higher at lower load conditions compared to higher load conditions, but NO_x and smoke pollutants were higher at higher load conditions relative to lower load conditions.

Keywords: diesel engine, direct injection, biodiesel, heat release rate, regulated emissions

Introduction

In the face of the unrelenting use of fossil fuels and its determental effects on human life and environment, finding alternative sources of energy has gained particular significance. Biodiesel, commonly referred to fatty acid methyl or ethyl esters, is produced by the transesterifcation process of the vegetable oils, waste cooking oils and animal fats in the presence of methanol or ethanol as catalyst. It is gaining increasing attention as alternative fuel for diesel engines over the past few years, owing to its clean burning and environmental friendly characteristics. It is renewable, technically feasible, environmentally acceptable, and readily available substitute fuel (Correa and Arbilla, 2006). It has ultra low sulphur (Ebiura *et al*., 2005) and is non toxic and biodegradable (Turrio-Baldassarri *et al*., 2004) with improved lubricating efficiency (Agarwal *et al*., 2003), higher flash point, higher cetane number and high oxygen content (Krahl *et al*., 2003). According to Ramadhas *et al*. (2005), biodiesel and its blends with fossil diesel can be used as alternative fuels in compression ignition (CI) engine without modification or adjustment in it.

In, Germany, Italy, France, Austria and Sweden, other European Community member countries and USA, specific legislations have been enacted to promote the production and use of biodiesel (Dube *et al*., 2007; Demirbas, 2007; Korbitz, 1999; Krawczyk, 1996).

India is producing around 6.7 million tons of non-edible oils from plants such as Karanji *(Pongamia glabra)*, castor, linseed, neem *(Azadirachta indica)*, kusum *(Schleichera trijuga)*, and palash (*Butea monosperma*) (Agarwal *et al*., 2003).

Many studies focussed on regulated emissions have revealed that biodiesel reduces CO, HC and PM emissions (Raheman and Ghadge, 2007; Lebeckas and Slavinskas, 2006; Dorado *et al*., 2003). However, if some authors claim decrease in NO_x pollutants with biodiesel (Agarwal and Rajamanoharan, 2009; Dorado *et al*., 2003; Peterson and Reece, 1996), majority has unanimously reported that NO_x emissions increase with biodiesel (Karabektas *et al*., 2008; Szybist *et al*., 2007; Agarwal *et al*., 2006; Usta, 2005). These discordant findings concerning the emissions of NO_x pollutants are still a dilemma for researchers working on the exhaust emissions of diesel engines fuelled with biodiesel, particularly when the engine is unmodified.

The current work is an effort to investigate, and hence compare the exhaust emissions including CO, HC, smoke and PM

*Author for correspondence; E-mail: naeem_138@hotmail.com

pollutants from an unmodified diesel engine fuelled with biodiesel (B100), diesel (D), and 20% biodiesel-80% diesel (v/v) blend (B20), together with cylinder pressure and heat release studies at different engine conditions. In addition to this, it has also been attempted to study the brake power (BP) and brake specific fuel consumption (BSFC) of the engine at these engine conditions. Prior to this, the authors have reported that B100 and B20 have shorter ignition delay, less maximum rate of pressure rise (MRPR), less brake specific energy consumption (BSEC), a low premixed combustion amount, early start of fuel injection, higher maximum combustion pressure (MCP), and more BSFC compared to fossil diesel (Shah *et al.*, 2009a).

Materials and Methods

Test engine, fuels and working conditions. The tests were performed on a turbocharged, direct injection, heavy duty and intercooled diesel engine (FAW-WDEW 4CK, China made) having a mechanical injection system and working without exhaust gas recirculation (EGR) or any other devices. No modification or adjustment was made in the engine. Detailed specifications of the engine (Shah *et al.*, 2009a, 2009b, 2008), are listed in Table 1. The engine was run on an electrical dynamometer (Schenck HT350, Germany) as shown in Fig. 1.

Three test fuels D, B100, and B20 were used in this study, using D as a reference or baseline fuel. Biodiesel was produced from the soybean oil by the process of transesterification, and the diesel was purchased from the pump, and is representative of fuel being sold in Beijing, China. The main properties of the test fuels are given in Table 2.

Table 1. Engine specifications.

Number of cylinders	4
Bore (mm)	110
Stroke (mm)	125
Displacement (litre)	4.752
Compression ratio	16.8
Rated power (KW/rpm)	117/2300
Maximum torque (N.m/rpm)	580/1400
Nozzle hole diameter (mm)	0.23
Number of nozzle holes	6

The experiments were performed in accordance with the engine conditions given in Table 3. Maximum torque speeds (1400 r/min and 1800 r/min) were selected for the study. The engine load (torque) was measured with the help of torque flange and was read along with speed and throttle position directly on monitor supported by a software "Automation System STARS Rev. 1.5" in the control room. In order to measure the fuel flow rate, PLU (Pier Berg) was used, and fuel flow rate was also read in the control room. Crank angle was found with the help of a sensor (2613A, Kistler Corporation) giving a signal for the top dead center (TDC) and the instantaneous pressure in the cylinder was found receiving the signals through Piezo-electric sensor (6125B, Kistler Corporation). These signals were stored on a high speed computer based

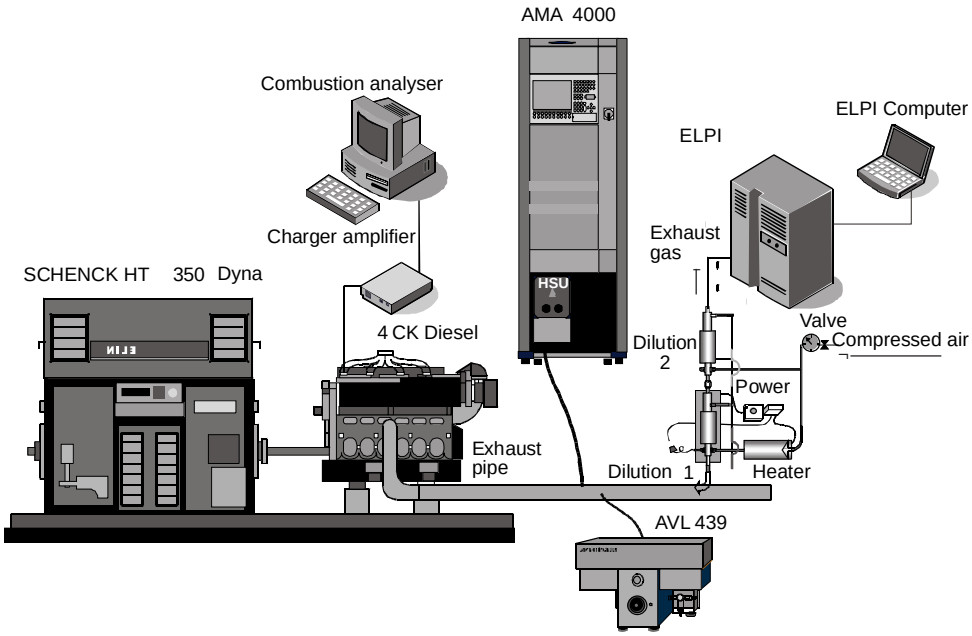

Fig. 1. Experimental setup.

Table 2. Properties of fuels.

Properties	Fuels and blends			Test Method*
	B100	B20	D	
Density (kg/m^3)	875	845.5	841	SH/T 0604
Viscosity (mm^2/s) at 20 ºC	7.1	4.3	4.0	GB/T 265
Lower heating value (MJ/kg)	37.3	41.7	42.8	GB/T 384
Sulphur content (mg/litre)	24.5	n/a	264	SH/T 0253-92
Cetane number	60	n/a	52	GB/T 386-91
Carbon content (%)	77	n/a	87	SH/T 0656-98
Hydrogen content (%)	12	n/a	13	SH/T 0656-98
Oxygen content (%)	11	n/a	0	Element analysis

*Chinese standard

Table 3. Engine conditions.

	Speed (r/min)	Load (%)
Engine condition 1	1400	10
Engine condition 2	1400	50
Engine condition 3	1800	50
Engine condition 4	1800	75

digital data acquisition system and were processed with specially developed software using combustion analyzer dewetron (DEWE-5000). Heat release analysis (HRA) was carried out with a special software using Dewetron (DEWE-5000). HRA was performed in accordance with the first law of thermodynamics using single-zone model and making simplified assumptions (Heywood, 1988). In order to measure the temperatures of engine oil and coolant, PT-100 (sensors) were used, while exhaust temperature was measured using thermocouple (k-series).

Exhaust emissions such as HC, CO, and NO_x were measured by heated flame ionization detector (FID), non-dispersive infrared analyzer (NDIR), and chemiluminescent detector (CLD), respectively, using analytical package AMA4000 (Austria). Smoke was measured with an opacimeter using AVL439, which measured the opacity of the exhaust emissions in term of light extinction coefficient (m^{-1}).

For the calculation of PM mass, electrical low pressure impactor (ELPI, Dekati Ltd. Finland) was used. An ELPI is a real time particle number concentration measuring device (Shah *et al.*, 2009b). It consists mainly of corona charger, a low pressure cascade impactor and a multichannel electrometer. Prior to introduction to the impactor, the particles are charged by the corona charger where the aerosol is cut-off by different size scopes, and thus electrometer detects their current which is converted into a particle concentration (He, *et al.*, 2008). In order to avoid overloading of the electrometer, the exhaust gas was diluted with dry, particle free and pressurized air using an ejector diluter (Dekati Ltd. Finland) having an overall dilution ratio of 64. The ejector diluter consists of a set of filters, a dryer, a temperature controller, a pressurized air heater and two diluters having a dilution ratio of 8 for each. The detailed specifications of the above discussed equipments are listed in Table 4.

Results and Discussion

Effect of biodiesel on BP and BSFC. As shown in the Fig. 2 (a), brake power (BP) of the engine was almost unaffected by B20; however, it decreased by 5.8%, 1.5%, 2.7%, and 3.3% at

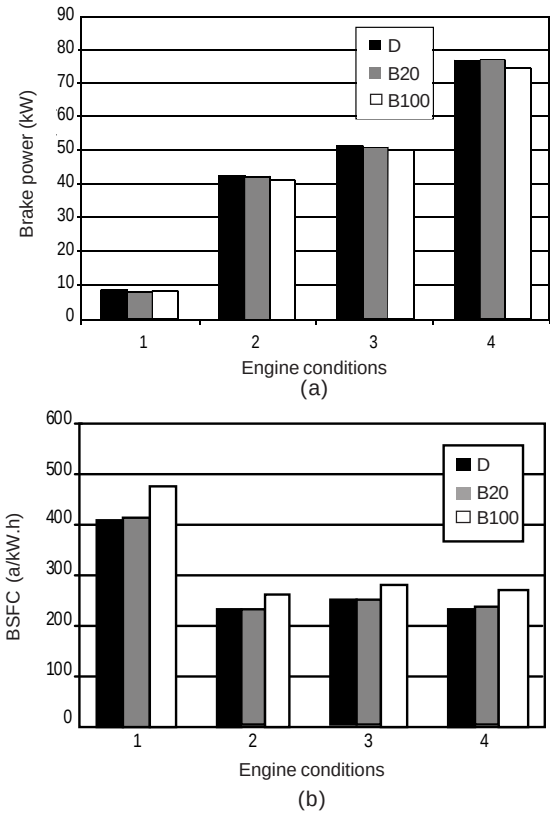

Fig. 2. Effect of biodiesel on (a) brake power and (b) BSFC, at different conditions.

engine conditions 1, 2, 3, and 4, respectively, in case of B100 compared to commercial diesel. This finding is consistent with those of previous studies that BP decreases with the use of biodiesel as compared to diesel (Lin *et al*., 2006). Kaplan *et al.* (2006) compared biodiesel from sunflower oil and fossil diesel and reported that the loss of torque and power ranged between 5% and 10%.

Brake specific fuel consumption (BSFC) is the mass of fuel consumed per brake power (kW) developed by the engine in one hour. Fig. 2 (b) shows a noticeable increase in BSFC of the engine with B100; however, there was a nominal increase in it with B20, relative to diesel. In case of B100, BSFC increased by 16.4%, 14.4%, 14%, and 17% at engine conditions 1, 2, 3, and 4, respectively, as compared with the diesel fuel. These findings are in good agreement with those of earlier studies (Turrio-Baldassarri *et al.*, 2004; Alam *et al.*, 2004). The Southwest Research Institute of USA has reported that fuel consumption with biodiesel from pure soybean oil increased from 13% to 18%, compared with diesel, while with B20, variation in BSFC ranged from -3% to 9% (Wedel,1999).

This decrease in BP and increase in BSFC with B100 is attributed to the lower heating value and more density of the biodiesel compared to fossil diesel. Tsolakis (2006) has reported that higher bulk modulus of biodiesel helps the pressure to be developed faster in the fuel injection system compared to the lower bulk modulus of diesel. Consequently, the fuel injection commences earlier in case of biodiesel with higher pressure and rate, resulting in the increase in mass of biodiesel compared to that of diesel at the same crank angle in degree (CAD). According to Choi *et al.* (1997), higher viscosity of biodiesel is helpful in reducing the fuel losses during the injection process compared to diesel. This reduction in fuel losses helps in faster development of pressure, and hence advances the injection timing.

Effect of biodiesel on the combustion. Figure 3 presents the cylinder pressure and HRR of the engine for the three test fuels used in this study. It is obvious that MCP of the engine is higher with B20 and B100, relative to diesel for all the engine conditions. Although the increase in MCP with B20 is very small, it becomes noticeable with B100 at all the engine conditions. Particularly at engine conditions 2 and 4, the MCP with B100 becomes 5.5% and 4.7% higher, respectively, relative to diesel fuel.

This increase in MCP with B100 and B20 is attributed to their physical and chemical properties. Higher cetane number, better fuel atomization, faster flame propagation speed, higher density, lower compressibility (higher bulk modulus), oxygen

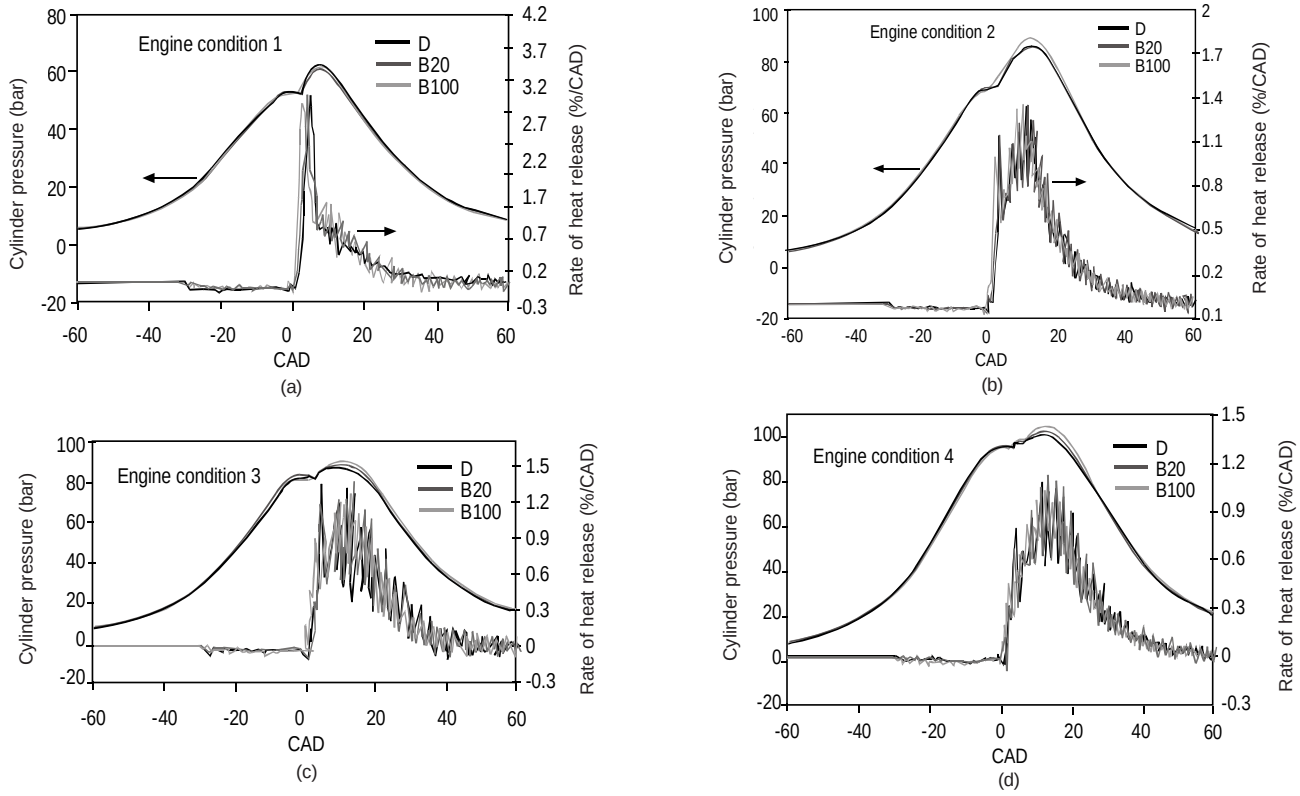

Fig. 3. Effect of biodiesel on the combustion of engine at different conditions.

enrichment and simple chemical structure of the biodiesel are responsible for advancing the combustion process. Higher cetane number of biodiesel reduces the ignition delay, thus results in earlier combustion due to which MCP becomes higher with B100 and B20, relative to diesel (Shah *et al.*, 2009a). Furthermore, biodiesel is an alkyl ester containing internal oxygen atoms which promote the burning of impurities under the same condition of use (Kegl, 2008).

In order to study the HRR, it is important to understand the premixed and diffusion combustion periods. The lowest point on HRR curve between premixed combustion peak and diffusion combustion peak is the point which divides the combustion into premixed and diffusion periods (Xiaoming *et al.*, 2005). According to Zhang and Van Gerpen (1996), heat release curves show a negative trend during the ignition delay period due to endothermic reaction in the combustion chamber (CC), which becomes positive when auto-ignition occurs. Heat release curves are deeper with diesel during this ID period; particularly, at engine condition 3 and 4 the trends are more prominent and distinguishable as shown in the Fig. 3. This indicates smaller endothermic heat with biodiesel, and hence justifies the claim that biodiesel having higher cetane number exhibits shorter ID.

Heat release curves reflect smaller premixed burning peaks with biodiesel, relative to diesel as shown in Fig.3. This may be due to the lower volatility and shorter ID with biodiesel compared to diesel. In case of diesel fuel, more fuel-air mixture is formed due to longer ID, which produces a larger premixed burn peak (Zhang and Van Gerpen, 1996).

Effect of biodiesel on the emissions. ***CO Emission.*** As presented in Fig. 4 (a), CO emissions decrease with B100 and B20 compared to diesel. Relative to diesel, B20 exhibits 19%, 12.5%, 12.3%, and 6.8% reduction in CO pollutants at engine conditions 1, 2, 3, and 4, respectively. There is 2.9%, 5%, 14.2%, and 6.8% decrease in CO emissions with B100 at engine conditions 1, 2, 3, and, 4 respectively, compared with commercial diesel. Similar results have also been reported by other researchers (Choi *et al.*, 1997; Krahl *et al.*, 1996). Last *et al.* (1995) fuelled a 4-stroke DI heavy duty engine with 10%, 20%, 30%, 50% and 100% biodiesel from soybean oil and reported that with respect to diesel fuel there were 10%, 8%, 18%, 6% and 14% reductions in CO emissions, respectively.

The oxygen enrichment and simple chemical structure of biodiesel are major contributors to the reduction of CO emissions with B100 and B20, compared with diesel. The oxygen enrichment in biodiesel promotes the combustion, hence reduces the CO emissions. Unlike fossil diesel, biodiesel has minor short-chain compounds capable of being converted to carbon dioxide (CO_2) more easily (Guarieiro *et al.*, 2008), and thus results in better oxidation and complete combustion. Higher cetane number is also an important factor for the reduction of the possibility of fuel-rich mixture formation, and hence for the reduction of CO emissions (Hansen and Jensen, 1997). Moreover, earlier start of fuel injection, shorter ID and MCP also play a vital role in the reduction of CO emissions.

The experimental results show that CO emissions are higher at condition 1 relative to condition 2 and at condition 3 relative to condition 4, for all the test fuels. This may be due to the large excessive air-fuel ratio and relatively larger ID at low loads (conditions 1 and 3) compared to higher loads (conditions 2 and 4) for the respective speeds. Consequently over-lean mixture area increases, and thus oxidation rate is decreased.

It is also evident from Fig. 4 (a) that CO emissions are higher at engine condition 3 relative to condition 2 which means these emissions are higher at higher speed relative to lower speed for all the test fuels. This increase in CO pollutants can be attributed to decrease in the temperature in the CC at higher speed compared to lower speed, because higher speeds increase the turbulence in the CC, and hence increase the heat loss to the CC walls, ultimately reducing the combustion temperature (Shah *et al.*, 2008). Moreover, Collier *et al.* (1995) have also reported that engine speed affects the swirl characteristics, injection timing and combustion temperature of the engine. So, this relatively lower temperature in CC plays an effective role in the reduction of oxidation rate of CO, and results in the increase of CO emissions.

HC emissions. HC emissions decrease by 19%, 20%, 20.8%, and 13% with B20 at engine conditions 1, 2, 3, and 4, respectively, relative to diesel fuel (Fig. 4(b)). The abatements in HC pollutants with B100, compared with the diesel are 43.8%, 44.6%, 46.3%, and 32.6% at engine conditions 1, 2, 3, and 4, respectively. These findings are consistent with those of Peterson and Reece (1996) who performed experiments on a diesel engine fuelled with blends of biodiesel with and without catalytic converter, and reported 50% reduction in HC emissions. Similar findings were also claimed by Last *et al.* (1995) who fuelled the engine with 10%, 20%, 30%, 50% and 100% biodiesel from soybean oil and reported that with respect to diesel fuel there were 28%, 32% and 75% reduction in HC emissions with 10%, 20% and 100% biodiesel, respectively.

Possible reasons for the reduction of HC emissions with biodiesel are additional oxygen content leading to more com-

plete and cleaner combustion, higher cetane number resulting in reduction in ID and the advanced fuel injection causing the increase in MCP, thus increasing the combustion temperature. Moreover, higher final distillation points for diesel fuel causes incomplete vaporization and burning of its final fraction, thus increasing the HC emissions with diesel (Turrio-Baldassarri *et al.*, 2004).

Fig. 4 (b) reveals more HC emissions at engine condition 1 relative to condition 2, and at engine condition 3 relative to condition 4 for the three test fuels. It also shows that HC pollutants are almost same at engine conditions 3 and 4 for the test fuels. Reasons for more HC emissions at lower loads relative to higher loads are the same as those for CO emissions.

NO_x emissions. B20 exhibits a nominal increase in NO_x pollutants at engine conditions 1 and 2; however, it reflects 2.2% and 5.5% increase in them at conditions 3 and 4, respectively, relative to diesel (Fig. 4(c)). In case of B100, there are 2%, 10%, 3.4%, and 7% increase in NO_x emissions at engine conditions 1, 2, 3, and 4, respectively, compared with diesel fuel. These results are in good agreement with those of other studies (Karabektas, *et al.*, 2008; Szybist *et al.*, 2007; Agarwal *et al.*, 2006; Usta, 2005).

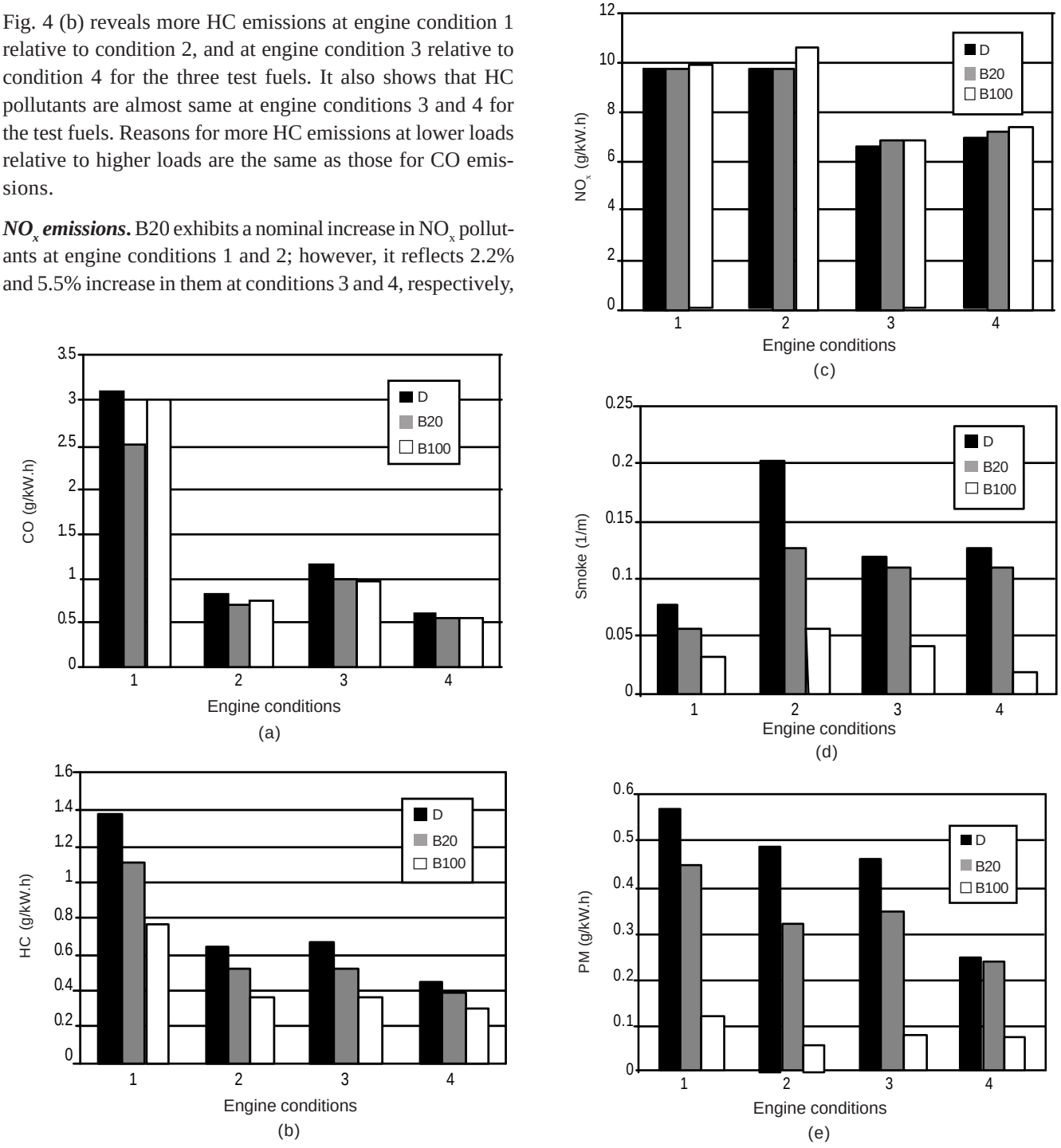

Fig. 4. Effect of biodiesel on (a) CO; (b) HC; (c) NOx; (d) smoke and (e) PM emissions.

Table 4. Specifications of the equipments used in the study

Dynamometer	Company: $Dynas_3$ Schenck Pegasus GmbH; Standard delivery scope: AC induction motor, torque measuring flange, speed measuring system, variable frequency driver, digital test standard controller x-actDE; asynchronous machine: radial forced draft, frequency exchange by eddy current brake, speed up to 10,000 r/min, low mass moment of inertia; frequency converter: high dynamical field-oriented current and torque regulation; full four quadrant operation, double IGBT technique; integrated main filter; torque-meter and speed acquisition: dynamically correct, high mechanical overload capacity, availability of an electronic R-cal, short and low inertia torque flange; speed acquisition: two separate sensors for converter and test standard control, 512 marks/revolution for $Dynas_3$ LI and HT, 1024 marks/revolution for $Dynas_3$ HD.
Fuel flow rate measuring device	Company: Pierburg-Gruppe PLU, Pierburg Luftfahrt Gearate Union GmbH, NEUSS; PLU V2: nominal measuring range 1 = 0.5...60 L/h, nominal measuring range 2 = 1...120 L/h; standard equipment: PLU 4000, temperature sensor PT 100 with transducer; optional equipment: inlet pressure reducers (regular fuels and alcohol-resistant), density meter with built-in PT1000 temperature sensor.
AMA 4000	Company: Pierburg Instruments GmbH Neuss Germany; flow rate: 10-15 L/min; dimensions: 665 mm × 900 mm × 2000 mm (W × D × H); weight: 450 kg; power distributor: 115V ± 10% 50/60 Hz, 230 V ± 10% 50/60 Hz; response time T-90 (via cooler): 3 sec (FID); ambient conditions: sample input pressure = ±300 hPa, temperature = 5-35°C; humidity = 5-80 %; FID 4000 (for non-diluted hot measurements): THC = 0 – 20.000 ppm C_3 (4 measuring ranges definable), CH_4 = 0 – 20.000 ppm C_1; CLD 4000 (for non-diluted hot measurements): NO_x = 0 – 10.000 ppm (4 measuring ranges definable); IRD 4000 measuring ranges: CO h = 0 – 10%, CO_2 h = 0 – 20% (4 measuring ranges difinable).
Combustion analyzer (DEWE-5000)	Company: DEWETRON GESMBH, Graz, Austria; no. of slots for DAQ or PAD modules: 16; total PCI – slots: 5; weight of the instrument: 17 kg; hard disk: 250 GB; data throughout: 30 to 45 MB/s; Power supply: 90 to 260 V_{ac}; display: 1280 × 1024 pixel; processor: Intel Pentium 4 (2.8 G Hz); Ram: 1 GB; operating system: Microsoft WINDOWS XP Professional; operating temperature: 0 - 50°C; storage temperature: -20 to +70°C; humidity: 10 to 80% non cond.
AVL 439 (Opacimeter)	Company: AVL GmbH Graz Austria; application area: engine test beds for static and steady state modes; method of operation (measurement principle): Beer-Lambert Law; gas flow rate: 40…45 L/min; measuring unit: measuring chamber, light unit, detector unit; warm up time: 20-30 min; measuring value out put: opacity N [%] or absorption k [m^{-1}]; measuring range: N = 0…100 % or k = 0…10 m^{-1}; rise time: 0.1 sec (at flow rate 40 L/min); sampling rate for opacity signal: 50 Hz; exhaust gas temperature: 0…600°C; Exhaust gas pressure: -100-+400 mbar; power supply: 230 V; dimensions: 650 mm × 420 mm × 450 mm (W × H × D); weight: 47 kg.
Electrical low pressure impactor (ELPI)	Company: Dekati Ltd. Finland; particle size range: 0.03-10 ìm with filter stage 0.007-10 ìm; number of channels: 12; time resolution: 2-3 sec; Operating conditions: ambient temperature = 5-40°C, ambient humidity = 0-90% non-condensing; aerosol conditions: gas temperature = < 60°C and < 200°C with heated impactor; weight: 35 kg; electric power: 110/220-240 V, 50-60 Hz, 200W; pressure under the first stage: 100 mbar; pump specifications (10 lpm ELPI): minimum 7 m^3/h at 100 mbar abs; computer specifications: Pentium processor, color monitor, MS-Windows 95™, 98™, NT 4.0™, XP™ or 2000™.
ELPI dilutor	Company: Dekati Ltd., Finland; sample air flow (inlet): 10 or 30 L/min; diluted sample flow (outlet): 60 L/min; dilution ratio: 1:8; dilution air pressure: 2 bar; temperature (operating conditions): 0-450°C; total length: 360 mm; max.diametre: 120 mm; inlet, outlet and exhaust: 12 mm male pipe for each; dilution air: 8 mm female; material: AISI 316; gaskets: copper.

Increase in NO_x pollutants with biodiesel may be due to the improved combustion caused by the advanced injection discussed earlier. Monyem and Van Gerpen (2001) and Senatore *et al.* (2000) have also reported increase in NO_x emissions and the role of advanced injection. Moreover, high oxygen concentration in biodiesel plays a significant role in the increase of MCP and temperature and thus increases the NO_x pollutants with biodiesel compared to fossil diesel. According to Cardone *et al.* (2002), physical properties of biodiesel like viscosity, density, compressibility and sound velocity play a significant role in increasing the fuel injection duration and thus are responsible for advancing the combustion process. This advanced combustion causes the increase in NO_x emissions with biodiesel, relative to commercial diesel.

It is worthwhile to note that NO_x pollutants of biodiesel are 10% and 7% higher than those of diesel fuel at engine conditions 2 and 4, respectively. These are the conditions at which percentage difference of two fuels in terms of their NO_x is higher, compared with other two conditions (conditions 1 and 3). As discussed earlier, relative to diesel, biodiesel has 5.5% and 4.7% higher MCP at engine conditions 2 and 4, respectively, which means that the percentage difference of two fuels in terms of their MCP is also higher at engine conditions 2 and 4 compared to other two conditions 1 and 3. This implies that higher the MCP, more are the NO_x pollutants. Higher MCP indicates higher temperature in the cylinder which in turn is responsible for higher NO_x emissions. This is the reason for emission of more NO_x with biodiesel compared to diesel, particularly at engine conditions 2 and 4.

It is important to consider that NO_x are higher at engine condition 2 (lower speed) relative to condition 3 (higher speed). Since at higher speed, CC temperature is lower compared to that at lower speed as discussed earlier so there are appreciable abatements in NO_x at condition 3 for the test fuels. This finding further strengthens the argument that higher temperature in the CC leads to increase in NO_x emissions.

***Smoke emissions*.** Smoke emissions were recorded using light extinction coefficient which is the absolute light absorption unit indicating the quantity of light absorbed at a distance of 1 m. Figure 4 (d) demonstrates that smoke emissions decrease by 25%, 36.6%, 9.1% and 13.6% with B20; and 56.5%, 71.7%, 64%, and 83% with B100 at engine conditions 1, 2, 3, and 4, respectively, relative to diesel fuel.

Decrease in smoke emissions with B20 and B100 is ascribed to increase in oxidation rate of soot with biodiesel compared to fossil diesel. According to Jung *et al.* (2006), oxidation velocity of biodiesel soot is about six times higher compared to that of diesel soot. Song *et al.* (2006) reported faster oxidation of soot by biodiesel of soybean oil compared with fossil diesel. Moreover, lower final boiling point of biodiesel reduces the probability of tar or soot to be formed which are often seen in diesel (Lapuerta *et al.*, 2002).

It is interesting to note that like NO_x emissions discussed above, percentage difference of biodiesel and diesel in terms of smoke opacity is also higher at engine conditions 2 and 4, compared with other two conditions i.e. 1 and 3. The only exception is that in case of NO_x, biodiesel shows higher increase, but in case of smoke it reveals higher abatement in emissions at both these engine conditions. This connotes the trade off between NO_x and smoke emissions of biodiesel.

It is clear from Fig. 4 (d) that smoke is higher at engine condition 2 relative to condition 1 for all the test fuels, and it is also higher at condition 4 relative to condition 3 with diesel and B20; however B100 shows lower smoke emissions at condition 4 compared to condition 3. This increase in smoke at higher load with respect to lower load is ascribed to the formation of rich mixture in CC. However, the decrease in smoke emissions with B100 may be due to the optimum air/fuel ratio that might have occurred at this load level for B100.

***PM emissions*.** PM emissions decrease by 21%, 34.7%, 25.3%, and 3.2% with B20; and 78.9%, 87.8%, 82.72%, and 71.3% with B100 at engine conditions 1, 2, 3, and 4, respectively, relative to diesel (Fig. 4(e)). Above findings are in good agreement with those of Canakci and Van Gerpen (2001) who reported 65% reduction from the tests performed on diesel engine fuelled with biodiesel from soybean oil.

The reduction in PM emissions with B20 and B100 is attributed to the oxygen enrichment resulting in more complete combustion, relative to diesel. In addition to this, lack of aromatic content in biodiesel is also responsible for the reduction of PM emissions, because aromatic content is considered as soot precursor contributing to the PM emissions (Lapuerta *et al.*, 2002). Moreover, nominal sulphur content in biodiesel may help in the reduction of PM emissions by biodiesel compared to diesel (Choi *et al.*, 1997). This sulphur content is responsible for the sulphate formation, and hence for PM emissions.

As shown in Fig. 4 (e), PM pollutants are higher at engine condition 1 compared to condition 2, and at engine condition 3 relative to condition 4 for the test fuels. This may be due to the higher HC emissions at engine conditions 1 and 3 as compared to their corresponding conditions 2 and 4 as shown in Fig. 4 (b).

Conclusions

Following important points have been concluded from the present experimental study:

- At different engine conditions, BP of the engine remained almost unaffected by B20, but it decreased by 1.5% to 5.8% with B100, relative to fossil diesel.
- There was a marginal increase in BSFC with B20; however, B100 exhibited 14% to 17% increase in BSFC as compared to diesel for different engine conditions.
- B20 revealed a nominal increase in MCP; however, B100 exhibited a noticeable increase in it which reached to 5.5% with B100, when compared with commercial diesel.
- Relative to B20 and B100, diesel showed deeper HRR curves during the ignition delay periods and larger premixed combustion peaks.
- At different engine conditions, B20 exhibited 6.8% to 19% reduction, and B100 reflected 3% to 14% abatement in CO pollutants, compared with commercial diesel. CO pollutants were higher at lower load relative to higher load, and at higher speed relative to lower speed.
- HC emissions were reduced by 13% to 20.8% with B20, and 32.6% to 46.3% with B100 as compared to diesel for different engine conditions. HC pollutants were higher at lower load relative to higher load.
- NO_x pollutants increased by 2.2% to 5.5% with B20, and 2% to 10% with B100, relative to fossil diesel fuel. NO_x emissions were greatly influenced by the MCP, and increased with increase in MCP. NO_x emissions were higher at higher load relative to lower load, and at lower speed as compared to higher speed.
- Smoke opacity was considerably affected by biodiesel, and reduced by 9% to 36.6% with B20 and 56.5% to 83% with B100 with respect to diesel, at different engine conditions. The MCP showed a significant impact on smoke emissions and a trade-off between smoke and NO_x was observed. Smoke emissions were higher at higher load, compared with lower load.
- B20 and B100 showed 3.2% to 34.7% and 71.3% to 87.8% abatement in PM emissions, respectively, as compared to the commercial diesel fuel. PM emissions were higher at lower load relative to higher load.

Acknowledgement

The authors acknowledge the financial supports of National Laboratory of Auto-Performance and Emission Test, Beijing Institute of Technology (BIT), Beijing, P. R. China under its project # 50576063.

References

Agarwal, A.K., Rajamanoharan, K. 2009. Experimental investigations of performance and emissions of Karanja oil and its blends in a single cylinder agricultural diesel engine. *Applied Energy* **86:** 106-112.

Agarwal, D., Sinha, S., Agarwal, A.K. 2006. Experimental investigation of control of NO_x emissions in biodiesel-fueled compression ignition engine. *Renewable Energy* **31:** 2356-2369.

Agarwal, A.K., Bijwe, J., Das, L.M. 2003. Wear assessment in biodiesel fuelled compression ignition engine. *Journal of Engineering for Gas Turbine Power* (ASME J) **125:** 820-826.

Alam, M., Song, J., Acharya, R., Boehman, A., Miller, K. 2004. Combustion and emission performance of low sulfur, ultra low sulfur and biodiesel blends in a DI diesel engine. *SAE Technical Paper Series* No. 2004-01-3024.

Canakci, M., Van Gerpen, J.H. 2001. Comparison of engine performance and emissions for petroleum diesel fuel, yellow grease biodiesel, and soybean oil biodiesel. *ASAE Annual International Meeting* 016050.

Cardone, M., Prati, M.V., Rocco, V., Seggiani, M., Senatore, A., Vitolo, S. 2002. *Brassica carinata* as an alternative oil crop for the production of biodiesel in Italy: engine performance and regulated and unregulated exhaust emissions. *Environmental Science and Technology* **36:** 4656-4662.

Choi, C.Y., Bower, G.R., Reitz, R.D. 1997. Effects of biodiesel blended fuels and multiple injections on D.I. diesel engines. *SAE Technical Paper Series* No. 970218.

Collier, A.R., Rhead, M.M., Trier, C.J., Bell, M.A. 1995. Polycyclic aromatic compound profiles from a light-duty direct-injection diesel engine. *Fuel* **74:** 362-367.

Correa, S.M., Arbilla, G. 2006. Aromatic hydrocarbons emissions in diesel and biodiesel exhaust. *Atmospheric Environment* **40:** 6821-6826.

Demirbas, A. 2007. Importance of biodiesel as transportation fuel. *Energy Policy* **35:** 4661-4670.

Dorado, M.P., Ballesteros, E., Arnal, J.M., Gomez, J., Gimenez, F.J.L. 2003. Testing waste olive oil methyl ester as a fuel in a diesel engine. *Energy Fuels* **17:** 1560-1565.

Dube, M.A., Tremblay, A.Y., Liu, J. 2007. Biodiesel production using a membrane reactor. *Bioresource Technology* **98:** 639-647.

Ebiura, T., Echizen, T., Ishikawa, A., Murai, K., Baba, T. 2005. Selective transesterification of triolein with methanol to methyl oleate and glycerol using alumina loaded with alkali metal salt as a solid-base catalyst. *Applied Catalyst. A: General.* **283:** 111-116.

Guarieiro, L.L.N., Pereira, P.A.P., Torres, E.A., da Rocha, G.O., deAndrade, J.B. 2008. Carbonyl compounds emitted by a diesel engine fuelled with diesel and biodiesel-diesel blends: Sampling optimization and emissions profiles. *Atmospheric Environment* **42:** 8211-8218.

Hansen, K.F., Jensen, M.G. 1997. Chemical and biological characteristics of exhaust emissions from a DI diesel engine fuelled with rapeseed oil methyl ester (RME). *SAE Technical Paper Series* No. 971689.

He, C., Ge, Y., Tan, J., Shah, A.N., Wang, B. 2008. Time-resolved emissions characteristics of gasoline vehicle particle number and size distributions. International Powertrains, Fuels and Lubricants Congress, Shanghai, China. *SAE Technical Paper Series* No. 08SFL-0207.

Heywood, J.B. 1988. *Internal Combustion Engine Fundamentals.* McGraw-Hill Book Co. Inc., New York, USA.

Jung, H., Kittleson, D.B., Zachariah, M.R. 2006. Characteristics of SME biodiesel-fueled diesel particle emissions and the kinetics of oxidation. *Environmental Science and Technology* **40:** 4949-4955.

Kaplan, C., Arslan, R., Surmen, A. 2006. performance characteristics of sunflower methyl esters as biodiesel. *Energy Sources, Part A.* **28:** 751-755.

Karabektas, M., Ergen, G., Hosoz, M. 2008. The effects of preheated cottonseed oil methyl ester on the performance and exhaust emissions of a diesel engine. *Applied Thermal Engineering* **28:** 2136-2143.

Kegl, B. 2008. Effects of biodiesel on emissions of a bus diesel engine. *Bioresource Technology* **99:** 863-873.

Korbitz, W. 1999. Biodiesel production in Europe and North America, an encouraging prospect. *Renewable Energy* **16:** 1078-1083.

Krahl, J., Munack, A., Bahadir, M., Schumacher, L., Elser, N. 1996. Review: Utilization of rapeseed oil, rapeseed oil methyl ester or diesel fuel: exhaust gas emissions and estimation of environmental effects. International Fall Fuels and Lubricant (1996) *SAE Technical Paper Series* No. 962096.

Krahl, J., Munack, A., Schroder, O., Stein, H., Bunger, J. 2003. Influence of biodiesel and different designed diesel fuels on the exhaust gas emissions and health effects. *SAE Transactions* **112:** 2447-2455.

Krawczyk, T. 1996. Biodiesel: Alternative fuel makes inroads but hurdles remain. *Inform* **7:** 801-814.

Labeckas, G., Slavinskas, S. 2006. The effect of rapeseed oil methyl ester on direct injection diesel engine performance and exhaust emissions. *Energy Conversion and Management* **47:** 1954-1967.

Lapuerta, M., Armas, O., Ballesteros, R. 2002. Diesel particulate emissions from biofuels derived from Spanish vegetable oils. *SAE Tech. Paper Ser.* No. 2002-01-1657.

Lapuerta, M., Armas, O., Rodriguez-Fernandez, J. 2008. Effect of biodiesel fuels on diesel engine emissions. *Progress in Energy and Combustion Science* **34:** 198-223.

Last, R.J., Kruger, M., Durnholz, M. 1995. Emissions and performance charateristics of a 4-stroke, direct injected diesel engine fuelled with blends of biodiesel and low sulfur diesel fuel. *SAE Technical Paper Series* No. 950054.

Lin, Y.C., Lee, W.J., Li, H., Hou, H.C. 2006. PAH emissions and energy efficiency of palm-biodiesel blends fueled on diesel generator. *Atmospheric Environment* **40:** 3930-3940.

Monyem, A., Van Gerpen, J.H. 2001. The effect of biodiesel oxidation on engine performance and emission. *Biomass and Bioenergy* **20:** 317–325.

Peterson, C.L., Reece, D.L. 1996. Emission testing with blends of esters of rapeseed oil fuel with and without a catalytic converter. *SAE Technical Paper Series* No. 961114.

Raheman, H., Ghadge, S.V. 2007. Performance of compresssion ignition engine with mahua *(Madhuca indica)* biodiesel. *Fuel* **86:** 2568-2573.

Ramadhas, A.S., Jayaraj, S., Muraleedharan, C. 2005. Characterization and effect of using rubber seed oil as fuel in the compression ignition engines. *Renewable Energy* **30:** 795-803.

Senatore, A., Cardone, M., Rocco, V., Prati, M.V. 2000. A comparative analysis of combustion process in D.I. diesel engine fuelled with biodiesel and diesel fuel. *SAE Technical Paper Series* No. 2000-01-0691.

Shah, A.N., Yun-shan, G.E., Jian-Wei, T., Zhi-hua, L. 2008. An experimental investigation of PAH emissions from a heavy duty diesel engine fuelled with biodiesel and its blend. *Pakistan Journal of Scientific and Industrial Research* **51:** 293-300.

Shah, A.N., Yun-shan, G., Chao, H., Baluch, A.H. 2009a. Effect of biodiesel on the performance and combustion parameters of a turbocharged compression ignition engine. *Pakistan Journal of Engineering and Applied Science* **4:** 61-69.

Shah, A.N., Yun-shan, G., Shaikh, M.A. 2009b. A comparative study on number size distribution of particles emitted from a heavy duty CI engine fuelled with biodiesel and its 20% blend. *Mehran University Research Journal of Engineering and Technology*. **28:** 205-213.

Song, J.H., Alam, M., Boehman, A.L., Kim, U.J. 2006. Examination of the oxidation behavior of biodiesel soot.

Combustion and Flame **146:** 589-604.

Szybist, J.P., Song, J., Alam, M., Boehman, A.L. 2007. Biodiesel combustion, emissions and emission control. *Fuel Process Technology* **88:** 679-691.

Tsolakis, A. 2006. Effects on particle size distribution from the diesel engine operating on RME-biodiesel with EGR. *Energy and Fuels*. **20:** 1418-1424.

Turrio-Baldassarri, L., Battistelli, C.L., Conti, L., Crebelli, R., Berardis, B.D., Iamiceli, A.L., Gambino, M., Iannaccone, S. 2004. Emission comparison of urban bus engine fuelled with diesel oil and biodiesel blend. *Science of the Total Environment* **327:** 147-162.

Xiaoming, L., Yunshan, G., Sijin, W., Xiukun, H. 2005. An experimental investigation on combustion and emissions characteristics of turbocharged DI engines fuelled with blends of biodiesel. *SAE Technical Paper Series* No. 2005-01-2199.

Usta, N. 2005. An experimental study on performance and exhaust emissions of a diesel engine fuelled with tobacco seed oil methyl ester. *Energy Conversion and Management* **46:** 2373-2386.

Wedel, R.V. 1999. *Emissions Reductions with Biodiesel. Handbook of Biodiesel*. US Department of Energy, USA.

Zhang, Y., Van Gerpen, J.H. 1996. Combustion analysis of esters of soybean oil in a diesel engine. *SAE Technical Paper Series* No. 960765.

Pak. J. Sci. Ind. Res. 2009 **52** (4) 228-230

Development of a Solar Fish Dryer

Adenike Boyo[a]* and Henry Boyo[b]

[a]Physics Department, Lagos State University, Ojo, Lagos, Nigeria

[b]Physics Department, University of Lagos, Akoka, Lagos, Nigeria

(received June 11, 2008; revised March 13, 2009; accepted April 6, 2009)

Abstract. The solar fish dryer developed for particular conditions of Bishop Village, Lagos, Nigeria absorbs sunlight with a flat plate collector for its air heater. Mirrors are appended to one of the collector sides to enhance collection of solar radiations. The dryer is a passive type, tailored to solve the energy needs of the people of the area. On days of high irradiance, temperature within the solar fish dryer can be as high as 80°C with relative humidity around 10%.

Keywords: renewable energy, flat plate collector, solar fish dryer, fish drying

Introduction

Principal profession of the male population of Bishop village of Lagos, Nigeria, is catching fish whereas local females work on its drying. The chief method commonly employed for fish preservation at the Bishop village is the smoke drying whereas on a small scale, fish is dried openly in the sun. In the absence of electric power, the local population did not have access to other means of food preservation such as refrigeration, freezing or any other method that requires electricity.

Sun drying in open air exposes seafood to contamination such as dust, flies, insects, birds etc., while the smoke drying technique can roast or scorch the fish. Protein and vitamin losses become a major concern at elevated temperatures (above 90 °C) at which fish is dried. The smoke drying method depends heavily on wood as fuel, a valuable commodity that can be utilized in building huts and canoes; smoke also pollutes the environment.

The solar fish dryer presently developed is powered by solar energy and requires minimum labour. Apart from the initial investment, the maintenance cost of the solar fish dryer is negligible. Fish is kept in an enclosure during drying process and is safe from contamination; it can be dried completely in a day under optimum sunshine conditions. The women of village, by employing this technique, can produce better-dried fish of improved quality, thus bringing in its better monetary value. Principally made for drying the fish, the dryer can be used for drying vegetables and other related foods, as well.

Principle involved. Food preservation is based on the removal of moisture from foods upto the level at which it cannot support the growth of microorganisms and, hence, stops spoilage of food (Desrosier and Desrosier, 1987).

* Author for correspondence; E-mail: nikeboyo@yahoo.com

In the developed solar fish dryer, solar energy is employed to heat the air that passes through the drying chamber and removes moisture from the fish along its convective path (Boyo, 2001).

Construction of solar fish dryer. Figure 1 shows essential features of the solar fish dryer. It is composed of a flat plate collector "C" (Ikejiofor, 1985; Sayigh, 1979) for air heating, a drying chamber "D" and mirrors A and B. The drying chamber is made of hard wood in the form of a stool which stands 80 cm above the ground. The base of the drying chamber is lined with blackened aluminium to absorb radiations and also to protect the wooden frame of the chamber from fish oil drippings when the dryer is in use. The outlets at the drying chamber are regulated in such a way that proper temperature for fish drying is attained (below 80° C). Mirrors 'A' and 'B' are put in place to converge sun rays towards collector plate and drying chamber "D".

The dryer can be positioned in such a way that its mirrors 'A' and 'B' face southward, so that while the sun traverses its path (east to west), it can function without human involvement. Otherwise it would be cumbersome to reorient the mirrors for receiving direct sunlight.

Collector plate "C", placed at a tilt angle of 40° relative to horizontal, allows the hot air flow into the drying chamber "D" *via* convective air drift, reducing humidity within the drying chamber (by the replacement of wet cool air through inflow of dry hotter air); it thus accelerates evaporation of moisture from surface of the fish. A fraction of heat is transferred from hot air to fish, which increases its temperature and helps in migration of moisture to the surface of fish.

The factors that enhance drying speed include:

1. High temperature
2. Low relative humidity

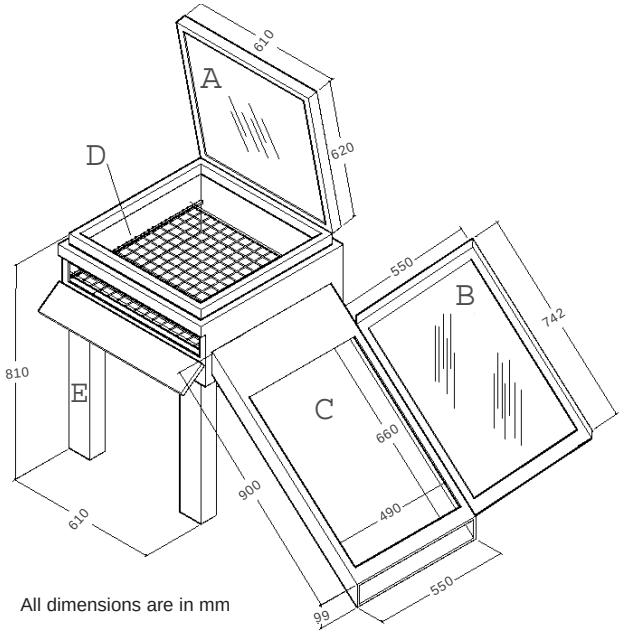

Fig. 1. Essential features of the solar fish dryer.

3. High wind speed
4. High porosity of the food
5. Large surface area to volume ratio of food

Attainable temperature analysis. The temperature inside the dryer does not increase indefinitely even when it is continuously supplied with energy by the sun at its best collector's tilt.

The energy analysis of the heating chamber is discussed herein. The heating chamber is a flat plate collector having a glass glazing and within it is a blackened aluminum sheet that serves as absorber.

Let:

Q_{rad} : be the effective solar irradiance on collector absorber plate

C_{ap} : heat capacity of the absorber plate.

T_{ap} : mean temperature of the absorber plate and

T_o : the ambient temperature.

Q_L : represents all the heat taken away from the absorber plate either by the air (it is supposed to heat) or the loss mechanisms at the collector in particular.

Q_{rad} and C_{ap} are constants.

The energy balance equation for the system takes the form:

$$Q_{rad} = C_{ap}\left(\frac{dT_{ap}}{dt}\right) + Q_L \qquad (1)$$

Experimental work by Sayigh (1979) showed agreement with what was expected, that is:

Q_L generally increases with the increasing difference $(T_{ap}\text{-}T_o)$. Q_L is taken to depend on $(T_{ap}\text{-}T_o)$ alone and with that, the second term in the Taylor's expansion of Q_L is $k(T_{ap}\text{-}T_o)$ which will be taken to approximate Q_L in our case.

$Q_L = k(T_{ap}\text{-}T_o)$ substituted into equation (**1**), gives,

(2)

Equation (2) can be rewritten as:

$$\frac{dT_{ap}}{dt} = \frac{[Q_{rad} - k(T_{ap} - T_0)]}{C_{ap}} \qquad (3)$$

The solution of equation (3) is,

$$T_{ap} = \left(\frac{Q_{rad}}{k}\right)\left[1 - \exp\left(-\frac{k}{C_{ap}}\right)\right] + T_0 \qquad (4)$$

From equation (4), one can draw the conclusion that plate temperature has an upper limit, $T_{ap} = \frac{Q_{rad}}{k} + T_o$, determined by the irradiance on the plate, the energy transfer rate from the plate to the air (the rate of useful air heating) and various losses (due to imperfect insulation etc).

Higher order terms in the Taylor's expansion for Q_{rad} would only reduce the steady state temperature T_{ap}. Since the air temperature from the collector would not exceed that of the absorber plate (if this indeed is the air heater), then with proper designing one can create the heating chamber of the dryer so that the temperature does not exceed particular values.

Q_{rad}

Maximum attainable temperature for the developed dryer was set to about 80 °C as required for fish drying so as to avoid over- cooking.

Results and Discussion

The data collected for the dryer, while drying fish at the Bishop village on the 6th of May 2006, (Fig. 2) was obtained with an autolog temperature and humidity sensor (RH-02) made by Pico Technology. This was set to sample data every 3 min. From the graph, temperature within the dryer was about 40 ºC above the ambient one at about 4:30 pm. It can be seen from the graph that the environment of Bishop Village has ambient humidity of approx 70% during the day. Thus, open sun drying would occur at a comparatively much slower rate in this place.

The average humidity inside the dryer between 12:30 pm and 5:30 pm was around 25%, which shows a relatively well-improved environment for drying compared to its surroundings.

It was observed that 50 ºC temperature was good enough for the initial drying of fish which was then gradually increased to 80 ºC to avoid cake-layer formation of the outer tissues.

At about 3:20 p.m., the dryer was momentarily opened (for about 3 min to check the dryness of the fish) causing the humidity to jump to about 54%. It is suggested that in the design of dryer, some arrangement for energy storage like coal or granite stones may be provided to preserve the heat inside the chamber especially during cloud cover (Boyo, 2003).

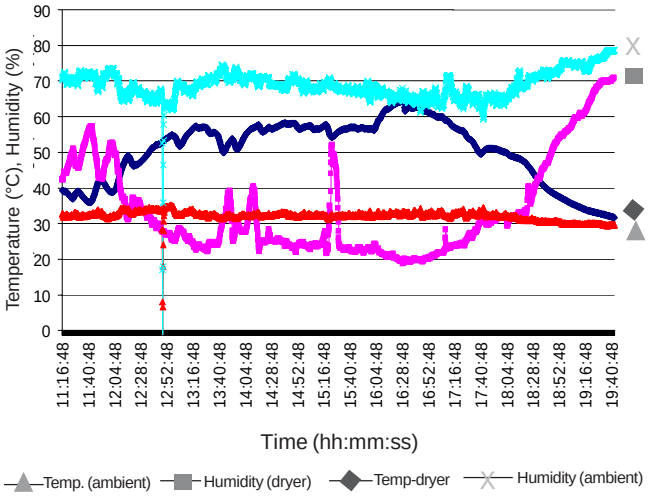

Fig. 2. Temperature and humidity profile inside and outside dryer during fairly clear sky on 6th June 2006.

The drying time required to dry any type of fish depends on the extent of dryness to be achieved. On a reasonably sunny day, when the dryer operates close to 80 ºC with humidity within 10%–30%, moisture content of thin slices of 2 kg of fish may be reduced by 76%. For thick slices, the problem of case hardening may occur which sets in when food is dried too rapidly. For the solution of this problem, common practice is to salt the fish so as to build up osmotic pressure that will encourage the diffusion of water onto the surface. A solar photovoltaic powered micro-controller will be incorporated in future design to regulate the temperature and humidity inside the dryer to suit specific products (Anyanwu, 2006).

Conclusion

The solar fish dryer, developed herein, provides optimum drying conditions for fish between 50 ºC to 80 ºC and humidity range of 10% to 30%. Under these conditions, the moisture content of about 2 kg of sliced fish was reduced by about 76% over a period of seven hours.

The solar fish dryer provides a convenient and hygienic way of drying the fish and is useful particularly for use in the Bishop Village, Nigeria. The wood (or coal) that would have been used for drying can now be spared for better utilization.

References

Anyanwu, A. 2006. Design and Construction of a User Friendly Universal Solar Food Dryer Using Programmable System on Chip. B. Sc. Thesis, Department of Physics. pp. 11-17, University of Lagos, Nigeria.

Boyo, A. O. 2003. Comparative efficiencies of different storage materials for solar collectors and their applications in solar drying. *Journal of Engineering Applications* **3:** 19-24.

Boyo, A.O. 2001. Solar radiation on inclined surfaces in Lagos, Nigeria. *The Nigerian Journal of Research And Review In Science*. **2:** 60-65.

Desrosier, N.W., Desrosier, J.N. 1987. *The Technology of Food Preservation*, 4th edition, CBS Publishers and Distributors, New Delhi, India.

Ikejiofor, I.D. 1985. Passive solar cabinet dryer for drying agricultural products. In: *Proceedings of the Workshop of the Physics and Technology of Solar Energy Conversion*. pp. 157-165, African Union of Physics, University of Ibadan, Nigeria.

Sayigh, A.A.M. 1979. The technology of flat plate collectors. In: *Solar Energy Conversion, An Introductory Course* 5th, pp. 101-124, University of Waterloo, Ontario, Canada August 6-19, 1978, Selected Lectures (A80-42435, 18-44) Pergamon Press, Toronto, Canada and New York, USA.